Hydrologic Performance of Sustainable Urban Drainage Systems in Cold Maritime Climates

Tarek Zaqout

Faculty of Civil and Environmental Engineering
University of Iceland
2022

Hydrologic Performance of Sustainable Urban Drainage Systems in Cold Maritime Climates

Tarek Zaqout

Dissertation submitted in partial fulfillment of a
Philosophiae Doctor degree in Environmental Engineering

Supervisor
Prof. Hrund Ólöf Andradóttir

Ph.D. committee

Prof. Hrund Ólöf Andradóttir

Asst. Prof. Johanna Sörensen

Prof. Ólafur Gestur Arnalds

Opponents
Prof. Tone Merete Muthanna
Asst. Prof. Ryan Winston

Faculty of Civil and Environmental Engineering
School of Engineering and Natural Sciences
University of Iceland

September 2022

Hydrologic Performance of Sustainable Urban Drainage Systems in Cold Maritime Climates

Dissertation submitted in partial fulfillment of a *Philosophiae Doctor* degree in Environmental Engineering

Faculty of Civil and Environmental Engineering
School of Engineering and Natural Sciences
University of Iceland
Hjarðarhagi 2-6
107, Reykjavík
Iceland

ISBN 978-9935-9647-9-3

Printing: Haskolaprent ehf.
Reykjavik, Iceland, September 2022

Abstract

Sustainable urban drainage systems (SUDS) are increasingly implemented to mitigate flood risk and augment environmental quality and wellbeing in cities. Vegetated swales are one of the most common SUDS components, yet they are among the least studied in cold climates. The goal of this research was to assess the performance of a grass swale in a cold maritime climate characterized by frequent freezing and thawing, rain-on-snow events, and repeated midwinter snowmelt. Synthetic runoff experiments, single-ring infiltration measurements, and continuous monitoring of soil and meteorological conditions were undertaken over two years in the BREEAM-certified neighborhood of Urriðaholt, Iceland. The grass swale infiltrated water during all seasons but at a lower rate in winter. Sparsely vegetated and barren areas were more susceptible to concrete frost formation and heave than well vegetated areas during repeated freeze-thaw. The dense vegetation in the grass swales and the intertwined root system aided the hydrological performance of the grass swale by enhancing the near-surface soil porosity while providing soil binding that resists structural deformation. Soil frost modeling indicated that while soil frost has decreased in the last 70 years, the freezing season shifted towards midwinter to coincide with the largest rain-on-snow events. This, combined with increasing rain-on-snow volume, suggests that the risk of urban flooding during winter may increase in the next decades with climate warming. Greenifying urban areas is essential to improve resilience and mitigate the adverse impacts of climate change.

Útdráttur

Blágrænar ofanvatnslausnir (BGO) eru í auknum mæli innleiddar til þess að draga úr flóðahættu, auka umhverfisgæði og vellíðan í borg. Gróðurrásir eru algeng útfærsla á BGO, en minnst kannaðar í köldu loftlagi. Markmið þessarar rannsóknar var að meta virkni gróðurrásar í köldu sjávarloftslagi, sem einkennist af tíðum umhleypingum frost og þíðu, regn-á snjó atburðum og snjóbráð á miðjum vetri. Framkvæmdar voru afrennslistilraunir, ísigsmælingar, og samfelldar mælingar á jarðvegi og veðurfari yfir tveggja ára tímabil í umhverfisvottaða hverfinu Urriðaholti, í Garðabæ. Gróðurrásin miðlaði vatni í jarðveg á öllum árstíðum, en þó með lægri skilvirkni vegna frostmyndunar að vetri. Strjál og gróðurlaus svæði voru næmari fyrir hýfingu og myndun steypufrosts í kjölfar endurtekinna frost-þíðu kafla en gras. Þétt blöð og samofið rótarkerfi grass hjálpuðu að viðhalda vatnafræðilegri virkni, með því að auka gleypni yfirborðs og binda jarðveg svo hann aflagist ekki. Hermanir á jarðvegshita gáfu til kynna að dregið hafi úr frosti á síðustu 70 árum, að frosttímabilið hafi styst í átt að mánuðum þar sem mesta rigning mælist á snjó. Þessi þróun samhliða meiri úrkomu á snjó gefur vísbendingu um að hætta á ofanflóðum í þéttbýli geti aukist á næstu áratugum með hlýnandi loftslagi. Að viðhalda grænum svæðum í borg er nauðsyneg til að auka viðnámsþol og draga úr neikvæðum áhrifum hnattrænar hlýnunar.

To my family.

Table of Contents

List of Figures

List of Tables

List of Publications

Appended papers

Zaqout, T., & Andradóttir, H. Ó. (2021). Hydrologic performance of grass swales in cold maritime climates: Impacts of frost, rain-on-snow and snow cover on flow and volume reduction. Journal of Hydrology, 597, 126159. https://doi.org/10.1016/j.jhydrol.2021.126159

Zaqout, T., Andradóttir, H. Ó., & Arnalds, Ó. (2022). Infiltration capacity in urban areas undergoing frequent snow and freeze-thaw cycles: Implications on Sustainable Urban Drainage Systems. Journal of Hydrology, 127495. https://doi.org/10.1016/j.jhydrol.2022.127495

Zaqout, T. Andradóttir, H. Ó., & Sörensen, J. Trends in soil frost formation due to climate change and the impacts on urban flood risk. [submitted].

Author's contribution to appended papers

Paper I: The author collected the data, developed the methods, analyzed the data, wrote the paper, and discussed the results together with the co-author of the article.

Paper II: The author collected and analyzed the data independently, wrote the paper and discussed the findings with the co-authors.

Paper II: The author collected part of the data, acquired the other data from external sources, modeling and data analyses were conducted by the author, and wrote the article and discussed the findings with the co-authors.

Abbreviations

BMPs	Best management practices
F	Frost
FTC	Freeze-thaw cycle
GCMs	Global climate models
IPCC	The Intergovernmental Panel on Climate Change
IUWM	Integrated urban water management
IUWRM	Integrated urban water resources management
K_{sat}	Saturated hydraulic conductivity
LID	Low impact development
N	Neutral soil conditions
PTF	Pedo-transfer functions
RoS	Rain-on-snow
S	Snow surface conditions
SHAW	Simultaneous heat and water model
SoF	Snow on frost surface conditions
SUDS	Sustainable urban drainage systems
SuDS	Sustainable drainage systems
T	Return period
TN	Total nitrogen
TP	Total phosphorus
TSS	Total suspended solids
W	Warm surface conditions

WSUD	Water sensitive urban drainage

Acknowledgments

First and foremost, I would like to express my sincere gratitude to my supervisor Prof. Hrund Ólöf Andradóttir, for her guidance, motivation, immense knowledge, and continuous support throughout my Ph.D. studies. This work would not have been possible without her. Secondly, I would like to thank my co-supervisor, Asst. Prof. Johanna Sörensen at the University of Lund, for the fruitful discussions that helped me widen my horizons during my studies, for her contributions to Paper II, and for co-authoring Paper III in this thesis. I would also like to express my gratitude to my Ph.D. committee member Prof. Ólafur Gestur Arnalds at the Agricultural University of Iceland (LBHÍ), for designing the experimental setup and co-authoring Paper II, as well as for the discussions and helpful comments with the entire thesis.

This work has been made possible and funded by the Icelandic Research Fund (Icelandic: Rannís; grant number 185398-053) and a one-year teaching grant from the University of Iceland. Moreover, Garðabær municipality and Urriðaholt ehf. are thanked for their financial and logistical support of the project.

Several people provided instrumental help in designing the experimental field program: Our technician Vilhjálmur Sigurjónsson at the University of Iceland, is thanked for his help with the experimental setup and immense support throughout my studies. Guðni Þorvaldsson and Berglind Orradóttir at The Agricultural University of Iceland are thanked for their help setting up the soil monitoring program. A special thank you goes to the Gardening Department at the University of Iceland, especially Hjalti Stefánsson, for lending us equipment used in the field.

I would like to thank Prof. Birgir Hrafnkelsson and Prof. Viðar Guðmundsson for their help with Paper III. In addition, I would like to thank Finnur Pálsson for lending us the snow measuring kit and Andri Gunnarsson for his practical advice and help with the field program.

I also would like to thank the Icelandic Meteorological Office for their instrumental help and support in making this work possible and for operating the Urriðaholt weather station, especially Óðinn Þórarinsson, Guðrún Nína Petersen, Gunnar Sigurðsson, and Tryggvi Hjörvar. I‘m also grateful for the help provided by Benedikt Sigurvinsson at Strendingur ehf., Garðabær Municipality, Urriðaholt ehf., the Department of Water Supply in Garðabær, and the Fire Department in Hafnarfjörður for providing the infrastructure and the connection to running water. I want to express my gratitude to Sigurður John Einarsson for helping with the field experiments.

Lastly, warm thanks go to my parents, brother, sister, and entire family for being supportive and loving. To all my friends in Palestine, Iceland, and Germany, I couldn‘t have asked for a better company.

1 Introduction

1.1 Motivation

Climate change and the rapid increase in urbanization have led to more frequent and damaging urban floods (Ashley et al., 2007; Huong & Pathirana, 2013). These floods have motivated a shift in urban drainage policy from a single-purpose approach of reducing runoff to a multi-functional approach that provides social, economic, and health benefits (Fletcher et al., 2015; Wong & Brown, 2009). Decentralized, infiltration-based stormwater management using Sustainable Urban Drainage Systems (SUDS) has gained increased popularity in recent decades (Barrett, 2008; Maksimovic et al., 2000). However, concerns still exist about their hydrological performance that may be negatively affected by winter conditions (Caraco & Claytor, 1997; Oberts, 2003). Yet, the most detailed cold climate studies focused on the performance of bioretention cells, which ranged from complete capture of runoff volumes to impeded infiltration in the presence of surface frost (e.g., Blecken et al., 2010; Khan et al., 2012; LeFevre et al., 2009; Muthanna et al., 2008; Paus et al., 2016; Roseen et al., 2009).

SUDS hydrological performance and effectiveness in reducing and treating surface runoff rely heavily on their filter media's capacity to infiltrate water (Davis et al., 2012; García-Serrana et al., 2017; Rujner et al., 2018). Soil infiltration capacity is mainly dependent on soil physical properties, type of soil, soil hydraulic conductivity, initial moisture content, and the type of vegetation on the surface. The hydrologic efficiency is also linked to the magnitude and intensity of runoff events (Davis et al., 2012). Bed slopes and surface roughness provided by vegetation also affect flow retardation and infiltration (Monrabal-Martinez et al., 2018). The conflicting reports on winter SUDS performance are, thus, partially linked to the complex interactions between the soil, vegetation cover, and climatic conditions. For example, even highly conductive soils, such as sandy loam (Paus et al., 2016), can form ice lenses that significantly impair infiltration. Frost type, largely governed by the pre-freezing soil water content, can play a more important role than frost depth (Muthanna et al., 2008). Concrete frost formation that fully blocks infiltration develops in saturated soils while granular and porous frost favoring infiltration forms in unsaturated or dry soils (Kane & Stein, 1983; Orradottir et al., 2008). A good drainage capacity is paramount to avoid high water content in the soil, which has been shown to enhance volume reduction and prevent frost formation (LeFevre et al., 2009; Muthanna et al., 2008).

In cold coastal regions, frequent rain-on-snow and freeze-thaw cycles are the key cause of urban flooding (Andradóttir et al., 2021). The repeated wetting of the soil by cold liquid water from melting snow and the lack of thermal insulation that can be provided by a continuous, seasonal snow cover render the soils susceptible to frequent freezing and thawing (Flerchinger et al., 2013; Moghadas et al., 2018; Muthanna et al., 2008). Frequent freeze-thaw cycles (FTCs) negatively affect ecosystem diversity and productivity because they cause changes in soil physical properties, lead to soil deformation, and affect water movement in the landscape (Fouli et al., 2013). The constant shift between liquid and solid

phases significantly alters the soil's hydraulic and thermal properties (Lundin, 1990) and is often difficult to quantify. Nevertheless, little is still known about urban runoff generation in cold maritime climates as most studies on rain-on-snow-induced floods have been in rural or mountainous regions (e.g., Freudiger et al., 2014; Garvelmann et al., 2015; Li et al., 2019).

With warmer temperatures in winter, more frequent midwinter snowmelt and rain-on-snow (RoS) events are expected, which generate voluminous runoff that can lead to extreme flooding (Dong & Menzel, 2020; Garvelmann et al., 2015; Hamlet et al., 2005). The hydrological processes during winter i.e., RoS, snowmelt, frost formation, and infiltration in frozen ground, are highly interlinked and less understood than the processes in temperate climates (Granger et al., 2011; Gray et al., 2001; Kane & Stein, 1983). As crucial as soil frost is to urban runoff generation, it is rarely considered when planning urban drainage systems (Maksimovic et al., 2000). A better understanding of SUDS in cold climates is essential to successfully transition cities into climate resilient areas in the northern hemisphere. To date, the hydrological performance of SUDS in cold climates, especially undergoing frequent freezing and thawing, is lacking. Therefore, to alleviate the uncertainties regarding SUDS efficiency in winter and enable more wide adoption of SUDS, a comprehensive, long-term assessment of SUDS in cold maritime climates is needed.

1.2 Objectives and research approach

The overarching goal of this research was to assess the hydrological performance of grass swales undergoing frequent soil freezing and thawing, rain-on-snow events, and intermittent midwinter snowmelt. A particular focus of this work is dedicated to understanding the complex interactions between the different winter hydrological processes, i.e., snow, frost, and RoS, and their relation to runoff generation and flood risks.

The research was organized into three scientific journal papers primarily based on field experiments, as well as modeling techniques and statistical analysis (Figure 1.1), to achieve the following specific goals:

- Assess the hydrologic performance of grass swales during different surface and weather conditions (**Paper I**),
- identify the drivers and the most important factors that affect the performance of grass swales in cold maritime climates (**Paper I**),
- investigate the spatiotemporal variations in infiltration in an urban area (**Paper II**),
- evaluate the role of vegetation and manufactured underlying soils on the infiltration capacity in urban areas (**Paper II**),
- investigate the trends in soil temperature and frost due to climate change (**Paper III**),
- understand the implications of climate change on winter flood risks (**Paper III**).

This work improved the understanding of the hydrological performance of grass swales undergoing cyclical freezing and thawing and emphasized the importance of soil infiltration and drainage capacity by conducting synthetic runoff experiments in a segment of a grass swale (**Paper I**; Figure 1.1). Additionally, it added to the knowledge of infiltration into frozen soils by using single-ring infiltration measurements in different terrains in an urban area, especially highlighting the benefits of using dense vegetation covers and carefully chosen coarse filter media material for SUDS in cold climates (**Paper II**). This research also

utilized the knowledge and data from the field program to numerically model soil temperature and frost to assess the long-term changes due to climate warming and their relation to urban flood risk, especially with the increase in rain-on-snow and frost-induced urban floods (**Paper III**). Therefore, this work contributes to the overall knowledge of urban drainage and climate resiliency to face current and future challenges.

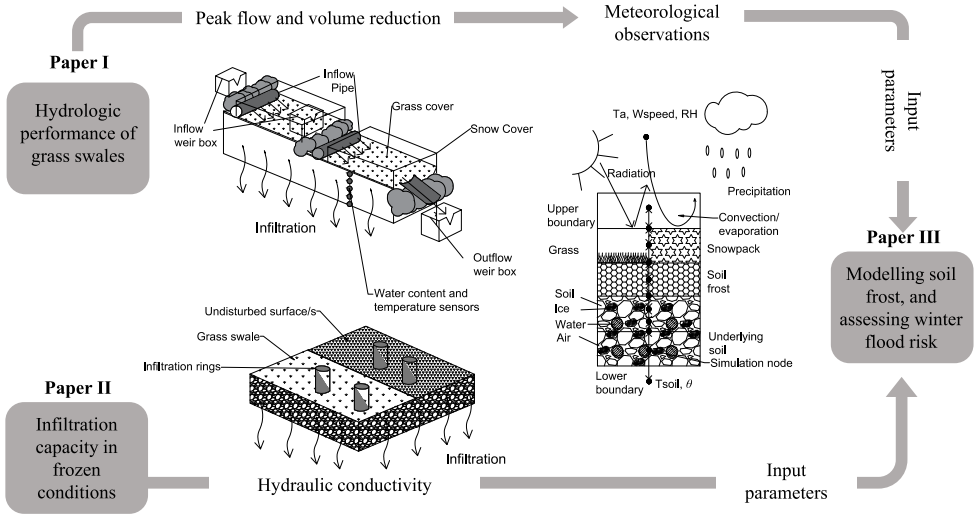

Figure 1.1 Schematic diagram of the thesis structure and key research contributions.

1.3 Thesis structure

The thesis starts with a general overview of the background, methods used, and main results. The focus of the background section is to introduce the key terms and give some more details on the challenges in urban drainage approaches, a brief introduction to cold climate processes, SUDS role, and implementation in Iceland. Then, the methods are briefly summarized, highlighting the range of methods used and the interconnection between the three papers. Following that, a summary of the main findings is presented. Lastly, the highlights of the findings in the three papers are discussed interconnectedly and in relation to the implications on SUDS design and operation and urban flood risk assessment.

Appended at the end of the thesis are the three scientific papers. **Paper I** evaluates the hydrologic performance of grass swales in a cold climate during different winter soil, surface, and meteorological conditions. Specifically, the impacts of soil frost, snow cover, cold temperatures, and the degree of soil saturation on runoff peak and volume reduction, time lag, and drainage capacity of the swale. **Paper II** assesses the infiltration capacity of the grass swale in comparison with different natural (undisturbed) terrains in an urban area in cold maritime conditions undergoing frequent freeze-thaw and snow cycles. The work also focused on the benefits of vegetation and manufactured soils in mitigating the impacts of soil freezing and thawing, namely concrete frost formation and structural deformation, which were pronounced in non or less vegetated areas. **Paper III** predicts frost depth and

timing in an urban area in the last 70 years using numerical modeling to overcome the lack of soil observations. The paper focused on the co-occurrence of rain-on-snow, snowmelt, and rainfall in the presence of frost to assess winter urban flood risks and the implications of climate change on frost formation and its coincidence with extreme events.

2 Background

2.1 Modern urban drainage challenges

Safe drinking water, flood protection measures, stormwater drainage, and wastewater disposal are essential for societies and have been used since the dawn of civilization as early as 5000 years ago in Mesopotamia (Marsalek, 2014). Urban drainage systems are facilities that deal with stormwater and water from domestic, industrial, and commercial sanitary flow "wastewater" (Chocat et al., 2007). In modern times, the goals of flood protection and public health have, to a great extent, been accomplished (Chocat et al., 2007), but less emphasis has been placed on environmental protection. But many problems still exist concerning the efficiency of urban drainage systems, and more issues continue to arise.

By 2030, more than 60% of the world's population is expected to live in urban areas (UN, 2019). Urbanization and the increase in impervious surfaces lead to higher runoff volumes and peaks due to poor infiltration, consequently leading to more frequent urban flooding accompanied by an increase in property damages and loss of life (Chocat et al., 2007; Huong & Pathirana, 2013; Marsalek, 2014). The impacts of urbanization also extend to water quality, as stormwater draining from urban areas is one of the primary sources of pollutants, including pathogens, trace organics, heavy metals, and nutrients. The rapid changes in the inflows from the combined sewer systems (wastewater and stormwater) and the introduction of new types of emerging pollutants like pharmaceuticals and microplastics (Geissen et al., 2015) result in an impairment in the performance of wastewater treatment plants and a deterioration in the quality of receiving waters. Moreover, urbanization affects the local microclimate creating what has been termed the "urban heat island," where urban areas tend to have higher temperatures than the surrounding areas (Huong & Pathirana, 2013). In the mid-20th century, those challenges urged planners to separate stormwater from wastewater to lower the amount of water being conveyed to treatment plants (Talebi & Pitt, 2019). In the past couple of decades, the adoption of sustainable urban drainage systems (SUDS) has been on the rise to compliment the use of direct channeling of surface water through networks of pipes and sewers to face the current and future needs and challenges.

A second concern is the change in climate that has occurred both globally and regionally since industrialization. The consensus is that global warming, at least in the past 50 years, is attributable to human activities (IPCC, 2022), which have changed the atmospheric and meteorological processes that define climate (Arisz & Burrell, 2006). This, in turn, has altered the weather patterns and is expected to increase weather extremes (Konisky et al., 2016), affecting the hydrological cycle and its processes. The quantification of the impacts of climate change on the hydrological cycle is primarily based on the predictions provided by the General Circulation Models (GCMs) that take into account the future changes in the production of greenhouse gases and their deposition into the atmosphere (Arisz & Burrell, 2006). Various climate scenarios have predicted that an increase in precipitation and air temperature will likely occur during this century, both on global and regional/local scales. In the Nordic and Baltic regions, the increase in temperature will be more variable and most

pronounced in winter (up to 4°C) by 2050 with respect to the 1961–1990 baseline (Thorsteinsson & Björnsson, 2012). In the northern hemisphere, the combined effect of increased precipitation intensity, the number of precipitation events, and the total precipitation volume might provide conditions that are expected to result in flooding (Thorsteinsson & Björnsson, 2012). In Iceland and Norway, which are partially ice-covered, runoff is predicted to increase by 3–40%. In Sweden, results based on 16 regional climate scenarios show that 100-year floods are expected to decrease in magnitude due to the reduction in snowmelt volumes in spring. Still, the rain-on-snow-related flooding is likely to increase (Thorsteinsson & Björnsson, 2012).

2.2 Climate resilience and Sustainable Urban Drainage Systems (SUDS)

The frequently asked question of how to best adapt urban areas to the newly posed challenges driven by urbanization and climate change is still persistent. In recent years, risk-based assessment approaches have been widely adopted (Zhou et al., 2012). Flood risk can be assessed by considering the exposure to hazards, which describes the probability and extent of flooding, and the vulnerability of areas, here urban, to the adverse effects of said hazards (Apel et al., 2009; Barroca et al., 2006). The focus of engineers and planners has shifted towards developing suitable adaptation strategies (Zhou et al., 2012) that include exposure and vulnerability assessment. That said, comprehensive, cost-effective, and sustainable urban flood mitigation measures are still lacking (Ashley et al., 2007), especially in large cities. Awareness of cities being complex interdependent systems is growing, but stormwater management strategies are still fragmented and largely controlled by the private sector (Ashley et al., 2010). Additionally, for centuries, stormwater management policies focused on structural engineering solutions rather than natural, non-structural ones (Ashley et al., 2007). To deal with those challenges and the increased uncertainty and complexity, efforts have been made to improve the resilience of urban areas before, during, and after flooding events (Sörensen et al., 2016). Resilience implies drainage systems' ability to adapt, self-organize, and increase the capacity to learn for future events (Ashley et al., 2007). Increasing the resilience of cities has become, however, an important and often talked about issue. Many progressive municipalities implemented laws that restrict developers to maintain the pre-development runoff peaks. Several countries around the world, especially in Europe and North America, encourage implementing, wherever possible, sustainable urban drainage systems (SUDS in the UK) or low impact development (LID in the US), as well as incorporating integrated urban water resources management (IUWRM) as part of the framework to increase resilience. There exist a plethora of terminologies that are in use today such as low impact development (LID), sustainable urban drainage systems (SUDS) or sustainable drainage systems (SuDS), water sensitive urban design (WSUD), best management practices (BMPs), and integrated urban water management (IUWM) (Fletcher et al., 2015). In this work, the term SUDS is used as it is seen to be more descriptive and follows the most authoritative guide to this kind of measures, *The SuDS Manual* (Woods Ballard et al., 2015).

SUDS constitute an approach through which urban stormwater is dealt with close to where it falls in a decentralized way (Sörensen, 2018). SUDS are a diverse set of installations that serve several functions and are meant to maintain the pre-development hydrological cycle

(Woods Ballard et al., 2015) by limiting imperviousness, reducing runoff peaks and volumes, promoting infiltration and evapotranspiration, and enhancing water quality by removing pollutants from stormwater runoff (Figure 2.1). Several design configurations of SUDS exist, including *infiltration-based systems* such as swales, filter strips, infiltration trenches, infiltration basins, and green roofs, *bioretention systems* such as rain gardens and bioretention cells, and *retention-based systems* such as wetlands and detention ponds, which can accommodate large storm events, as well as *stormwater harvesting techniques* (Fletcher et al., 2013, 2015; Wong & Brown, 2009; Woods Ballard et al., 2015). SUDS can also improve the quality of life in urban spaces by making them pleasant, vibrant, and resilient to changes (Wong & Brown, 2009), by improving air quality, regulating the microclimate, reducing noise, and providing recreational benefits (Woods Ballard et al., 2015). In this work, however, the focus is on the hydrological benefits of SUDS.

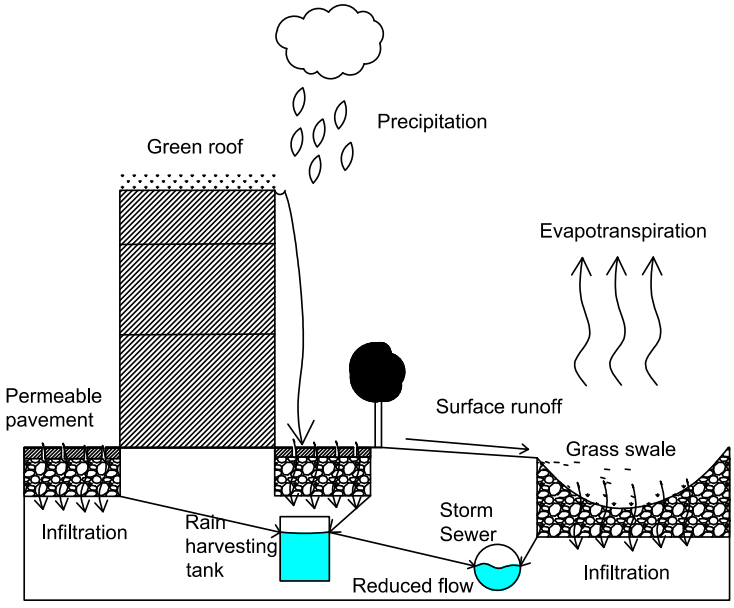

Figure 2.1 Schematic diagram of the hydrological benefits of sustainable urban drainage systems (SUDS).

SUDS provide various hydrological benefits such as reducing and delaying runoff peaks, infiltration, volume storage, flow attenuation, and replenishing the groundwater table (Davis et al., 2012). SUDS also contribute to pollutant removal mechanisms such as filtration, particle entrapment, and settling (Luell et al., 2021; Monrabal-Martinez et al., 2018). Several factors can influence the efficiency of SUDS, such as soil characteristics (Deletic & Fletcher, 2006; García-Serrana et al., 2017), surface area and slope (Monrabal-Martinez et al., 2018), surface roughness and vegetation height (Bäckström, 2002; Davis et al., 2012; García-Serrana et al., 2017), and the initial degree of saturation (Rujner et al., 2018). Designing and planning SUDS is subject to local expertise and specific site and weather conditions (Rujner et al., 2018). Despite their increasingly wide adoption, limited information still exists on the factors affecting their hydrological performance (Fardel et al., 2020). The ambiguity in those

parameters resulted in a wide range of reported hydrologic benefits of such stormwater control measures (Ekka et al., 2021). While the soil's physical properties, i.e., textural class, bulk density, porosity, can be relatively easily measured, soil hydraulic characteristics such as the saturated hydraulic conductivity, K_{sat}, field capacity and wilting point, and water retention curves, are more difficult to determine (Kanso et al., 2018). Such difficulties can be overcome by using pedo-transfer functions (PTF) to estimate the hydraulic properties of soils from routinely measured physical properties (Castellini & Iovino, 2019; Saxton & Rawls, 2006). Nonetheless, soils are extremely heterogeneous and infiltration capacity can differ greatly from one point to another within the same SUDS element (Ahmed et al., 2015), which can lead to an inaccurate prediction of the system performance. It is essential, therefore, to study the local conditions at the site including soils, vegetation, and local weather patterns to insure successful implementation of SUDS.

2.3 Grass swales

Vegetated or grass swales are one of the most common and oldest stormwater control measures, which are simple open channels that convey stormwater runoff from roads or parking lots (Luell et al., 2021). Grass swales are typically designed to convey runoff longitudinally from impervious areas to the next stormwater control measure or to the sewer system (Davis et al., 2012). Additionally, they contribute to total volume reduction via infiltration and temporary storage, runoff attenuation and peak reduction, and outflow delay allowing for more infiltration (Davis et al., 2012; Deletic, 2001; Rujner et al., 2018). Swales are used as a replacement to the traditional underground piping system and can include different configurations that vary according to local conditions and means of use. Swales can be in the form of bioswales, infiltration swales, grassed swales, and wet and dry swales (Woods Ballard et al., 2015). High flow and volume reduction can be obtained by grass swales as high as 100% (Davis et al., 2012; García-Serrana et al., 2017; Monrabal-Martinez et al., 2018). Grass swales can also achieve high pollutant removal efficiencies of up to 99% of total suspended solids (TSS), total phosphorus (TP), and total nitrogen (TN) (Bäckström, 2002). Yousef et al. (1987) reported values ranging between 25% to 35% for TP removal and between 7% and 56% for TN removal (Deletic & Fletcher, 2006; Yousef et al., 1987).

Storm events characteristics such as intensity and duration, together with the catchment characteristics, i.e., the total drainage area, landcover, and topography, determine the volume and flow characteristics being drained into swales (Davis et al., 2012; Gavrić et al., 2019). Therefore, the hydrological efficiency of grass swales is highly dependent on the timing and magnitude of such inflows (Rujner et al., 2018). More importantly, the performance of grass swales is governed by their soil's hydraulic properties, antecedent moisture content, surface roughness, vegetation characteristics (e.g., height, density, and stiffness), and slope (Bäckström, 2002; Davis et al., 2012; Ekka et al., 2021; Gavrić et al., 2019; Morbidelli et al., 2016; Rujner et al., 2018). Gravel or coarse sand materials are not preferred as filter media in swales as they are unsuitable for supporting vegetation (U.S. EPA, 1999). However, sufficiently coarse soils such as sand (minimum infiltration capacity of 21 cm/h), loamy sand (6.1 cm/h), or sandy loam with infiltration rates of 2.6 cm/h are recommended. Shafique et al. (2018) studied a grass swale adjacent to a parking lot with a media consisting of sandy loam soil that achieved volume reductions in the range of 40–75% depending on rainfall intensity with higher efficiencies achieved during small events. However, high volume reduction (88%) was also observed by Deletic & Fletcher (2006), who studied a swale with

silty clay materials that had a saturated hydraulic conductivity of 3.6 cm/h. This might be attributed to the presence of macropores that promote infiltration regardless of the soil type. In a study by Purvis et al. (2019) the hydrological performance of a bioswale that had a high-flow, sand-based media was investigated and the swale was able to infiltrate 37 out of 39 events without generating substantial overflow or underdrain volume, including a 86.1 mm storm event.

2.4 Cold climate concerns

The implementation of SUDS still faces several hurdles, particularly in cold climates (Caraco & Claytor, 1997). The reduction in infiltration capacity and pollutant removal efficacy during winter raises concerns about the hydrological benefits of SUDS in cold climatic regions (Bäckström & Viklander, 2000). The urban hydrological cycle in winter is more complex than in summer (Thorolfsson, 2012). A large portion of precipitation falls as snow and accumulates in snowpacks, air temperature and evapotranspiration are low, frost develops in the soil, and the runoff processes are altered (Bäckström & Viklander, 2000; Maksimovic et al., 2000). Consequently, complications, including clogging of inlets, freezing of pipes, and frost heave can arise (Bengtsson & Westerström, 1992). Snowfall captures pollutants during its passage through the air due to its large surface area compared to rainfall. It continues to accumulate pollutants on the ground, which can be later released into receiving waters during melt (Westerlund & Viklander, 2006). In a study by Sillanpää & Koivusalo (2013), it was found that the snowpack can store up to 50% of the total suspended solids in the catchment. Additionally, the accumulated sediments and particles within the snowpack can accelerate the clogging of the topsoil in infiltration-based practices (Monrabal-Martinez et al., 2019). The runoff resulting from snowmelt is also more voluminous than rainfall, and the contributing area is greater in winter due to frozen and/or saturated soils, which otherwise are permeable (Westerström, 1984). As such, pervious areas can initially infiltrate meltwater but start to encounter a progressive reduction in infiltration capacity as the soil moisture storage begins to fill up or refreeze (Buttle, 1990; Buttle & Xu, 1988).

Frozen soil is a continuum of particles: large air-filled pores, intermediate ice-filled pores, small liquid water-filled pores, and liquid water films around particles (Lundin, 1990). Three conditions are normally present in a frozen soil: unfrozen water in the finest pores, frozen water in the intermediate pores, and air in the largest pores (Stähli et al., 1999). This happens because complete saturation of the soil does not usually occur, and the largest pores are still air-filled at the onset of freezing (Stahli et al., 1996). Water movement in frozen soils becomes more complicated when the soil is not completely saturated. Then, water movement in the large air-filled pores plays a significant role. The air-filled pores permit water movement via vapor diffusion or rapid liquid water flow during transient conditions (Flerchinger et al., 2013). Therefore, water movement into frozen soils cannot only be explained by the liquid water domain, which is in contact with the solid particles, but also by the rapid water flow within the largest pores filled with air at the onset of infiltration. The macropores' size governs the flow of water in frozen soils. For soils with no cracks, infiltration capacity is significantly lowered by large amounts of ice in the soil (Thunholm et al., 1989). High ice content in the soil is caused by high pre-freezing water content in the soil or by refreezing infiltrated meltwater during winter (Andersland & Ladanyi, 1994). Infiltration rates in frozen soils range from 0.24 mm/h to 300 mm/h, and the high rates are

dominant in dry soils (Kane & Stein, 1983). In addition to water content, the actual distribution of ice and ice lenses in the soil profile governs the infiltration process. Upon freezing water is expelled from the aggregates to some of the macropores/cracks in the soil profile, and the remaining space within the cracks can still allow significant infiltration into the soil which can be maintained throughout the winter (Thunholm et al., 1989). When freeze-thaw cycles occur, ice in the soil can thaw and move to the cracks or if snowmelt water infiltrates into the soil, the infiltrated water may refreeze in the macropores and form ice blocks, thereby reducing infiltration capacity. Soil permeability is affected by various factors including the presence and depth of frost, and ice content in the soil which is related to heat and water transfer at the soil surface and in the soil profile. Soil freezing and thawing can change soil properties and structure. Changes in soil aggregate stability due to freezing alters soil structure and pore continuity which can alter infiltration capacity even after the soil has thawed (Flerchinger et al., 2013).

Several studies assessed the hydrologic performance of SUDS in a cold climate (e.g., Khan et al., 2012; LeFevre et al., 2009; Muthanna et al., 2008; Paus et al., 2016; Paus & BrasKerud, 2014; Roseen et al., 2009). The hydrologic efficiency of SUDS can be assessed using different metrics, e.g., peak flow reduction, lag time, and stormwater volume reduction, which can all be quite variable based on the design and event intensity (Davis et al., 2012; Kratky et al., 2017). A wide range of peak flow reduction values has been reported for bioretention cells in cold climates, from complete capture of runoff to almost no capture (Kratky et al., 2017). In a study by Roseen et al. (2009), six SUDS elements were tested, including bioretention cells, swales, and retention ponds; frost penetration was observed in all tested practices but did not affect the performance significantly. As such, the peak flow reduction achieved by surface and subsurface SUDS elements were similar. However, a slower percolation rate was observed and attributed to the presence of frost. Swales were the most affected by seasonal variations and it was recommended to oversize them. Another study by Géhéniau et al. (2015) assessed the hydrologic performance of bioretention cells in Quebec, Canada, and found that the system retained 35% of the total runoff during winter and 60% during summer. They also concluded that the hydraulic retention efficiency is highly reliant on the initial moisture content and the length of the dry period. Similar conclusions were reported by Muthanna et al. (2008) in Trondheim, Norway, where bioretention performance was assessed during winter. Muthanna et al. (2008) found that the peak flow reduction was reduced from 42% for the entire study period to 27% in winter. Also, in Trondheim, Norway, both the peak flow reduction and the total volume reduction achieved by a bioretention cell were significantly lower in April (13%) compared to August (26%) (Muthanna, Viklander, Gjesdahl, et al., 2007). In an Alpine region, Fach et al. (2011) investigated the performance of grass swales and found that the swale fulfilled its function properly despite the top layer being frozen for some time and the storage capacity of the swale was sufficient to store the precipitation until the conditions improved. They also found that when the temperature was below 0 °C, the hydraulic conductivity was reduced when the initial moisture content was high. The system's flow attenuation or volume reduction capacity is, however, dependent on the incoming flow rate. For instance, Khan et al. (2012) found that bioretention cells in Calgary, Canada, captured 100% of events less than 32 mm during winter, while 91% for larger events.

Despite the reported reduction in hydrologic efficiency of the different SUDS elements in cold climates, the consensus is that they remain functional during the freezing season. However, the planning, design, and operation of SUDS require several considerations for

optimal performance. It is pivotal to use soils with sufficient permeability to drain the system prior to freezing. Many studies in cold climates recommended the use of coarse soils with a sand content of > 90% and low fines content (silt and clay) of < 10% for the filter media (Blecken et al., 2010; Denich et al., 2013; Géhéniau et al., 2015; LeFevre et al., 2009; Muthanna, Viklander, Gjesdahl, et al., 2007; Muthanna et al., 2008) to avoid frost formation and prevent the high total suspended solids in snowmelt from blocking pore spaces. In a biofilter column study, Blecken et al. (2010) used a filter media consisting of an upper sand layer with 5% silt and 14% fine gravel and a lower layer with medium to fine sand, which they recommended over the typical sandy loam soils. Moghadas et al. (2016) tested two frozen soils in the laboratory, coarse soil and the other fine-textured, and arrived at the same conclusions. It is often recommended to use an efficient, gravel-based drainage layer and underdrains for SUDS in cold climates to enhance their performance and reduce the risk of freezing (LeFevre et al., 2009; Muthanna et al., 2008; Roseen et al., 2009). The choice of coarse material for filtering media in SUDS might help mitigate frost formation and maintain permeability during winter, but that might come at the expense of water quality by reducing the contaminant removal efficiency (Kratky et al., 2017). Another factor that might compromise the water quality performance of SUDS in cold climates is freeze-thaw cycles. Despite the perceived benefits of macropores and preferential flow paths to enhance infiltration capacity, excessive soil deformation, large cracks, and changes in structure due to frequent freeze-thaw cycles, a characteristic of cold maritime regions, might lead to bypass flows and lower pollutant removal performance. Plants and mulch layer play an important role in improving both the hydrological and water treatment benefits of SUDS (Muthanna et al., 2007). Vegetation also increases the near-surface soil porosity, strengthens the soil via the root system, reduces freeze-thaw impacts, and constitutes a tool to add foliage to the urban environment (Prince George's County, 1999).

2.5 SUDS in Iceland

In the past two decades, the awareness of SUDS has gradually increased in Iceland. A pivotal moment was when the municipality of Garðabær, in the Capital Region of Iceland, planned a new neighborhood integrated with SUDS to protect the water level and quality in the shallow 13-ha lake at the bottom of the catchment. Planning documents stipulate local landowners to infiltrate water on-site. Only excess surface runoff infiltrates into the green surfaces and then is separately conveyed via underdrains discharging into a network of grass swales that leads towards the lake. Urriðaholt became the first Building Research Establishment's Environmental Assessment (BREEAM) certified neighborhood in Iceland.

Besides the large conveyance grass swales, a diverse set of SUDS components were implemented in Urriðaholt (Figure 2.2): roadside grass swales, permeable pavements, rain gardens, and green roofs to deal with stormwater runoff locally. Sited on a hill (88 m a.s.l), special precautions had to be made to slow down runoff velocity. For example, the conveyance grass swales were undulating with steps to reduce flow speed.

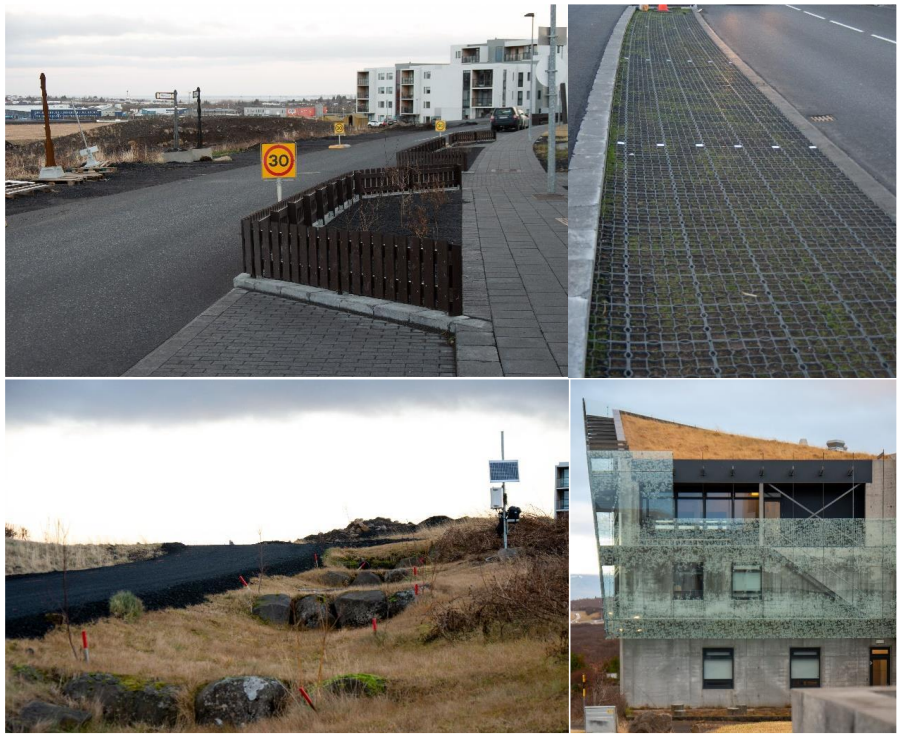

Figure 2.2 Examples of the different SUDS components in Urriðaholt (Johanna Sörensen, 2019). Rain garden (top left), permeable pavement (top right), grass swale (bottom left), and green roof (bottom right).

Several research studies on SUDS performance in Iceland have been conducted in the past decade. Vollertsen (2010) investigated the performance of wet ponds in improving water quality and heavy metals removal. Ágústsson (2015) studied the water retention potential of green roofs in relation to climatic conditions in Reykjavík. The tested green roofs achieved good water retention on an average of 17–56%, with grass turf showing much higher water retention capabilities than the sedum-moss turf. Similar findings were reported by Einarsdóttir (2018), assessing the seasonal variations in green roofs' hydrological performance but found that the overall runoff retention achieved by the green roofs was slightly higher, 47–61%.

The successful implementation of SUDS requires a regulatory and policy framework, including incorporating SUDS throughout the municipal planning process, clearly identifying collaborators' roles, and assigning responsibilities from planning and design to construction, operation, and maintenance stages (Pétursdóttir, 2016). But most importantly, a detailed description of the site needs to be available at the onset of any SUDS project, including the specific meteorological, hydrological, and geological data. The specific climatic conditions in Iceland, i.e., frequent freeze-thaw cycles and shallow, intermittent snow cover during winter, add more complexity to the design and sizing of SUDS. Especially, that Iceland is the largest volcanic area in Europe which contributes to the domination of volcanic ash on Icelandic soils (Andosols and Vitrisols), which are characterized by having high water holding capacity, prone to organic matter accumulation, and having high field capacity and wilting point, which means that soils are excessively wet

for extended periods making them susceptible to frost formation (Arnalds, 2015). Furthermore, the textural class of Andosols tends to contain high fine material as brown Andosols are usually dominated by silt loam and loam textures, while Vitrisols are often of sandy loam or loamy sand textures (Arnalds, 2004). Thus, special considerations and care must be taken when implementing SUDS in Iceland, adding to the need for more comprehensive studies on their functionality. In 2018, the University of Iceland collectively launched a SUDS research center in Urriðaholt in collaboration with the municipality of Garðabær, Urriðaholt ehf., and the Icelandic Meteorological Office (IMO) (University of Iceland, 2018). The goal of the center was to learn from the early implementation of SUDS in Iceland in order to aid future adoption.

3 Study area

Iceland is located in the North Atlantic between the latitudes 63°23´N and 66°32´N and longitudes 13°30´W and 24°32´W. Because of its proximity to the arctic circle, the solar altitude is small, resulting in a substantial difference between summer and winter day length (Figure 3.1; inset map). Several factors influence the weather of Iceland, and because of its latitude, it receives considerably low total radiation, and heat transfer is carried out from oceanic and atmospheric circulations (Einarsson, 1984). Cyclones often intensify in winter and pass over the island causing rapid pressure variations bringing precipitation and strong winds. The maritime city of Reykjavík is the capital of Iceland, located by the coastline in the southwestern corner of Iceland (Figure 3.1). The local climate undergoes large decadal variations associated with the location of storm tracks across the North Atlantic Ocean, the position of the sea ice margin to the north of the country, and the phase of the North Atlantic Oscillation (Andradóttir et al., 2021). The weather is characterized by cool summers and mild winters, frequent changes in meteorological conditions and relatively high precipitation, and shallow intermittent snow cover, resulting in a high frequency of freeze-thaw cycles, rain-on-snow events, and midwinter snowmelt. Table 3.1 summarizes the annual maximum, minimum, and average weather conditions in Reykjavík.

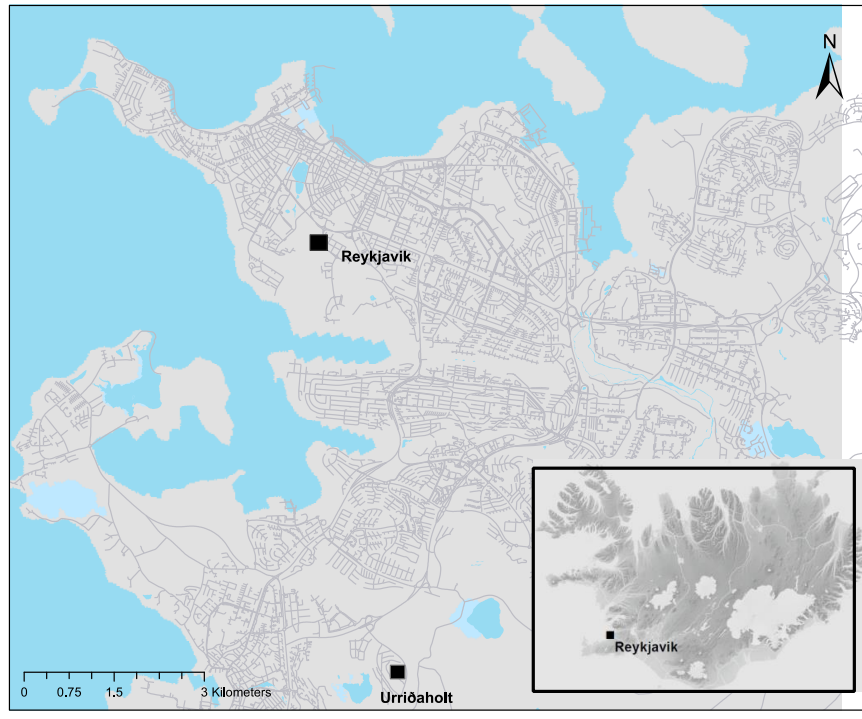

Figure 3.1 Greater capital area of Reykjavík, Iceland. The two study sites are marked as squares, and water bodies are in light blue.

To study the hydrologic performance of sustainable drainage systems (SUDS) in a cold maritime climate, the residential neighborhood Urriðaholt in Garðabær, Iceland, on the outskirts of Reykjavík (64°4'18.46" N, 21°54'37.11" W) was chosen as a study site (**Paper I**, **II**, and **III**). Downstream of the built environment, open pervious areas surround the grassed swales system, which has different vegetation covers, e.g., Nootka lupine (*Lupinus nootkatensis*), dwarf shrub heath, as well as barren lands. For soil dynamics modeling, the long-term assessment of soil frost formation, changes and trends in soil temperature, and winter urban flood risks, the city of Reykjavík was chosen as a study site, where the longest record of meteorological observations exists (**Paper III).** The weather station No. 1 is situated in an open grassed area (50 m a.s.l) next to the Icelandic Meteorological Office (IMO) headquarters in Bústaðavegur 7, Reykjavík (64°07'39.1" N, 21°54'08.5" W). The weather station is located 2.5 km from the ocean and approximately 3 km from Reykjavík city center. The city of Reykjavík has an area of 273 km^2, is densely populated (approx. 135,000 inhabitants), and the drainage system is dominated by combined sewers.

Table 3.1 Summary of the annual meteorological observations in Reykjavík (1949–2018).

Meteorological variable	**Unit**	**Max.**	**Min.**	**Avg.**	**Std. Dev.**
Air temperature	°C	6.1	2.9	4.8	0.7
Relative humidity	%	82	75	78	1.6
Air pressure	hPa	1011	1001	1006	2.3
Wind speed	$m\ s^{-1}$	7.4	3.6	5.5	1.0
Precipitation	mm	1125	560.3	825.8	140.7
Rainfall[1]	mm	891.2	378.4	615.8	111.1
Snowfall[1]	mm	396	63.7	210	70
Snow depth[2]	cm	51	7.0	24	9.2

Note: [1] Rainfall and snowfall data are corrected from total daily precipitation depth. [2] Snow depth statistics are derived from the annual maximum snow depth in cm.

4 Methods

This Chapter provides an overview of the methods used. More details are available in the appended papers.

4.1 Continuous monitoring

4.1.1 Soil moisture content and temperature

A grass swale was chosen in the study site (Urriðaholt) to be instrumented with five water content reflectometers (type CS650 Campbell Scientific Inc.). Each sensor has two parallel 30-cm long rods. The sensors were placed horizontally in the swale at 10-cm intervals at 5, 15, 25, 35, and 45 cm depths from the soil surface below the turf layer (Figure 4.1). Readings were logged by a multiplexer data logger (Campbell Scientific Inc.) every 1 minute. Prior to the field installation, a soil-specific laboratory calibration was conducted. Soil samples were extracted from the swale and were left to air dry for a week (Caldwell et al., 2018). Then, the soil was repacked in layers into PVC cylinders. The probes were inserted into the soil, and they were wetted gradually by adding water to the samples (Figure 4.2). The sensor's permittivity output was recorded after it stabilized, and the concurrent volumetric water content was measured. The square root of permittivity and the measured water content were plotted, and a linear calibration equation was derived.

Figure 4.1 Pictures of the installation of soil water content and temperature sensors in the swale (November 6th, 2018).

Figure 4.2 Calibration of water content reflectometers in the laboratory of the University of Iceland.

On September 10, 2019, three water content reflectometers were installed in a lupine field adjacent to the study swale in **Paper I** (Figure 4.3). The sensors were installed at 5, 15, and 25 cm depths from the surface to compare the swale with the dense vegetation cover with an undisturbed terrain with a less dense vegetation cover in terms of water movement, temperature changes, and frost formation. Laboratory calibration was not possible; instead, the probes were calibrated in the field. The probes were driven into the soil, and the permittivity output was recorded. A soil sample was collected from the same spot and taken back to the laboratory to measure the volumetric water content. Then the soil was deliberately wetted, and the same procedure was repeated. Finally, a calibration equation was derived.

Figure 4.3 Water content reflectometers installed at the lupine field next to the swale.

4.1.2 Meteorological data

Ten-minute weather data (e.g., air temperature, precipitation, and relative humidity) were collected from a weather station installed in February 2019 and operated by the Icelandic Meteorological Office (IMO) on behalf of the Garðabær municipality (Figure 4.4). The station is located approx. 100 m downstream from the location of the measurements. Hourly temperature, snow depth, precipitation, and radiation data were also acquired from the Reykjavik No. 1 station located on a hilltop 6 km away from the study site.

Figure 4.4 A picture of the chosen study swale in Urriðaholt in the foreground and the weather station in Urriðaholt in the background.

4.2 Field experiments in Urriðaholt

4.2.1 Synthetic runoff experiments in a grass swale

This work aimed to investigate the impact of cold climate on the hydrologic efficiency and ability of SUDS to infiltrate stormwater and reduce runoff peaks and volumes (**Paper I**). To that end, synthetic runoff experiments were conducted in a 5.8 m long, trapezoidal swale section in Urriðaholt with an average bed width of 2 m and a longitudinal slope of 3.3%. The side slopes ranged between 10 and 22% (Figure 4.5).

A portable water delivery system, consisting of a 1 m^3 water tank filled with water from a nearby fire hydrant, was designated to feed the swale with simulated runoff inflows ranging between 0.2 l/s to 4.2 l/s. The inflow and outflow rates were measured using V-notch weirs and level transducers for the duration of the experiment (20–30 minutes). Runoff peak reduction, total volume reduction, lag time, areal efficiency (area of the flow relative to the surface area of the swale), and drainage capacity (the reduction in liquid water content after 24 hours of the simulated event) were derived from the inflow and outflow hydrographs. A total of 63 runoff simulations were conducted from March 2019 to August 2020 to capture winter, the transitional period of thawing during spring, and warm conditions. The assessment was based on classifying the surface conditions as frost (F), snow on frost (SoF),

snow (S), neutral conditions (N) of nonfrozen and no snow conditions in winter, and warm conditions during summer (W). An example of the experiments conducted in different seasons and surface conditions is shown in Figure 4.6.

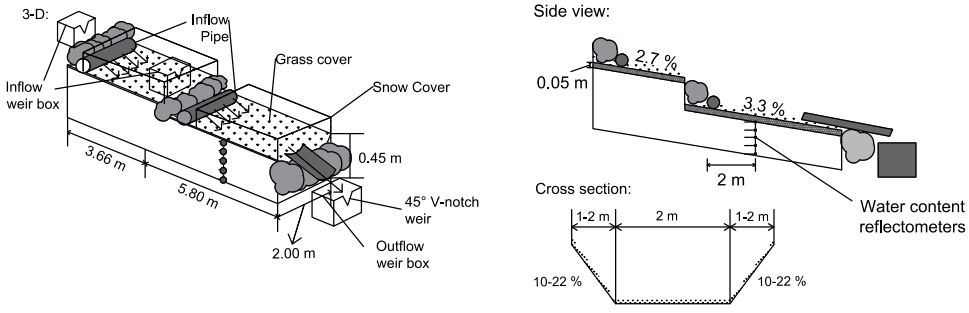

*Figure 4.5 Schematic of the experimental setup, the swale dimensions and slopes, the location of the inflow and outflow measurements, water content and soil temperature sensors, and the water delivery system (**Paper I**).*

Figure 4.6 Synthetic runoff experiments conducted in different seasons, climatic and surface conditions in Urriðaholt, Iceland.

4.2.2 Single-ring infiltration measurements

Paper II investigated the changes in infiltration capacity between summer and winter in three different surface covers in the Urriðaholt study site, including a grass swale subject to the same hydro-climatological conditions. The approach taken in **Paper II** was to use single-ring infiltrometers to assess the seasonal evolution of infiltration capacity and the spatial variations at the top 20 cm of soil that is prone to frost formation, frost heave, deformation, and frequent freeze-thaw cycles in a cold maritime climate. A total of 28 measurement campaigns have been conducted from 2018 to 2020 in a grass swale designed to infiltrate water and two adjacent undisturbed permeable terrains: an area vegetated with Nootka lupine (*Lupinus nootkatensis*) introduced for restoring deteriorated ecosystems, a barren area, and dwarf shrub heath. Each surface cover has a different plant density and root characteristics and constitutes large areas in public or undeveloped urban areas. A particular focus was on relating infiltration capacity to surface frost and structural deformations as well as soil moisture content and drainage.

A total of 8 infiltration rings were installed at the study site in the summer of 2018. The infiltrometers were placed close to one another, with easy access to water supply along a walking path (Figure 4.7). The rings were 22.5 cm in diameter and 40 cm in height. The infiltrometers were gently hammered to establish good contact with the soil and minimize disturbances down to 15–17 cm depths perpendicular to the slope of the soil surface. Four infiltration rings were added in the grass swale in the summer of 2019 in order to account for the spatial variability. A mesh was placed within the infiltration ring to ensure that the water poured into the ring uniformly spread over the surface. An initial volume of water was added instantly at time $t = 0$ until the water level within the ring stabilized, and using a stopwatch, the recording of time was started. The water level or ponded depth was maintained at approximately 5 cm by adding water continuously using graduated cylinders with volumes of 1 and 2 L. The added volume was recorded every 5 min and timed using a timer. The experiment was discontinued when the added volume remained constant for three consecutive iterations, which occurred after approximately 45–60 min during summer and 30–45 min during winter. The measurements were conducted once every 3–4 weeks to minimize the disturbance of the study site prior to each measurement. Before each infiltration measurement, the surface, water, and air temperatures were measured using a handheld thermometer. Pictures were taken of the terrain surface within the rings. The presence of surface frost was noted by visually observing the presence of ice lenses. Soil structural changes and frost heave were evaluated by measuring the distance between the pre-set soil surface elevation and the surface elevation on the measurement day using a hand-held measuring tape.

Figure 4.7 Single-ring infiltrometers at the grass swale (top left), lupine field (top right), barren area (bottom left), and heath field (bottom right).

4.2.3 Support measurements (snow, frost, and radiation)

In winter, snow cover depth and density were measured in the field regularly and prior to the experimental runs. On average, three snow cores were extracted from each test site using a cylinder (Figure 4.8). Snow temperature at the surface and the bottom of the snowpack was measured using a handheld thermometer. The overall accuracy of the snow depth measurements was determined to be 3–16%, and for the snow density, 1–13%. The presence of frost was also investigated based on surface hardness by inserting a blade into the soil and visually noting the presence of ice crystals in the uppermost 5 cm (Orradottir et al., 2008).

For one winter (Decemeber 2019–April 2020), a pyranometer was installed at 2 m at the weather station in Urriðaholt to measure the incoming and outgoing radiation at the site (Figure 4.9). The instrument was borrowed from the National Power Company in Iceland (Landsvirkjun) and operated by the IMO. The radiation measurements from the Urriðaholt study site were comparable to the data collected at the main station Reykjavík No.1 for in- and outgoing radiation (Figure 4.10). The longwave radiation in the Reykjavík station deviated largely from the measurements in Urriðaholt as a malfunction of the instrument was reported by the IMO. This comparison supports the use of the incoming solar radiation from the Reykjavík station for Urriðaholt for model runs (**Paper III**).

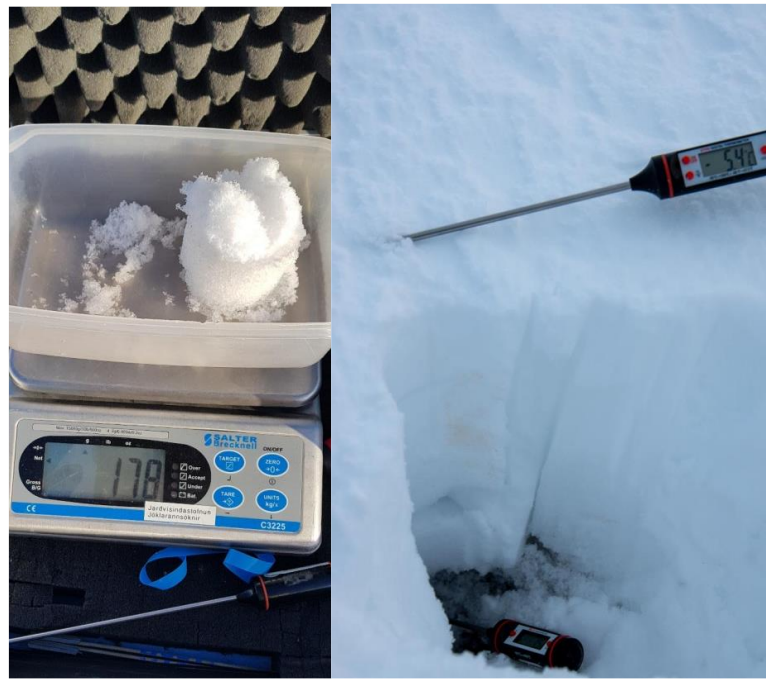

Figure 4.8 Example of the snow depth and density measurements in the study site Urriðaholt (13.01.2020).

Figure 4.9 A picture of the pyranometer installed at the Urriðaholt weather station during the winter of 2019/2020.

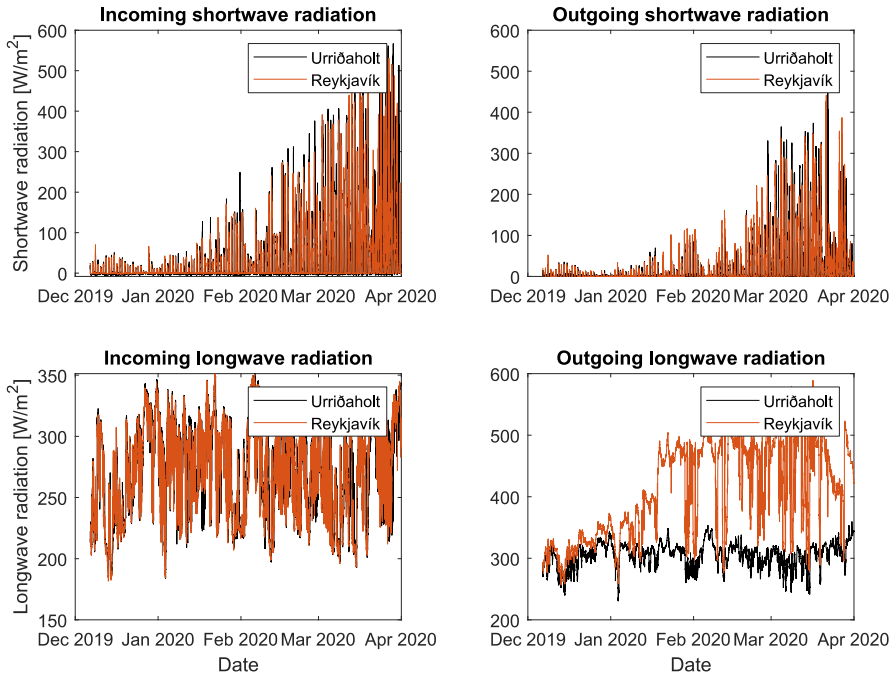

Figure 4.10 Comparison between the incoming and outgoing shortwave and longwave radiation observations at the Urriðaholt station and Reykjavík station.

A camera was installed at the Urriðaholt station directed upwards, viewing the open area downstream of the catchment, where the measurements took place. Another camera was set up at the top of the hill at the study site to monitor the snow cover conditions during the snow season (Figure 4.11). This gave an indication of the locations where melt started, which mostly began at the roofs of the buildings.

Figure 4.11 Snapshots of the camera view in Urriðaholt at the weather station (left) and the top of the hill (right).

4.3 Analyses and modeling

4.3.1 Statistical analyses

In **Paper I**, the significant difference between the hydrological performance metrics (i.e., peak flow reduction, relative infiltrated volume, lag time, areal efficiency, and drainage capacity) was determined using the one-way analysis of variance (ANOVA) and the Student's t-test. The assessment was based on the surface and soil conditions, i.e., the seasonal variations in the grass swale's performance. The drivers for the hydrological performance metrics in **Paper I** were quantified with a two-step linear regression analysis. In the first step, the correlation of performance with each external driver (i.e., inflow rate, antecedent degree of saturation, surface and soil temperature, and snow depth) was considered. In the second step, a multiple linear regression analysis was conducted first with the primary drivers. Single and multiple linear regression analyses were performed for the performance metrics using indicators such as inflow rate, surface and soil temperature, degree of saturation, and snow depth by adding one indicator at a time to each model. For each performance indicator, the model with the best coefficient of determination was chosen. Parameters that did not enhance the model performance were eliminated from the analysis.

Similarly, in **Paper II**, the statistical differences between the measurement locations, i.e., grass swale, lupine, and barren, were determined to assess the spatial variations in infiltration capacity between the test points. The differences between terrains were analyzed by performing multiple comparisons using the student's t test to look for significant differences. Data used for analysis were transformed when required to account for the assumptions of normality. The normality of the data was tested using the Kolmogorov-Smirnov test (K-S) and Shapiro-Wilk test. The normality is accepted at a p-value > 0.05. The spatial variation within the swale was assessed by comparing the arithmetic mean of the infiltration rates from each of the six infiltrometers.

4.3.2 Long-term indicators and trends

In Paper II, the seasonal number of air freeze-thaw cycles and the freezing and thawing indices were calculated to assess the intensity of these air temperature variations using the degree-day method (Andersland & Ladanyi, 1994). The air freezing degree days (FDD) were estimated as the sum of the daily average temperatures below zero ($T_{avg} < 0$ °C) during winter (November to March), and the thawing degree days (TDD) were estimated as the sum of the daily average temperatures above freezing ($T_{avg} > 0$ °C). A soil frost cycle was derived based on the average daily temperature at 5 cm depth so that if the soil temperature dropped below zero for one day, it would be counted as a cycle. Maximum frost penetration was derived as the maximum soil depth at which the average daily temperature was below zero. A rain-on-snow (RoS) event was defined as a day with precipitation concurrent with a reduction in snow depth. A snow cycle was defined as 24 hours with a snow depth of > 1 cm measured at 9 AM.

In **Paper III**, to investigate the changes in frost formation behavior, frost timing, and coincidence with surface runoff due to climate change, trends were assessed using the Mann-Kendall test (Kendall, 1948; Mann, 1945), and the significance of the slope using the Theil-Sen method (Sen, 1968; Theil, 1950). These methods were chosen for their simplicity

because they are non-parametric, i.e., the data does not need to conform with any particular distribution, allows for missing data, and can be used for small datasets.

4.3.3 Soil temperature and frost modeling

The SHAW model is a physically-based, one-dimensional, coupled heat and water transfer model. To calibrate and test the model, hourly weather and soil temperature data were compiled from the high-resolution 10-minute data collected from the residential neighborhood Urriðaholt. Then, calibrated parameters of the model for Urriðaholt were used as a basis for simulating soil temperature and frost in Reykjavík from 2007 to 2018, and recalibration was done manually. Afterward, the model was run with daily timesteps using the long-term weather observations from 1949 to 2018 (i.e., air temperature, relative humidity, and wind speed) and the simulated incoming solar radiation due to the lack of measurements from 1949 to 2007.

4.3.4 Bivariate frequency analysis using copulas

The copula method was used to estimate the joint probability of two hydrological variables occurring simultaneously and derive the joint return periods for winter events. The annual maximum rainfall, snowmelt, and RoS were derived from the observed daily data in Reykjavík. The annual maximum frost depth was derived from the daily simulated frost depth using the SHAW model.

The approach to understanding the co-action of hydrological inputs and soil frost was to estimate the joint probability of occurrence of two winter hydrological events. The combined daily precipitation and snow depth measurements at 9 A.M., annual maximum rainfall, snowmelt, and rain-on-snow in the presence of soil frost were calculated. Rainfall was distinguished from snowfall based on a temperature threshold, T_{RH} (°C), that incorporated relative humidity, RH (%), following the method presented by Feiccabrino et al. (2015). With this definition, all precipitation within a given day was classified either as dry or wet, when in some instances, it can be in both forms. Snowmelt was defined based on the reduction of snow depth, ΔSD, converted to snow water equivalents assuming a snow density, ρ_s, of 200 kg/m^3, in relation to a water density, ρ_w, of 1000 kg/m^3. If precipitation was recorded together with a reduction in snow depth, it was assumed to be rainfall. The magnitude of RoS was taken as the sum of the rain and liquid snowmelt volume (mm) estimated from measured snow depth (in cm) as presented in Andradóttir et al. (2021).

Each of the annual daily maximum datasets was fitted to a distribution using the maximum likelihood method. The goodness of fit was assessed using the Kolmogorov-Smirnov, Cramer-von Mises, and Anderson-Darling tests. Then, the distribution with the lowest Akaike (AIC) and Bayesian Information Criteria (BIC) was chosen. As such, maximum snowmelt during frost was fitted to the lognormal distribution, maximum frost during snowmelt to the Weibull distribution, maximum rainfall during frost to the lognormal distribution, maximum frost during rainfall was found to fit the Weibull distribution, maximum RoS during frost, and maximum frost during RoS were both fitted to the Weibull distribution. The return periods were then derived for each of the co-acting hydrological variables (Chow et al., 1988).

The copula method was used to estimate the joint distribution C ($F_x(x)$, $F_y(y)$) = C (u_1, u_2) of two dependent variables based on their marginal distributions of the annual maximum values fitted to a theoretical distribution $F_x(x) = u_1$ and $F_y(y) = u_2$ (Chen, 2019; Lian et al., 2013; Zellou & Rahali, 2019). Due to their simplicity, the four Archimedean copulas most widely used for hydrological analyses (i.e., Clayton, Gumbel, Joe, and Frank) were tested (Nelsen, 2007). The three pairs of winter flood-inducing hydrological variables (i.e., maximum snowmelt during frost, rainfall during frost, and RoS during frost) were then fitted to one of the bivariate Archimedean copulas using the maximum likelihood method. The bivariate copula family that best fits the pair was chosen based on the highest log-likelihood and lowest AIC and BIC (Zellou & Rahali, 2019).

5 Results and discussion

This chapter briefly overviews the main findings of the papers discussed together. More is found in the appended publications.

5.1 Hydrologic performance of grass swales in a cold climate

The synthetic runoff experiments showed a significant reduction in the hydrologic performance of the grass swale during winter (**Paper I**). The reduction in infiltration capacity in the grass swale was mainly attributed to shallow frost within the top 5 cm soil horizon, consistent with previous findings (e.g., Khan et al., 2012; LeFevre et al., 2009; Muthanna et al., 2008; Paus et al., 2016; Roseen et al., 2009). Soil frost was identified as the key indicator for reduced hydrologic performance, as there was a drop in peak flow reduction and volume reduction during frost and snow on frost conditions. Similarly, it negatively affected the ability of the soil to drain within 24 hours after the end of an event (i.e., Drainage Capacity). The areal efficiency of the swale, determined by the wet area at the surface, was most affected by the snow cover. A large variance was noted in the experimental runs during snow only conditions suggesting that not only snow presence but also snow characteristics such as depth and density were influential factors. The effect of frost on the grass swale's infiltration performance was corroborated with single-ring infiltration measurements (**Paper II**). Infiltration decreased by approximately one-third during wintertime, from an average of 98 cm/h in summer and fall to 63 cm/h in winter. Two out of the six test locations in the swale were significantly higher than the rest, indicating large variations in infiltration capacity. The two test locations at the lupine site also differed significantly (p-value < 0.05) but were within the same range. The two barren test locations were not statistically different from each other.

The performance fluctuated synoptically due to intermittent frost formation throughout winter (**Paper I** & **II**). Three different soil conditions were identified during winter; frozen soil, during which the peak flow reduction and volume reduction were very limited; partially frozen soil, allowing for moderate but significantly lower flow attenuation; and neutral soil conditions (non-frozen) (**Paper I**). Regardless of frost presence, infiltration occurred in all experimental runs, which was attributed to macropore flow maintained by the vegetation cover of the swale and the fact that the soil was relatively coarse and well-drained, minimizing the impacts of sub-freezing temperatures. Similar findings were reported by Khan et al., 2012 and Paus et al., 2016 for bioretention cells in Canada and Norway, where it was found that, during winter, bioretention cells achieved high peak flow reduction, i.e., up to 92% and between 55 and 100%, respectively. Paus et al. (2016) concluded that a soil with a hydraulic conductivity of at least 10 cm/h was required for the bioretention cells to function properly during the freezing season. The infiltration capacity in the grass swale during winter was considerably higher than this threshold (avg. 63 ± 53 cm/h: Paper **II**). In **Paper I**, it was found that the average peak flow reduction during winter was only 13%, which can be explained by the short residence time and high velocity in the grass swale,

which functions as a conveyance measure rather than a retention measure in this site. The hydraulic head of water ponding on the surface in retention-based systems increases the infiltration capacity compared with water flowing over a permeable surface (Davis et al., 2012). This was also found in **Paper II** when constant head infiltration measurements were conducted in the grass swale, which explains the very high infiltration rate measured compared with findings in **Paper I**. This explanation was also supported by the findings from Roseen et al. (2009), as they found that between various SUDS configurations, grass swales were the most affected during winter for the same reason. The hydraulic loading used in the synthetic runoff experiments was relatively high for the surface area of the swale. While, for example, Khan et al. (2012) used inflow rates of 25 cm/h, in **Paper I**, hydraulic loadings as high as 131 cm/h were used. The vegetation type in the different contrasting systems might also explain the low peak flow reduction during winter in the swale compared to, e.g., bioretention cells in the studies mentioned above. For instance, the vegetation in the bioretention cell tested by Khan et al. (2012) was comprised of eight trees of various species, which indicates the presence of a large and interconnected root system that enhances the near-surface porosity, especially when water is ponding on the surface for extended periods. Bioretention cells often include a mulch layer and a deeper filtering media compared to grass swales (Barrett, 2008; Woods Ballard et al., 2015).

In comparison, the filtering media in the studied grass swale was limited to 45 to 50 cm, while it was 120 cm and 75 cm for Khan et al. (2012) and Paus et al. (2016), respectively. Additionally, in **Paper I** and **II**, the grass swales tested did not have specific drainage layers or underdrains, which is considered common practice for bioretention systems (Prince George's County, 1999). In cold climatic conditions in general and coastal cold regions in specifically, it is recommended to use well-drained soils to avoid the adverse effects of repeated frost formation (LeFevre et al., 2009; Muthanna et al., 2008).

5.2 Role of vegetation and engineered soil

The vegetation cover and the underlying engineered soil in the grass swales studied in **Paper I** and **II** played an important role in the hydrologic performance during winter. In **Paper I**, infiltration was observed during all measurement campaigns at the lower layers (> 5 cm) despite the frozen top layer of soil, which showed no changes in water content during the synthetic events conducted when the top layer was frozen. This was attributed to the macropores provided by the roots system and the good hydraulic conductivity of the soil (sandy loam) in the man-made grass swale. The vegetation was also highly influential to infiltration, especially during winter (**Paper II**). The grass swale had the highest infiltration rate in winter compared to the less vegetated and non-vegetated terrains in the urban environment (**Paper II**). The intertwined root system provided resistance to frost heave and helped maintain the soil porosity. Soil composition was also shown to be of high importance, as the soil drainage capacity was much higher in the grass swale during winter compared to the lupine field (14% per 24 hours vs. 4% per 24 hours), which was attributed to the fact that the lupine field had a considerably higher fines content (silt and clay) compared to the man-made grass swale. The near-surface soil porosity in the swale was also significantly higher (52% vs. 39%), which indicates a larger voids volume available for water infiltration aided by the dense roots of the grass. The lowest infiltration capacity was measured in the barren area, which lacked vegetation. In the barren terrain, concrete frost was observed during the

second winter of the measurements, and large cracks were observed at the surface after the thaw period in spring.

Icelandic Andosols often have a very low bulk density in the range of 0.3–0.8 g/cm^3 and are characterized by having high hydraulic conductivity, while the Vitrisols found in Iceland can have a higher bulk density up to 1.2 g/cm^3 (Óskarsson et al., 2004). Orradottir et al. (2008) found that the infiltration capacity of Andosols can reach as high as 37 cm/h during summer. However, coarse-grained tephra layers may exist in the soil, hindering its infiltration capacity (Arnalds, 2008). That said, the high water-holding capacity of Andosols and the often-thin fluctuating snow cover render them susceptible to frost formation (Kane & Stein, 1983; Orradottir et al., 2008). **Paper II** concluded that the man-made grass swales with sandy loam soils were more resilient to structural changes than the undisturbed soils. The soil in the lupine field contained higher fines content than the grass swale, which might have also led to severe freezing and structural changes. Fine-textured soils are more susceptible to frost formation (Shanley & Chalmers, 1999).

Such limitations must, therefore, be taken into account when planning SUDS. For soil and water conservation, restoration of deteriorated ecosystems, and combating deforestation, ecosystem engineers sometimes intentionally introduce new plant communities (Vetter et al., 2018). One species that was introduced to Iceland in the 1940s is the Nootka lupine (*Lupinus nootkatensis*), which turned out to become a problematic, invasive species. Lupine fixes atmospheric nitrogen, which changes the nitrogen cycle in the soil. Lupine builds up nutrients, organic matter and enhances the water storage capacity of soils, which was sought to offset land degradation and desertification in Iceland. This can potentially subject surfaces with lupine vegetation to frost formation and decreased winter infiltration, which was observed during the infiltration measurement campaigns in **Paper II**. Bare grounds within the built environment also tend to be more affected by human activity and increased compaction than vegetated terrains due to the lack of a root system that can sustain porosity (Barbosa et al., 2020). Leaving robust vegetated landscapes undisturbed with native plants might be a cost-effective solution for peak flow and volume reduction. Therefore, stormwater control measures that provide SUDS in cold maritime regions should aim to minimize non-vegetated or impermeable areas and promote the integration of green surfaces with native species for flood mitigation.

5.3 Effects of frequent freeze-thaw cycles

In **Paper II**, the influence of freeze-thaw cycles (FTCs) was shown to be detrimental to the hydrologic performance, especially during the winter with more cyclical conditions typical for a cold maritime climate. The two winters during which the infiltration measurements took place were distinctively different. The winter of 2018/2019 was dominated by a long-standing snow cycle lasting for 32 consecutive days with a maximum snow depth of 31 cm. In comparison, the following winter of 2019/2020, which was representative of a typical winter in Iceland, had a total of 13 snow cycles, 21 freeze-thaw cycles, and a maximum snow depth of only 12 cm. During the first winter, the infiltration capacity was not impeded in the grass swale compared to summer. In fact, it slightly increased. In contrast, the less vegetated area with lupine and the barren field became less infiltrative during winter, with a reduction to almost half of that during summer. The less and non-vegetated areas were susceptible to severe soil deformation resulting from freeze-thaw cycles. In the second winter, frost heave

was observed in the lupine field after 3 FTCs, concurrently with a 58% reduction in infiltration capacity. The soil structure collapsed in one of the lupine test locations (L1) after 5 FTCs, forming large cracks resulting in very rapid macropore flow that bypassed the soil matrix. The soil also collapsed in the other lupine test location (L2) after 7 FTCs during the second winter, and a similarly high bypass flow rate was measured. In a study by Eigenbrod (2011), similar behavior was observed with an increase in infiltration following freeze-thaw cycles that led to the soil becoming fissured. Eigenbrod (2011) also found that infiltration increases with the increase in freeze-thaw cycles. Meanwhile, the infiltration capacity in the barren area dropped by 34% following only one freezing cycle, developing concrete frost after that for the rest of winter 2019/2020. However, the grass swale was neither affected by structural deformation nor infiltration-inhibiting frost despite a slight reduction in infiltration rates. To assess the impact of freeze-thaw cycles on the infiltration capacity, a proxy, the number of snow cycles, was used to represent the fluctuations at both the soil surface and soil, and the infiltration capacity was found to be inversely related to the number of snow cycles. This suggests that the cyclical conditions during winter negatively affected infiltration. Such behavior was consistent for both studied winters and across all test locations.

One of the hurdles in implementing SUDS in cold maritime climate lies in the fact that, unlike cold inland regions with an intact snow cover for most of the winter which insulates the ground until late in the season, the soil is excessively wet and subjected to repeated freezing. In **Paper I**, it was observed that the most severe freezing events occurred after either real or simulated storm events. This has resulted in a lower near-surface effective soil porosity leading to a reduction in the available subsurface storage, specifically at the top frozen 5 cm soil horizon. The wetting of the soil, which in some cases was combined with the removal of the snow cover, rendered the soil more susceptible to temperature fluctuations, as evidenced in the sharp reduction in soil temperature following these events. Results in **Paper II** also show that the repeated midwinter melt and RoS events, assessed by relating the number of snow cycles to the infiltration capacity in all tested terrains, were detrimental to the hydrologic efficiency. Those cyclical conditions experienced in cold maritime regions are also expected to increase and become more widespread due to climate change, making them more relevant to urban drainage and flood risk assessment (**Paper III**).

Soil freezing and thawing can lead to significant volume change up to 30% (Eigenbrod, 2011), even after one freezing cycle. In **Paper II**, frost heave was not quantified, but an observable rise of the soil surface at the lupine field was seen resulting from the expansion of the ice lenses occupying the pore spaces and consequently leading to structural changes and the formation of large cracks when the soil thaws. In the barren test area, frost heave was visible after only one FTC, and after 3 FTCs, the infiltration capacity plunged to only 4 mm/h. Compared with the grass swale, the sparsely vegetated field (i.e., lupine) had a higher degree of saturation throughout the study period, especially during winter. Kane & Stein (1983) concluded that the formation of infiltration-inhibiting concrete frost was favored by high soil moisture content at the onset of freezing. Another effect of freeze-thaw cycles is the formation of cracks. While macropores might be beneficial in alleviating urban flood risks by increasing infiltration during winter, flow through large preferential paths reduces the pollutant removal efficiency associated with water movement through porous media. This contradicts the integral function of SUDS, which ultimately aim to preserve the integrity of receiving waters. This effect can be particularly dangerous in cold regions, where snow that accumulates more pollutants than rainfall-induced runoff is often cleared from

streets and deposited in roadside swales (Andradottir & Vollertsen, 2015; Gavrić et al., 2019). Bypass flow through cracks and fissures has been observed to severely limit solute removal within the top 1 m of soils (Flury et al., 1994). The rapid water seepage observed following the severe structural deformation in the lupine and barren suggests a potential water quality risk. Structural changes due to freezing and thawing resulted in a semi-permanent decrease in the infiltration capacity of 29% and 26%, in the lupine and barren, respectively, between summer 2019 and 2020, while the grass swale increased infiltration by 50%.

5.4 Impacts of climate change on frost formation and urban flood risk

Soil frost was identified as the most crucial parameter that affected the hydrological performance and the infiltration capacity of SUDS during wintertime (**Paper I** & **II**). The successful implementation of SUDS in cold maritime climates requires a better understanding of the frost formation processes and timing as it influences their use as a flood mitigation measure in urban areas. With a changing climate, soil temperature, water movement in the soil, and frost are predicted to be altered. Therefore, it is essential to quantify this change to accurately assess the long-term feasibility of SUDS and urban flood risk. In **Paper III**, the Simultaneous Heat and Water (SHAW) model was used to simulate soil temperature, water content, and frost at the Urriðaholt study site (where the soil was monitored at different depths during 2018–2022) and in Reykjavík (soil measurements available from 2007 to 2018). The aim was to investigate the trends in soil temperature and frost in the last 70 years using available meteorological records from 1949 as inputs. The SHAW model in **Paper III** predicted soil temperature with high accuracy in the Urriðaholt study site at all soil depths where soil physical properties are known, i.e., at 5, 15, 25, 35, and 45 cm (R^2 = 0.97–0.99 for the calibration and validation periods). Good agreement between measured and simulated soil temperature was achieved during winter. However, the R^2 values were lower in winter compared to the entire year (0.71–0.83 for winter 2018/2019, 0.91–0.93 for winter 2019/2020, 0.66–0.88 for winter 2020/2021, and 0.83–0.88 for winter 2021/2022). The model's overall performance was good and agreed with the observed values in terms of capturing the soil temperature variations, soil freezing and thawing behavior, and frost timing, especially at the top three layers of the soil that are of interest as they are most susceptible to frost and therefore influential to urban flooding. The observations of soil temperature in Reykjavík from 2007 to 2018 were used to calibrate the model. The modeled soil temperature for the station in Reykjavík agreed well with the observations (R^2 = 0.91–0.92). Table 5.1 summarizes the performance of metrics used to assess the model simulation results. In order to understand the long-term impacts of climate warming on soil temperature and frost formation, the soil temperature in the Reykjavík station was estimated from 1949 to 2018 at 10, 20, and 50 cm depths.

The maximum soil frost depth for the study period was 39 cm (Table 5.2) in 1949. Consistently, the lowest soil temperature at the surface (-3.7 °C) and 10 cm (-2.6 °C) was also simulated for the winter of 1949. The maximum number of days with soil frost in any given calendar year was 153 days, which was in 1951. Meanwhile, the minimum number of frost days was 26 days in 1987 and the shortest period of continuous frost lasted only four days in 1987. The average number of freeze-thaw cycles in a year is 3.65; the maximum was

eight cycles, occurring twice in 1965 and 1971. The trend analysis showed that, between the years 1949 and 2018, soil frost depth decreased significantly (p-value < 0.05). A similar trend was also observed in the total number of days with soil frost at 5 cm depth. In the last 70 years, soil frost has become less persistent, as the number of days with continuous soil frost decreased significantly (p-value < 0.05). This suggests that the instances of intermittent formation of soil frost have increased during winter. The increase in the frequency of intermittent frost and, therefore, freeze-thaw cycles can also be seen in the significant increase in the minimum asoil temperature at 10 cm depth in Reykjavík for the simulation period of 1949 to 2018.

*Table 5.1 The SHAW model performance of hourly soil temperature and water content in the grass swale in Urriðaholt 2018–2022 and soil temperature in Reykjavík 2007–2018 (**Paper III**).*

		Calibration		**Validation**	
Soil temperature		R^2	RMSE	R^2	RMSE
Reykjavík	All seasons	0.91–0.92	0.98–1.64	-	-
	Winter	0.30–0.94	0.82–2.53	-	-
Urriðaholt	All seasons	0.98–0.99	0.66–0.89	0.97–0.98	0.71–0.93
	Winter 1, 2	0.71–0.94	0.40–1.08	-	-
	Winter 3, 4	-	-	0.66–0.88	0.66–0.99
Volumetric water content					
Urriðaholt	All seasons	0.10–0.43	0.02–0.06	0.2–0.44	0.01–0.06

Notes: Winter 1, 2, 3, and 4 refer to the four winters between 2018 and 2022.

*Table 5.2 Summary of modeled long-term surface and subsurface winter conditions in Reykjavík from 1949–2018 (**Paper III**).*

Winter conditions	**Unit**	**Max.**	**Min.**	**Avg.**	**Std. Dev.**
T_{soil} at 10 cm	°C	17.5	-2.6	6.1	5.2
Snow depth[1]	cm	48.0	1.0	7.0	6.7
Frost depth [cm]	cm	39	0.1	9.9	8.1
No. days with soil frost	day	153	26	85.8	30
No. days with continuous frost	day	158	4.0	65.6	41
No. of soil FTCs	-	8.0	1.0	3.65	2.0

Notes: [1] Observed snow depth values from the Reykjavík station No. 1.

The total volume of RoS events co-occurring with soil frost was higher than rainfall or snowmelt alone during frost (Table 5.3). The 2 and 5-year return periods corresponding to 20 to 30 mm of RoS coinciding with frost depths of 11 and 20 cm have a co-probability of occurrence of 4.7–27%, which are events that are predicted to occur once every 4 years,

resulting in considerable surface runoff. In contrast, a 2-year snowmelt event occurring with a similar frost depth has a total event depth of only 10 mm, and a 2-year rainfall during a frost event has a total depth of 15 mm. Furthermore, the timing of soil frost formation is shifting towards midwinter, however, insignificantly (p-value > 0.05) represented as a shift in the first day of frost in the year (1–364/5) at any soil layer. In contrast, the last day of soil frost during winter has decreased significantly (p-value < 0.05). The timing of the largest winter hydrological inputs is also coinciding with the timing of the deepest frost. The total number of days with soil frost each month during the simulation period indicates that most occurrences of soil frost were towards the peak of winter, i.e., during December, January, February, and March, with January and February being the highest. That coincided with the largest RoS events occurring in February and March with an average of 9 and 11 mm, but less so in January (avg. 8.5 mm).

*Table 5.3 Joint probability of occurrence during one year for the maximum RoS volume during the maximum frost depth for different return periods (T) during winter (**Paper III**).*

		Max. frost depth during RoS [cm]						
		0.7	11.2	19.5	25	29.4	35.1	39.1
Max. RoS during frost [mm]	**T [yrs.]**	1	2	5	10	20	50	100
3.0	1	**0.977**	0.491	0.197	0.095	0.049	0.020	0.01
20.1	2	0.492	**0.266**	0.111	0.054	0.028	0.011	0.006
30.0	5	0.195	0.110	**0.047**	0.023	0.012	0.005	
35.4	10	0.099	0.056	0.024	**0.012**	0.006		
40.1	20	0.050	0.028	0.012	0.006			
45.5	50	0.020	0.011	0.005				
49.2	100	0.010	0.006					

The increase in air temperature, liquid precipitation, intermittent midwinter snowmelt, and RoS events in cold climates are all expected outcomes brought about by climate change (Andradóttir et al., 2021; Dong & Menzel, 2020; Garvelmann et al., 2015; Nygren et al., 2021; Wever et al., 2014; Würzer et al., 2016). In **Paper III**, the SHAW model results show a reduction in soil frost depth and the total number of frost days over the past 70 years. Additionally, it was found that a shift in the timing of frost formation has occurred as the first and the last days of frost have been shifting towards midwinter, coinciding with the maximum RoS and snowmelt events in January and February rather than in early spring. Il Jeong & Sushama (2018) found that 80% of the annual maximum daily runoff from January to May was due to RoS. In Iceland, Andradóttir et al. (2021) found that the urban flooding events correlating with the highest number of insurance claims coincided with the same period resulting from RoS. There has also been a decrease in the duration of continuous frost during winter in Iceland, which is consistent with a more intermittent frost and an increase in freeze-thaw cycles. In the long term, and under a consistently warming climate, an increase in infiltration capacity during winter can be expected (Clilverd et al., 2011; Jyrkama & Sykes, 2007). Other studies even argued that frost will cease to exist and will not affect future infiltration and runoff processes (Ford et al., 2020). In the short run, however, such a shift from cold to temperate climates may increase the risk of flooding because of an increase in magnitude and frequency of frost and RoS-induced runoff generation. Over the

Conterminous United States, Li et al. (2019) found that 70% of extreme runoff events have some contributions from RoS. In Slovenia, Sezen et al. (2020) found that the magnitude of extreme RoS-induced flooding is predicted to increase between 1981 and 2100 based on the RCP 4.5 climate scenario. The heterogeneous nature of urban areas is also a factor that influences melt rates depending on proximity to buildings, snow removal practices and the application (or lack thereof) of deicers, and human activity (Buttle & Xu, 1988). Buttle & Xu (1988) observed that the snowmelt rate was 600% higher in suburban areas than in open fields. They theorized that some variations (mostly increases) in runoff response due to snowmelt might have been due to RoS events where impervious surfaces (roads, roofs, and sidewalks) also contributed to runoff. These surfaces are mostly snow-free and would only contribute to runoff in case of RoS.

One of the reasons RoS events can be more damaging to infrastructure and cause severe flooding is that they often occur after a cold spell followed by a quick warming period that is not long enough to thaw the ground and release clogging from inlets. The combined volume of snowmelt and rainfall, together with a high degree of imperviousness resulting from ground frost and a reduced hydraulic capacity in the drainage system, can all contribute to catastrophic flooding events. In maritime climates characterized by frequent freeze-thaw cycles, repeated snowmelt throughout winter contributes to two distinct phenomena (1) the formation of icy layers within the snowpack or hardened surface layer on the snow surface, and (2) snowmelt infiltration into the underlying soil reducing the soil moisture storage and often refreezing in the soil. Thus, at the onset of RoS events, rapid runoff generation can occur from an abnormally large contributing area resulting in increased flooding potential even for relatively low-intensity rainfall and RoS events (Bengtsson & Westerström, 1992; Buttle & Xu, 1988; Westerström, 1984). Furthermore, the degree to which the ground is frozen may govern runoff generation and account for the variations in runoff response in **Paper I**, which was also noted for real snowmelt and RoS observed by Taylor (1982). Observations made by Kane & Stein (1983) indicated that the period when air temperature is below zero prior to snow accumulation and the degree of saturation in the soil determined the potential for frost formation to a large extent. This supports the notion that the cold maritime climate could be subject to such conditions throughout winter as the thin fluctuating snow cover does not provide prolonged insulation of the ground and contributes to increasing water content in the underlying soil. In **Paper III**, it was found that the joint probability of maximum RoS volume during maximum frost depth was 10 mm higher than snowmelt during frost and 5 mm higher than rainfall for the same return periods. A moderate maximum daily RoS events ($T < 2$ years) can be considered not to pose risk. That said, if such an event occurred simultaneously with a moderate frost event (10–20 cm depth), it could result in a large joint event which can occur regularly ($T < 4$ years) and lead to significant runoff volumes. Similarly, Moghadas et al. (2018) found that a frequent rain-on-snow event (return period = 1.4 years) caused almost five times greater runoff volume compared to a 10-year event occurring in the summer in Kiruna, Sweden. However, they attributed this large runoff volume to the joint occurrence of rain and snowmelt simultaneously. The reliance on design storms and intensity-duration-frequency (IDF) curves stands in the way of optimizing urban drainage systems in cold climates, where, in some areas, up to 50% of the annual precipitation falls in solid form as snow (Semadeni-Davies, 2006). Complications resulting from cold temperatures such as clogging of inlets, frozen ground, and undersized drainage networks are often overlooked when managing stormwater in the northern hemisphere (Thorolfsson, 2012). In those regions, the urban drainage systems have to be designed to mitigate freezing. Thus, a paradigm shift from the

current urban drainage strategies to a more sustainable, multi-purpose approach has taken shape in the past 30 years. That said, more research is still needed to assess the hydrologic benefits of SUDS on a larger scale, especially since most studies on SUDS in cold climates were either conducted in the laboratory or were at a pilot scale.

6 Summary and future perspectives

Urbanization and climate change are exerting increased pressure on urban drainage systems and leading to extreme flooding in different parts of the world. Despite the shift in stormwater management from a single-purpose to a multi-disciplinary approach in recent decades, implementing sustainable urban drainage systems (SUDS) in cold climates is still lacking and less understood than in temperate climates due to concerns regarding soil freezing. Maritime cold climates are both wet and mild, with air temperatures fluctuating around the freezing point and mild precipitation falling year-round. This thesis assessed the hydrological performance of a grass swale undergoing frequent soil freezing and thawing, rain-on-snow events, and intermittent midwinter snowmelt. This work improves the understanding of SUDS efficiency and fills the gaps in knowledge in an attempt to achieve a wider implementation of SUDS in cold regions. To that end, a comprehensive field program was implemented in a neighborhood (Urriðaholt) designed with a SUDS network comprised of grass swales and other undisturbed natural surfaces meant to maintain the pre-development water cycle to preserve a nearby shallow lake (Urriðavatn). The assessment of SUDS consisted of synthetic runoff experiments conducted in a chosen grass swale for a period of 18 months, single-ring infiltration measurement in a grass swale and different undisturbed terrains for 28 months, continuous monitoring of soil moisture content and temperature at two different locations (i.e., grass swale and a lupine field) from November 2018 until now, ad-hoc snow measurement campaigns for four consecutive winters (2018–2022), as well as monitoring the meteorological conditions at the study site using a dedicated weather station. Additionally, modeling of soil temperature, soil frost depth, duration, and timing was carried out. The model results were validated using the soil observations from the study site Urriðaholt. They then were used to construct a long-term record of soil temperature and frost in Reykjavík for the past 70 years to assess the trends in frost formation and its relation to urban flood risk in light of climate change.

The findings of this work indicate that the hydrological performance of the studied grass swale was reduced during winter, especially in the presence of soil frost. However, the swale remained functional throughout the study period and achieved peak flow reduction of an average of 13% during winter compared with 26% in spring and 38% in summer, while achieving a volume reduction of an average of 22% in winter vs. 30–60% in summer. The hydrological performance was less affected by the snow cover and the initial degree of saturation, specifically during winter. The drainage capacity of the swale 24 hours following an event was low during the study period and ranged between 20 to 30%. The infiltration capacity in the grass swale was maintained during winter and was less affected by freeze-thaw cycles than in the less vegetated (i.e., lupine) or barren areas. The frequent freezing and thawing of the soil led to a reduction in infiltration capacity of the grass swale, but the impacts were more pronounced in the lupine field and the barren terrain with observable frost heave and structural deformation that led to a collapse in the soil. The relatively better performance in the grass swale compared to the other terrains was attributed to the presence of an intertwined, soil-binding root system that enhanced the near-surface porosity, infiltration, drainage capacity, and mitigated the effects of frequent volume changes in the soil. The soil texture in the grass swale, which was engineered by limiting the fines content

in the soil (silt and clay < 5%), contributed to the better performance of the swale compared with other undisturbed areas that contained fines content of > 15%.

The modeling results show that frost depth has decreased in the last 70 years in Reykjavík. However, an increase in freeze-thaw cycles has been observed, the freezing season has shortened, and the timing of the occurrence of maximum frost depth has shifted towards midwinter to coincide with the largest rain-on-snow events. A trend expected to exacerbate winter urban flooding, especially that rain-on-snow was found to have a high joint probability of occurrence with frost and generates larger runoff volume than snowmelt or rainfall alone.

The findings of this thesis suggest that the stormwater control measures that provide sustainable urban drainage solutions in cold maritime areas should aim to minimize non-vegetated or impermeable areas and promote the integration of green surfaces to reduce surface runoff. The implementation of SUDS in cold climates must take into account winter conditions for optimal performance. The incorporation of an effective, gravel-based drainage layer with an underdrain can improve the hydrological performance along with carefully selecting soil types and vegetation. The increase in freeze-thaw cycles and its coincidence with rain-on-snow events might lead to an increase in urban flood risks in cold climates, which further motivates a shift towards increasing climate resilience within cities and a wider spread of sustainable development.

Despite the increase in their use in recent years, the adaptation of SUDS for winter operations remains challenging, especially at the catchment scale. Most research on the hydrological performance of SUDS in cold climates focused on frozen columns in laboratories or pilot-scale studies. Urban catchments are heterogeneous than their rural counterparts, exhibiting considerable spatial variability within small areas. Following the research in this thesis, a better understanding of the winter hydrological performance of different SUDS elements such as grass swales, permeable pavements, detention ponds, and rain gardens is still needed, especially at larger scales. Climate change impacts must also be taken into account when assessing the future of stormwater and flood control measures. The changing storm patterns present challenges regarding predicting rainfall and/or snowmelt volumes that need to be considered for planning and sizing urban drainage systems and, consequently, SUDS efficiency and operations. Integrating sustainable adaptation measures and risk-based management perspectives is essential to lessen the effects of weather extremes on a global and regional scale in the coming decades. Flood risk assessment and management have traditionally been the domain of hydrologists, water resources engineers, and statisticians and were especially looked at from a catchment perspective. In light of climate change, a broader, multidisciplinary approach that improves the understanding of the climatic context of urban flooding is needed. The use of regional climate models (RCMs) generated from general circulation models (GCMs) can prove beneficial and open exciting possibilities for integrating SUDS in the urban drainage scheme and flood prediction and prevention measures.

References

Ágústsson, Á. E. (2015). *Græn þök á Íslandi. Greining á vatnsheldni grænna þaka miðað við íslenska veðráttu* [Thesis]. https://skemman.is/handle/1946/21735

Ahmed, F., Gulliver, J. S., & Nieber, J. L. (2015). Field infiltration measurements in grassed roadside drainage ditches: Spatial and temporal variability. *Journal of Hydrology*, *530*, 604–611. https://doi.org/10.1016/j.jhydrol.2015.10.012

Andersland, O. B., & Ladanyi, B. (1994). *An Introduction to Frozen Ground Engineering*. Springer US. https://doi.org/10.1007/978-1-4757-2290-1

Andradóttir, H. Ó., Arnardóttir, A. R., & Zaqout, T. (2021). Rain on snow induced urban floods in cold maritime climate: Risk, indicators and trends. *Hydrological Processes*, *35*(9), e14298. https://doi.org/10.1002/hyp.14298

Andradottir, H. O., & Vollertsen, G. E. G. (2015). Temporal Variability of Heavy Metals in Suburban Road Runoff in a Rainy Cold Climate. *Journal of Environmental Engineering*, *141*(3), 04014068. https://doi.org/10.1061/(ASCE)EE.1943-7870.0000894

Apel, H., Aronica, G. T., Kreibich, H., & Thieken, A. H. (2009). Flood risk analyses—How detailed do we need to be? *Natural Hazards*, *49*(1), 79–98. https://doi.org/10.1007/s11069-008-9277-8

Arisz, H., & Burrell, B. C. (2006). Urban Drainage Infrastructure Planning and Design Considering Climate Change. *2006 IEEE EIC Climate Change Conference*, 1–9. https://doi.org/10.1109/EICCCC.2006.277251

Arnalds, O. (2004). Volcanic soils of Iceland. *CATENA*, *56*(1), 3–20. https://doi.org/10.1016/j.catena.2003.10.002

Arnalds, O. (2008). Soils of Iceland. *Jokull*, *58*, 409–421. https://doi.org/10.1007/978-94-017-9621-7

Arnalds, O. (2015). *The Soils of Iceland*. Springer Netherlands. https://doi.org/10.1007/978-94-017-9621-7

Ashley, R., Faram, M., Chatfield, P., Gersonius, B., & Andoh, R. (2010). *Appropriate Drainage Systems for a Changing Climate in the Water Sensitive City* (p. 877). https://doi.org/10.1061/41099(367)76

Ashley, R., Garvin, S., Pasche, E., Vassilopoulos, A., & Zevenbergen, C. (2007). *Advances in Urban Flood Management*. CRC Press.

Bäckström, M. (2002). Sediment transport in grassed swales during simulated runoff events. *Water Science and Technology: A Journal of the International Association on Water Pollution Research*, *45*(7), 41–49.

Bäckström, M., & Viklander, M. (2000). Integrated stormwater management in cold climates. *Journal of Environmental Science and Health, Part A*, *35*(8), 1237–1249. https://doi.org/10.1080/10934520009377033

Barbosa, L. A. P., Munkholm, L. J., Obour, P. B., & Keller, T. (2020). Impact of compaction and post-compaction vegetation management on aggregate properties, Weibull modulus, and interactions with intra-aggregate pore structure. *Geoderma*, *374*, 114430. https://doi.org/10.1016/j.geoderma.2020.114430

Barrett, M. E. (2008). Comparison of BMP Performance Using the International BMP Database. *Journal of Irrigation and Drainage Engineering*, *134*(5), 556–561. https://doi.org/10.1061/(ASCE)0733-9437(2008)134:5(556)

Barroca, B., Bernardara, P., Mouchel, J. M., & Hubert, G. (2006). Indicators for identification of urban flooding vulnerability. *Natural Hazards and Earth System Sciences*, *6*(4), 553–561. https://doi.org/10.5194/nhess-6-553-2006

Bengtsson, L., & Westerström, G. (1992). Urban snowmelt and runoff in northern Sweden. *Hydrological Sciences Journal*, *37*(3), 263–275. https://doi.org/10.1080/02626669209492586

Blecken, G.-T., Zinger, Y., Deletić, A., Fletcher, T. D., Hedström, A., & Viklander, M. (2010). Laboratory study on stormwater biofiltration: Nutrient and sediment removal in cold temperatures. *Journal of Hydrology*, *394*(3), 507–514. https://doi.org/10.1016/j.jhydrol.2010.10.010

Buttle, J. M. (1990). Effects of suburbanization upon snowmelt runoff. *Hydrological Sciences Journal*, *35*(3), 285–302. https://doi.org/10.1080/02626669009492430

Buttle, J. M., & Xu, F. (1988). Snowmelt Runoff in Suburban Environments. *Hydrology Research*, *19*(1), 19–40. https://doi.org/10.2166/nh.1988.0002

Caldwell, T. G., Bongiovanni, T., Cosh, M. H., Halley, C., & Young, M. H. (2018). Field and Laboratory Evaluation of the CS655 Soil Water Content Sensor. *Vadose Zone Journal*, *17*(1), 170214. https://doi.org/10.2136/vzj2017.12.0214

Caraco, D., & Claytor, R. (1997). *Stormwater BMP Design: Supplement for Cold Climates*. U.S. Environmental Protection Agency.

Castellini, M., & Iovino, M. (2019). Pedotransfer functions for estimating soil water retention curve of Sicilian soils. *Archives of Agronomy and Soil Science*, *65*(10), 1401–1416. https://doi.org/10.1080/03650340.2019.1566710

Chen, L. (2019). *Copulas and Its Application in Hydrology and Water Resources / by Lu Chen, Shenglian Guo.* (1st ed. 2019.). Springer Singapore. https://doi.org/10.1007/978-981-13-0574-0

Chocat, B., Ashley, R., Marsalek, J., Matos, M. R., Rauch, W., Schilling, W., & Urbonas, B. (2007). Toward the Sustainable Management of Urban Storm-Water. *Indoor and Built Environment*, *16*(3), 273–285. https://doi.org/10.1177/1420326X07078854

Chow, V. T., Maidment, D. R., & Mays, L. W. (1988). *Applied Hydrology*. McGraw-Hill.

Clilverd, H. M., White, D. M., Tidwell, A. C., & Rawlins, M. A. (2011). The Sensitivity of Northern Groundwater Recharge to Climate Change: A Case Study in Northwest Alaska1. *JAWRA Journal of the American Water Resources Association*, *47*(6), 1228–1240. https://doi.org/10.1111/j.1752-1688.2011.00569.x

Davis, A. P., Stagge, J. H., Jamil, E., & Kim, H. (2012). Hydraulic performance of grass swales for managing highway runoff. *Water Research*, *46*(20), 6775–6786. https://doi.org/10.1016/j.watres.2011.10.017

Deletic, A. (2001). Modelling of water and sediment transport over grassed areas. *Journal of Hydrology*, *248*(1–4), 168–182. https://doi.org/10.1016/S0022-1694(01)00403-6

Deletic, A., & Fletcher, T. D. (2006). Performance of grass filters used for stormwater treatment—A field and modelling study. *Journal of Hydrology*, *317*(3–4), 261–275. https://doi.org/10.1016/j.jhydrol.2005.05.021

Denich, C., Bradford, A., & Drake, J. (2013). Bioretention: Assessing effects of winter salt and aggregate application on plant health, media clogging and effluent quality. *Water Quality Research Journal*, *48*(4), 387–399. https://doi.org/10.2166/wqrjc.2013.065

Dong, C., & Menzel, L. (2020). Recent snow cover changes over central European low mountain ranges. *Hydrological Processes*, *34*(2), 321–338. https://doi.org/10.1002/hyp.13586

Eigenbrod, K. D. (2011). Effects of cyclic freezing and thawing on volume changes and permeabilities of soft fine-gained soils. *Canadian Geotechnical Journal*. https://doi.org/10.1139/t96-079-301

Einarsdóttir, H. (2018). *Árstímabundin virkni léttra gróðurþaka á Íslandi* [Thesis]. https://skemman.is/handle/1946/29501

Einarsson, M. (1984). *Climate of Iceland*. Elsevier.

Ekka, S. A., Rujner, H., Leonhardt, G., Blecken, G.-T., Viklander, M., & Hunt, W. F. (2021). Next generation swale design for stormwater runoff treatment: A comprehensive approach. *Journal of Environmental Management*, *279*, 111756. https://doi.org/10.1016/j.jenvman.2020.111756

Fach, S., Engelhard, C., Wittke, N., & Rauch, W. (2011). Performance of infiltration swales with regard to operation in winter times in an Alpine region. *Water Science and Technology*, *63*(11), 2658–2665. https://doi.org/10.2166/wst.2011.153

Fardel, A., Peyneau, P.-E., Béchet, B., Lakel, A., & Rodriguez, F. (2020). Performance of two contrasting pilot swale designs for treating zinc, polycyclic aromatic hydrocarbons and glyphosate from stormwater runoff. *Science of The Total Environment*, *743*, 140503. https://doi.org/10.1016/j.scitotenv.2020.140503

Feiccabrino, J., Graff, W., Lundberg, A., Sandström, N., & Gustafsson, D. (2015). Meteorological Knowledge Useful for the Improvement of Snow Rain Separation in Surface Based Models. *Hydrology*, *2*(4), 266–288. https://doi.org/10.3390/hydrology2040266

Flerchinger, G. N., Lehrsch, G. A., & McCool, D. K. (2013). Freezing and Thawing | Processes. In *Reference Module in Earth Systems and Environmental Sciences* (p. B9780124095489053000). Elsevier. https://doi.org/10.1016/B978-0-12-409548-9.05173-3

Fletcher, T. D., Andrieu, H., & Hamel, P. (2013). Understanding, management and modelling of urban hydrology and its consequences for receiving waters: A state of the art. *Advances in Water Resources*, *51*, 261–279. https://doi.org/10.1016/j.advwatres.2012.09.001

Fletcher, T. D., Shuster, W., Hunt, W. F., Ashley, R., Butler, D., Arthur, S., Trowsdale, S., Barraud, S., Semadeni-Davies, A., Bertrand-Krajewski, J.-L., Mikkelsen, P. S., Rivard, G., Uhl, M., Dagenais, D., & Viklander, M. (2015). SUDS, LID, BMPs,

WSUD and more – The evolution and application of terminology surrounding urban drainage. *Urban Water Journal*, *12*(7), 525–542. https://doi.org/10.1080/1573062X.2014.916314

Flury, M., Flühler, H., Jury, W. A., & Leuenberger, J. (1994). Susceptibility of soils to preferential flow of water: A field study. *Water Resources Research*, *30*(7), 1945–1954. https://doi.org/10.1029/94WR00871

Ford, C. M., Kendall, A. D., & Hyndman, D. W. (2020). Effects of shifting snowmelt regimes on the hydrology of non-alpine temperate landscapes. *Journal of Hydrology*, *590*, 125517. https://doi.org/10.1016/j.jhydrol.2020.125517

Fouli, Y., Cade-Menun, B. J., & Cutforth, H. W. (2013). Freeze–thaw cycles and soil water content effects on infiltration rate of three Saskatchewan soils. *Canadian Journal of Soil Science*, *93*(4), 485–496. https://doi.org/10.4141/cjss2012-060

Freudiger, D., Kohn, I., Stahl, K., & Weiler, M. (2014). Large-scale analysis of changing frequencies of rain-on-snow events with flood-generation potential. *Hydrology and Earth System Sciences*, *18*(7), 2695–2709. https://doi.org/10.5194/hess-18-2695-2014

García-Serrana, M., Gulliver, J. S., & Nieber, J. L. (2017). Infiltration capacity of roadside filter strips with non-uniform overland flow. *Journal of Hydrology*, *545*, 451–462. https://doi.org/10.1016/j.jhydrol.2016.12.031

Garvelmann, J., Pohl, S., & Weiler, M. (2015). Spatio-temporal controls of snowmelt and runoff generation during rain-on-snow events in a mid-latitude mountain catchment. *Hydrological Processes*, *29*(17), 3649–3664. https://doi.org/10.1002/hyp.10460

Gavrić, S., Leonhardt, G., Marsalek, J., & Viklander, M. (2019). Processes improving urban stormwater quality in grass swales and filter strips: A review of research findings. *Science of The Total Environment*, *669*, 431–447. https://doi.org/10.1016/j.scitotenv.2019.03.072

Géhéniau, N., Fuamba, M., Mahaut, V., Gendron, M. R., & Dugué, M. (2015). Monitoring of a Rain Garden in Cold Climate: Case Study of a Parking Lot near Montréal. *Journal of Irrigation and Drainage Engineering*, *141*(6), 04014073. https://doi.org/10.1061/(ASCE)IR.1943-4774.0000836

Geissen, V., Mol, H., Klumpp, E., Umlauf, G., Nadal, M., van der Ploeg, M., van de Zee, S. E. A. T. M., & Ritsema, C. J. (2015). Emerging pollutants in the environment: A challenge for water resource management. *International Soil and Water Conservation Research*, *3*(1), 57–65. https://doi.org/10.1016/j.iswcr.2015.03.002

Granger, R., Gray, D., & Dyck, G. (2011). Snowmelt Infiltration to Frozen Prairie Soils. *Canadian Journal of Earth Sciences*, *21*, 669–677. https://doi.org/10.1139/e84-073

Gray, D. M., Toth, B., Zhao, L., Pomeroy, J. W., & Granger, R. J. (2001). Estimating areal snowmelt infiltration into frozen soils. *Hydrological Processes*, *15*(16), 3095–3111. https://doi.org/10.1002/hyp.320

Hamlet, A. F., Mote, P. W., Clark, M. P., & Lettenmaier, D. P. (2005). Effects of Temperature and Precipitation Variability on Snowpack Trends in the Western United States. *Journal of Climate*, *18*(21), 4545–4561. https://doi.org/10.1175/JCLI3538.1

Huong, H. T. L., & Pathirana, A. (2013). Urbanization and climate change impacts on future urban flooding in Can Tho city, Vietnam. *Hydrology and Earth System Sciences*, *17*(1), 379–394. https://doi.org/10.5194/hess-17-379-2013

Il Jeong, D., & Sushama, L. (2018). Rain-on-snow events over North America based on two Canadian regional climate models. *Climate Dynamics*, *50*(1), 303–316. https://doi.org/10.1007/s00382-017-3609-x

IPCC. (2022). *Climate Change 2022: Impacts, Adaptation, and Vulnerability. Contribution of Working Group II to the Sixth Assessment Report of the Intergovernmental Panel on Climate Change* [[H.-O. Pörtner, D.C. Roberts, M. Tignor, E.S. Poloczanska, K. Mintenbeck, A. Alegría, M. Craig, S. Langsdorf, S. Löschke, V. Möller, A. Okem, B. Rama (eds.)]]. Cambridge University Press. In Press.

Jyrkama, M. I., & Sykes, J. F. (2007). The impact of climate change on spatially varying groundwater recharge in the grand river watershed (Ontario). *Journal of Hydrology*, *338*(3), 237–250. https://doi.org/10.1016/j.jhydrol.2007.02.036

Kane, D. L., & Stein, J. (1983). Water movement into seasonally frozen soils. *Water Resources Research*, *19*(6), 1547–1557. https://doi.org/10.1029/WR019i006p01547

Kanso, T., Tedoldi, D., Gromaire, M.-C., Ramier, D., Saad, M., & Chebbo, G. (2018). Horizontal and Vertical Variability of Soil Hydraulic Properties in Roadside Sustainable Drainage Systems (SuDS)—Nature and Implications for Hydrological Performance Evaluation. *Water*, *10*(8), 987. https://doi.org/10.3390/w10080987

Kendall, M. G. (1948). *Rank correlation methods*. Griffin.

Khan, U. T., Valeo, C., Chu, A., & van Duin, B. (2012). Bioretention cell efficacy in cold climates: Part 1 — hydrologic performance. *Canadian Journal of Civil Engineering*, *39*(11), 1210–1221. https://doi.org/10.1139/l2012-110

Konisky, D. M., Hughes, L., & Kaylor, C. H. (2016). Extreme weather events and climate change concern. *Climatic Change*, *134*(4), 533–547. https://doi.org/10.1007/s10584-015-1555-3

Kratky, H., Li, Z., Chen, Y., Wang, C., Li, X., & Yu, T. (2017). A critical literature review of bioretention research for stormwater management in cold climate and future research recommendations. *Frontiers of Environmental Science & Engineering*, *11*(4), 16. https://doi.org/10.1007/s11783-017-0982-y

LeFevre, N. J., Davidson, J. D., & Oberts, G. L. (2009). Bioretention of Simulated Snowmelt: Cold Climate Performance and Design Criteria. *Cold Regions Engineering 2009*, 145–154. https://doi.org/10.1061/41072(359)17

Li, D., Lettenmaier, D. P., Margulis, S. A., & Andreadis, K. (2019). The Role of Rain-on-Snow in Flooding Over the Conterminous United States. *Water Resources Research*, *55*(11), 8492–8513. https://doi.org/10.1029/2019WR024950

Lian, J., Xu, K., & Ma, C. (2013). Joint impact of rainfall and tidal level on flood risk in a coastal city with a complex river network: A case study of Fuzhou City, China. *Hydrology and Earth System Sciences*, *17*, 679–689. https://doi.org/10.5194/hess-17-679-2013

Luell, S. K., Winston, R. J., & Hunt, W. F. (2021). Monitoring the Water Quality Benefits of a Triangular Swale Treating a Highway Runoff. *Journal of Sustainable Water in the Built Environment*, *7*(1), 05020004. https://doi.org/10.1061/JSWBAY.0000929

Lundin, L.-C. (1990). Hydraulic properties in an operational model of frozen soil. *Journal of Hydrology*, *118*(1), 289–310. https://doi.org/10.1016/0022-1694(90)90264-X

Maksimovic, C., Saegrov, S., Milina, J., & Thorolfsson, S. (2000). *Urban drainage in specific climates, v. II: Urban drainage in cold climates—UNESCO Digital Library*. https://unesdoc.unesco.org/ark:/48223/pf0000122599

Mann, H. B. (1945). Nonparametric Tests Against Trend. *Econometrica*, *13*(3), 245–259. JSTOR. https://doi.org/10.2307/1907187

Marsalek, J. (2014). *Urban Water Cycle Processes and Interactions: Urban Water Series - UNESCO-IHP*. CRC Press.

Moghadas, S., Gustafsson, A.-M., Viklander, P., Marsalek, J., & Viklander, M. (2016). Laboratory study of infiltration into two frozen engineered (sandy) soils recommended for bioretention: Laboratory Study of Infiltration into Frozen Engineered Soil. *Hydrological Processes*, *30*(8), 1251–1264. https://doi.org/10.1002/hyp.10711

Moghadas, S., Leonhardt, G., Marsalek, J., & Viklander, M. (2018). Modeling Urban Runoff from Rain-on-Snow Events with the U.S. EPA SWMM Model for Current and Future Climate Scenarios. *Journal of Cold Regions Engineering*, *32*(1), 04017021. https://doi.org/10.1061/(ASCE)CR.1943-5495.0000147

Monrabal-Martinez, C., Aberle, J., Muthanna, T. M., & Orts-Zamorano, M. (2018). Hydrological benefits of filtering swales for metal removal. *Water Research*, *145*, 509–517. https://doi.org/10.1016/j.watres.2018.08.051

Monrabal-Martinez, C., Meyn, T., & Muthanna, T. M. (2019). Characterization and temporal variation of urban runoff in a cold climate—Design implications for SuDS. *Urban Water Journal*, *16*(6), 451–459. https://doi.org/10.1080/1573062X.2018.1536758

Morbidelli, R., Saltalippi, C., Flammini, A., Cifrodelli, M., Picciafuoco, T., Corradini, C., & Govindaraju, R. S. (2016). Laboratory investigation on the role of slope on infiltration over grassy soils. *Journal of Hydrology*, *543*, 542–547. https://doi.org/10.1016/j.jhydrol.2016.10.024

Muthanna, T. M., Viklander, M., Gjesdahl, N., & Thorolfsson, S. T. (2007). Heavy Metal Removal in Cold Climate Bioretention. *Water, Air, and Soil Pollution*, *183*(1), 391–402. https://doi.org/10.1007/s11270-007-9387-z

Muthanna, T. M., Viklander, M., & Thorolfsson, S. T. (2007). An evaluation of applying existing bioretention sizing methods to cold climates with snow storage conditions. *Water Science and Technology: A Journal of the International Association on Water Pollution Research*, *56*(10), 73–81. https://doi.org/10.2166/wst.2007.745

Muthanna, T. M., Viklander, M., & Thorolfsson, S. T. (2008). Seasonal climatic effects on the hydrology of a rain garden. *Hydrological Processes*, *22*(11), 1640–1649. https://doi.org/10.1002/hyp.6732

Nelsen, R. B. (2007). *An Introduction to Copulas*. Springer Science & Business Media.

Nygren, M., Giese, M., & Barthel, R. (2021). Recent trends in hydroclimate and groundwater levels in a region with seasonal frost cover. *Journal of Hydrology*, *602*, 126732. https://doi.org/10.1016/j.jhydrol.2021.126732

Oberts, G. L. (2003). Cold climate BMPs: Solving the management puzzle. *Water Science and Technology: A Journal of the International Association on Water Pollution Research*, *48*(9), 21–32.

Orradottir, B., Archer, S. R., Arnalds, O., Wilding, L. P., & Thurow, T. L. (2008). Infiltration in Icelandic Andisols: The Role of Vegetation and Soil Frost. *Arctic, Antarctic, and Alpine Research*, *40*(2), 412–421. https://doi.org/10.1657/1523-0430(06-076)[ORRADOTTIR]2.0.CO;2

Óskarsson, H., Arnalds, Ó., Gudmundsson, J., & Gudbergsson, G. (2004). Organic carbon in Icelandic Andosols: Geographical variation and impact of erosion. *CATENA*, *56*(1), 225–238. https://doi.org/10.1016/j.catena.2003.10.013

Paus, K. H., & BrasKerud, B. C. (2014). Suggestions for designing and constructing bioretention cells for a nordic climate. *Journal of Water Management and Research*, *70*, 139–150.

Paus, K. H., Muthanna, T. M., & Braskerud, B. C. (2016). The hydrological performance of bioretention cells in regions with cold climates: Seasonal variation and implications for design. *Hydrology Research*, *47*(2), 291–304. https://doi.org/10.2166/nh.2015.084

Pétursdóttir, E. (2016). *Key Factors for the Implementation of Sustainable Drainage Systems in Iceland* [Thesis]. https://skemman.is/handle/1946/24846

Prince George's County. (1999). *Low-impact Development: An Integrated Design Approach*. MD Department of Environmental Resources.

Purvis, R. A., Winston, R. J., Hunt, W. F., Lipscomb, B., Narayanaswamy, K., McDaniel, A., Lauffer, M. S., & Libes, S. (2019). Evaluating the Hydrologic Benefits of a Bioswale in Brunswick County, North Carolina (NC), USA. *Water*, *11*(6), 1291. https://doi.org/10.3390/w11061291

Roseen, R. M., Ballestero, T. P., Houle, J. J., Avellaneda, P., Briggs, J., Fowler, G., & Wildey, R. (2009). Seasonal Performance Variations for Storm-Water Management Systems in Cold Climate Conditions. *Journal of Environmental Engineering*, *135*(3), 128–137. https://doi.org/10.1061/(ASCE)0733-9372(2009)135:3(128)

Rujner, H., Leonhardt, G., Marsalek, J., Perttu, A.-M., & Viklander, M. (2018). The effects of initial soil moisture conditions on swale flow hydrographs. *Hydrological Processes*, *32*(5), 644–654.

Saxton, K. E., & Rawls, W. J. (2006). Soil Water Characteristic Estimates by Texture and Organic Matter for Hydrologic Solutions. *Soil Science Society of America Journal*, *70*(5), 1569–1578. https://doi.org/10.2136/sssaj2005.0117

Semadeni-Davies, A. (2006). Winter performance of an urban stormwater pond in southern Sweden. *Hydrological Processes*, *20*(1), 165–182. https://doi.org/10.1002/hyp.5909

Sen, P. K. (1968). Estimates of the Regression Coefficient Based on Kendall's Tau. *Journal of the American Statistical Association*, *63*(324), 1379–1389. JSTOR. https://doi.org/10.2307/2285891

Sezen, C., Sraj, M., Medved, A., & Bezak, N. (2020). Investigation of Rain-On-Snow Floods under Climate Change. *Applied Sciences-Basel*, *10*(4), 1242. https://doi.org/10.3390/app10041242

Shafique, M., Kim, R., & Kyung-Ho, K. (2018). Evaluating the Capability of Grass Swale for the Rainfall Runoff Reduction from an Urban Parking Lot, Seoul, Korea. *International Journal of Environmental Research and Public Health*, *15*(3), 537. https://doi.org/10.3390/ijerph15030537

Shanley, J. B., & Chalmers, A. (1999). The effect of frozen soil on snowmelt runoff at Sleepers River, Vermont. *Hydrological Processes*, *13*(12–13), 1843–1857. https://doi.org/10.1002/(SICI)1099-1085(199909)13:12/13<1843::AID-HYP879>3.0.CO;2-G

Sillanpää, N., & Koivusalo, H. (2013). Catchment-scale evaluation of pollution potential of urban snow at two residential catchments in southern Finland. *Water Science and Technology*, *68*(10), 2164–2170. https://doi.org/10.2166/wst.2013.466

Sörensen, J. (2018). *Urban, pluvial flooding: Blue-green infrastructure as a strategy for resilience* [Doctoral Thesis (compilation), Faculty of Engineering (LTH), Lund University]. https://doi.org/10.3390/w8080332

Sörensen, J., Persson, A., Sternudd, C., Aspegren, H., Nilsson, J., Nordström, J., Jönsson, K., Mottaghi, M., Becker, P., Pilesjö, P., Larsson, R., Berndtsson, R., & Mobini, S. (2016). Re-Thinking Urban Flood Management—Time for a Regime Shift. *Water*, *8*(8), 332. https://doi.org/10.3390/w8080332

Stahli, M., Jansson, P. E., & Lundin, L. C. (1996). Preferential water flow in a frozen soil—A two-domain model approach. *Hydrological Processes*, *10*(10), 1305–1316.

Stähli, M., Jansson, P.-E., & Lundin, L.-C. (1999). Soil moisture redistribution and infiltration in frozen sandy soils. *Water Resources Research*, *35*(1), 95–103. https://doi.org/10.1029/1998WR900045

Talebi, L., & Pitt, R. (2019). Chapter 7—Water Sensitive Urban Design Approaches in Sewer System Overflow Management. In A. K. Sharma, T. Gardner, & D. Begbie (Eds.), *Approaches to Water Sensitive Urban Design* (pp. 139–161). Woodhead Publishing. https://doi.org/10.1016/B978-0-12-812843-5.00007-1

Taylor, C. (1982). The Effect on Storm Runoff Response of Seasonal-Variations in Contributing Zones in Small Watersheds. *Nordic Hydrology*, *13*(3), 165–182.

Theil, H. (1950). A rank-invariant method of linear and polynomial regression analysis, 1-2; confidence regions for the parameters of linear regression equations in two, three and more variables. *Indagationes Mathematicae*, *1*(2). https://ir.cwi.nl/pub/18446

Thorolfsson, S. T. (2012). *Specific Problems in Urban Drainage in Cold Climate (SP-UDCC)*. 888–899. https://doi.org/10.1061/40583(275)86

Thorsteinsson, T., & Björnsson, H. (2012). *Climate Change and Energy Systems: Impacts, Risks and Adaptation in the Nordic and Baltic countries*. Nordic Council of Ministers. http://urn.kb.se/resolve?urn=urn:nbn:se:norden:org:diva-705

Thunholm, B., Lundin, L.-C., & Lindell, S. (1989). Infiltration into a Frozen Heavy Clay Soil. *Hydrology Research*, *20*(3), 153–166. https://doi.org/10.2166/nh.1989.0012

UN. (2019). *World Population Prospects—The 2019 revision*. https://population.un.org/wpp/

University of Iceland. (2018). *Samstarf um rannsóknarmiðstöð um blágrænar regnvatnslausnir*.

https://www.hi.is/frettir/samstarf_um_rannsoknarmidstod_um_blagraenar_regnvatnslausnir

U.S. EPA. (1999). *Storm Water Technology Fact Sheet Vegetated Swales*. https://nepis.epa.gov/Exe/ZyPURL.cgi?Dockey=200044A8.txt

Vetter, V. M. S., Tjaden, N. B., Jaeschke, A., Buhk, C., Wahl, V., Wasowicz, P., & Jentsch, A. (2018). Invasion of a Legume Ecosystem Engineer in a Cold Biome Alters Plant Biodiversity. *Front. Plant Sci.* https://doi.org/10.3389/fpls.2018.00715

Vollertsen, G. E. G. (2010). *Removal of heavy metals in a wet detention pond in Reykjavik* [Thesis]. https://skemman.is/handle/1946/5631

Westerlund, C., & Viklander, M. (2006). Particles and associated metals in road runoff during snowmelt and rainfall. *Science of The Total Environment*, *362*(1), 143–156. https://doi.org/10.1016/j.scitotenv.2005.06.031

Westerström, G. (1984). *Snowmelt runoff from Porsön residential area, Luleå*. *4*, 315–323. http://urn.kb.se/resolve?urn=urn:nbn:se:ltu:diva-38161

Wever, N., Jonas, T., Fierz, C., & Lehning, M. (2014). Model simulations of the modulating effect of the snow cover in a rain-on-snow event. *Hydrology and Earth System Sciences*, *18*(11), 4657–4669. https://doi.org/10.5194/hess-18-4657-2014

Wong, T. H. F., & Brown, R. R. (2009). The water sensitive city: Principles for practice. *Water Science and Technology*, *60*(3), 673–682. https://doi.org/10.2166/wst.2009.436

Woods Ballard, B., Wilson, S., Udale-Clarke, H., Illman, S., Scott, T., Ashley, R., & Kellagher, R. (2015). *The SUDS manual (C753). CIRIA: London, UK.* ISBN 978-0-86017-759-3

Würzer, S., Jonas, T., Wever, N., & Lehning, M. (2016). Influence of Initial Snowpack Properties on Runoff Formation during Rain-on-Snow Events. *Journal of Hydrometeorology*, *17*(6), 1801–1815. https://doi.org/10.1175/JHM-D-15-0181.1

Yousef, Y. A., Hvitved-Jacobsen, T., Wanielista, M. P., & Harper, H. H. (1987). Removal of contaminants in highway runoff flowing through swales. *Science of The Total Environment*, *59*, 391–399. https://doi.org/10.1016/0048-9697(87)90462-1

Zellou, B., & Rahali, H. (2019). Assessment of the joint impact of extreme rainfall and storm surge on the risk of flooding in a coastal area. *Journal of Hydrology*, *569*, 647–665. https://doi.org/10.1016/j.jhydrol.2018.12.028

Zhou, Q., Mikkelsen, P. S., Halsnæs, K., & Arnbjerg-Nielsen, K. (2012). Framework for economic pluvial flood risk assessment considering climate change effects and adaptation benefits. *Journal of Hydrology*, *414–415*, 539–549. https://doi.org/10.1016/j.jhydrol.2011.11.031

Appendix A

Paper I

Journal of Hydrology 597 (2021) 126159

Contents lists available at ScienceDirect

Journal of Hydrology

journal homepage: www.elsevier.com/locate/jhydrol

Research papers

Hydrologic performance of grass swales in cold maritime climates: Impacts of frost, rain-on-snow and snow cover on flow and volume reduction

Tarek Zaqout *, Hrund Ólöf Andradóttir

Faculty of Civil and Environmental Engineering, University of Iceland, Hjarðarhagi 6, 107 Reykjavik, Iceland

ARTICLE INFO

This manuscript was handled by Corrado Corradini, Editor-in-Chief

Keywords:
Grass swales
SuDS
Infiltration into frozen soils
Rain on snow
Flow reduction
Drainage capacity

ABSTRACT

Sustainable urban drainage solutions (SuDS) are a diverse set of design options that mitigate floods and improve water quality. Grass swales are the sole component of SuDS that transports runoff over long distances to downstream recipients. A deeper understanding of the performance of grass swales in different winter conditions is important in order for cities to achieve a greater climate resiliency. The goal of this study was to assess the impacts of frequent rain-on-snow, and freeze–thaw cycles on the hydrologic performance of grass swales. A total of 63 field synthetic runoff experiments were performed in a 5.8 m long section of a grass swale in the Urriðaholt neighborhood, Gardabaer, Iceland over 18 months. A three-fold reduction in peak flow attenuation was observed in winter (avg. 13%) compared to summer (avg. 38%) for hydraulic loadings ranging between 19 and 131 cm/h. The reduction in the performance of the swale was primarily due to frost formation and secondarily due to snow. The frequent rainfall, snowmelt, and rain-on-snow events elevated the soil water content and rendered the swale media susceptible to frost formation. The formation of pore ice within the 5 cm soil horizon led to a considerable reduction in soil porosity, which negatively affected the infiltration capacity, and shortened runoff lag times. Snow affected the performance by concentrating the flow in narrow channels, which reduced the effective area of infiltration, but also led to longer lag times and stored a portion of the runoff water within its pack. Despite the deterioration in the swale's efficiency in winter, infiltration was observed in all synthetic runoff experiments, indicating that frost was either porous/granular, or heterogeneous in nature. The swale served its purpose to moderately reduce runoff peaks and volumes, especially for small and medium events. This research highlights the importance of effectively draining infiltration-based systems in cold climates to avoid the adverse effects of low temperatures.

1. Introduction

Urban densification, together with intensifying weather, are exerting pressure on the conventional stormwater management systems and thus leading to more frequent and serious urban floods (Davis et al., 2012; Dietz and Clausen, 2008; Khan et al., 2012). Sustainable urban Drainage Systems (SuDS) have been increasingly implemented as a low impact stormwater control measure (SCM) to reduce runoff quantity and improve its quality. SuDS involve a wide range of design options with the goal of disposing stormwater in local waterways and mimicking the natural hydrological cycle. Vegetated swales are the sole component of SuDS elements that is intended to convey runoff across a watershed, while also performing the traditional functions of infiltrating and storing runoff, recharging the water table, and trapping and removing sediments and pollutants (Ahmed et al., 2015; Gavrić et al., 2019; Rujner et al., 2018). Hence, swales are paramount in making urban areas more climate resilient. The hydrological performance of swales during real and simulated runoff events has been extensively studied in temperate climates (e.g., Abu-Zreig et al., 2004; Davis et al., 2012; Deletic and Fletcher, 2006; García-Serrana et al., 2017; Liu et al., 2016; Rujner et al., 2018; Shafique et al., 2018). A swale's hydrological and hydraulic performance is observed through reduced runoff volumes and delayed peak flows. The infiltration capacity of swales and their ability to store water are largely dependent on soil physical properties, type of soil, soil hydraulic conductivity, initial moisture content, and the area of the vegetated surface. A swale's infiltration capacity is also linked to the magnitude and intensity of runoff events (Davis et al., 2012). Bed slopes and surface roughness provided by vegetation also affect flow retardation and infiltration (Monrabal-Martinez et al., 2018; Rujner et al., 2018).

* Corresponding author.
E-mail addresses: tarek@hi.is (T. Zaqout), hrund@hi.is (H.Ó. Andradóttir).

https://doi.org/10.1016/j.jhydrol.2021.126159
Received 30 October 2020; Received in revised form 9 February 2021; Accepted 3 March 2021
Available online 9 March 2021

SuDS water treatment and flood mitigation performance are negatively affected by winter conditions (Roseen et al., 2009). Even in highly conductive soils, such as sandy loam (Monrabal-Martinez et al., 2018; Paus et al., 2015), frost can clog the pores and form ice lenses that impair infiltration. In this regard, frost type is more important than frost depth (Muthanna et al., 2008). Frost type is largely governed by the pre-freezing soil water content, as saturated soils are more prone to concrete frost formation that blocks infiltration. Unsaturated or dry soil conditions promote granular and porous frost, both of which favor infiltration (Fach et al., 2011; LeFevre et al., 2009; Muthanna et al., 2008; Orradottir et al., 2008). A good drainage capacity is paramount to avoid high water content buildup, which has been shown to enhance volume reduction and prevent frost formation (LeFevre et al., 2009; Monrabal-Martinez et al., 2018; Muthanna et al., 2008).

Another factor known to promote urban flooding is the presence of snow. Winter runoff events become more voluminous with the addition of meltwater (Moghadas et al., 2018; Valeo and Ho, 2004). Being snow accumulation or snow deposit areas, SuDS are more prone to snowmelt compared to other vegetated urban areas (Bäckström and Viklander, 2000; Valeo and Ho, 2004). This is particularly true for swales, which are designed as channels or depressions and often located next to roads. When subjected to repeated freeze–thaw and rain-on-snow (RoS) cycles, icy layers form within the snowpack that prevent infiltration (Caraco and Claytor, 1997), and can contribute to instantaneous runoff generation during RoS and snowmelt events (Garvelmann et al., 2015; Muthanna et al., 2008). Moreover, the lack of a continuous insulating snow cover, as common in inland regions, renders coastal soils more susceptible to repeated meltwater infiltration and re-freezing contributing to impermeable frost formation (Orradottir et al., 2008). The repeated freezing and thawing processes can, however, alter soil aggregate stability and pore continuity, resulting in the creation of preferential flow paths that may promote infiltration (Flerchinger, 2013; Paus et al., 2015).

Little research exists on the performance of SuDS during frost, snow, and RoS in cold maritime climates. The most detailed studies on SuDS winter performance focused on bioretention cells, which exhibited anything from complete capture of runoff volumes to impeded infiltration in the presence of surface frost (e.g., Paus et al., 2015; Blecken et al., 2007; Khan et al., 2012; LeFevre et al., 2009; Muthanna et al., 2008). The different responses were attributed to a combination of soil hydraulic conductivity and drainage capacity, and the nature of runoff, whether it involves RoS or snowmelt (Muthanna et al., 2008; Paus et al., 2015). The effects of frost formation, soil saturation, and, more importantly, infiltration capacity were not investigated in depth in these studies. In addition, the number of snowmelt and RoS events were too few to clearly distinguish them from pure rainfall events. The studied bioretention cells included an underdrain and thick vegetation (e.g., Khan et al., 2012; Muthanna et al., 2008; Paus et al., 2015), which help keep the soil dry, prevent frost formation, and enhance infiltration. This differs from the relatively uniform vegetation cover and dense roots system of grass swales, many of which do not include an underdrain. Results from the bioretention cells may, therefore, not translate to grass swales. Particularly, the bioretention cells' good overall performance in cold climates might be attributed to the fact that they are designed to temporarily pond water (Woods Ballard et al., 2015), which ultimately infiltrates the soil through preferential flow paths and macropores despite the frozen filter media (Khan et al., 2012). Swales, however, are designed to convey water and have a much shorter residence time. Very limited documentation exists on the functioning of grass swales in cold climates, especially during frozen conditions and in the presence of snow.

To the authors' knowledge, a systematic study of the hydrologic

Fig. 1. Urridaholt urban catchment in Gardabær. The location of the study swale (dot), swale network (double line), the drainage area for the swale (crosshatch), building plots (even shade), streets (single heavy line), and lake Urridavatn (triangle).

performance of SuDS during frost, snow, and, more specifically, RoS has not been conducted. RoS and intermittent mid-winter snowmelt events that have historically been associated with cold maritime climates are now becoming more common and severe in various regions around the globe due to climate change (Dong and Menzel, 2020; Garvelmann et al., 2015). Frequent RoS and freeze–thaw cycles were found to be responsible for 83% of water related insurance claims in the capital of Iceland (Arnardóttir, 2020). It is therefore essential to better understand the complex interconnections between soil, snow, and frost in order to successfully integrate such systems in stormwater management strategies. The goal of this study, therefore, was to assess the performance of grass swales under frost, RoS, and snow conditions. 63 synthetic runoff experiments were conducted in a swale segment in a residential neighborhood from March 2019 to August 2020. The tests were conducted during a range of snow, frost, and low temperatures to allow comparisons between these different conditions.

2. Methods

2.1. Site description

Urridaholt is the first BREEAM (Building Research Establishment's Environmental Assessment Method) certified neighborhood in Iceland. Sited on a hill in the Gardabaer municipality in the greater capital area (64° 4′18.46″ N, 21° 54′37.11″ W), the drainage network was designed to protect the water level and quality in the shallow 13-ha Urridavatn lake at the bottom of the catchment (Fig. 1). For that purpose, excess runoff that infiltrates into roadside swales, detention ponds, and front lawns from the 10-ha catchment area is conveyed via underdrains and discharged as concentrated flows into a network of swales that lead towards the lake. The main swale extends from the top of the hill towards the lake, with mild sloping sections separated by check dams to attenuate the flow.

Table 1
Summary of soil characteristics determined in the laboratory using samples extracted from the study swale.

Soil characteristics	
Soil texture	Sandy loam
Gravel: sand: fines	15–20:75–82:2.5–4
Bulk density (ρ_s)	1.2–1.42
Porosity (ϕ)	0.46–0.53
Organic content	2–8%
Saturated hydraulic conductivity (K_{sat})	6.23 ($\pm$0.10) $\times$ 10^{-5} m/s

The swale was constructed in 2009, using local material without specific layering. The vegetation cover is 1 to 3 cm tall grass during winter and 5 to 10 cm in summer. The 45 cm swale media is comprised of mostly sand mixed with a small portion of gravel and fine sediments (Table 1), based on three samples from the top 30 cm horizon extracted in accordance with ASTM D7263 (ASTM, 2009) and analyzed in accordance with ASTM D6913 (ASTM, 2017) and USDA Soil Textural Classification (USDA, 1987). Three replicas were tested in the laboratory to determine the soil's saturated hydraulic conductivity, K_{sat}, using a constant head permeability test in accordance with ASTM D2434 (ASTM, 2019). Intact soil samples were also collected. Soil porosity and bulk density were then determined. The bed below the 45 cm soil horizon consists of hard compacted clay lying on top of rock.

2.2. Experimental design

Synthetic runoff experiments were conducted in a 5.8 m long, trapezoidal swale section with an average bed width of 2 m (Fig. 2) and longitudinal slope of 3.3%. The side slopes ranged between 10 and 22%. A portable water delivery system, consisting of a 1 m^3 water tank filled with water from a nearby fire hydrant, was designated to feed the swale with simulated runoff inflows. Water was pumped from the tank into a smaller upstream reservoir equipped with a 45° V-notch weir. Flow rates were regulated by ensuring a constant water level in the delivery tank. The overflow from the inflow weir box was distributed evenly over the bottom channel of the swale. The overland flow that did not infiltrate (runoff) was collected using a plastic sheet inserted 20 cm beyond the turf and was directed into the outflow weir box at the end of the swale section.

The runoff simulations were performed using constant inflow rates of 0.2 l/s (very low), 0.65–1.0 l/s (low), 2.0 l/s (medium), and 4.2 l/s (high flow) for a duration of 20–30 min. The experimental runs were timed to target a range of surface and soil conditions (Table 2). On each day, two to three experiments were conducted consecutively with a 30 to 45-minute resting period in between to to allow for all water in the depressions to infiltrate, and to limit the duration of the experiment. A total of 63 runoff simulations were conducted in the period from March 2019 to August 2020 to capture data for winter, the transitional period of thawing during spring, and warm summers when swales are biologically active.

2.3. Data collection

Long-term monitoring. The swale was equipped with five water

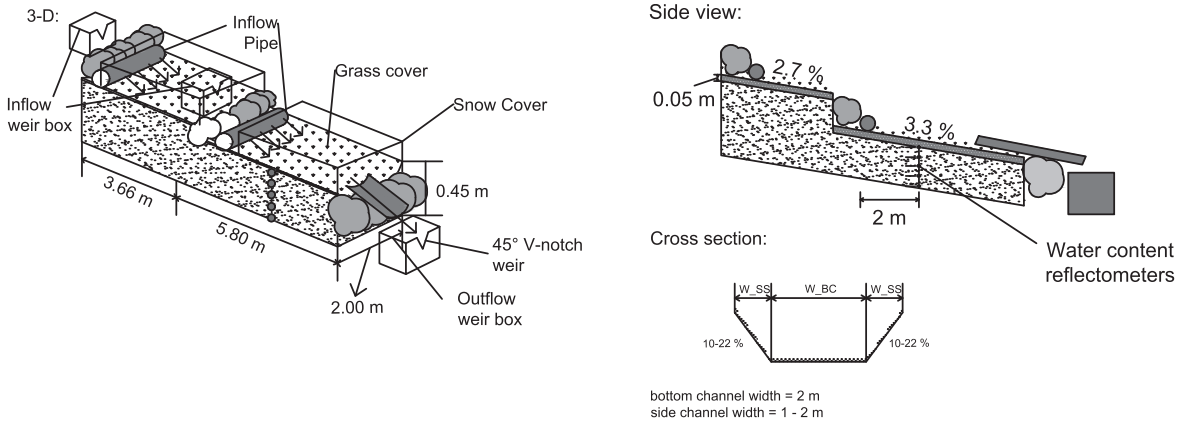

Fig. 2. Schematic of the experimental setup, the swale dimensions and slopes, the location of the inflow and outflow measurements, water content and soil temperature sensors, and the delivery system.

Table 2
Range of experimental initial conditions during the period of spring 2019 to summer 2020.

	DS_{ini} (%)	T_{air} (°C)	T_{surf} (°C)	Q_{in} (l/s)	SD (cm)
Average	70	6.1	5.6	2.0	17.5
Range	49–90	−3 to 19	−1 to 20	Very low: 0.2 Low: 0.65 to 1.0 Medium: 2 ± 0.2 High: 4.2 ± 0.3	2 to 30

Notes: Q_{in} = inflow rate; DS_{ini} = initial degree of saturation; T_{air} = air temperature; T_{surf} = soil surface temperature; SD = snow depth.

content reflectometers that continuously measured volumetric water content and temperature (type CS650, Campbell Scientific, Inc., accuracy ± 1%, Caldwell et al., 2018). The water content reflectometers were installed at the middle of the lower swale section at depths of 5, 15, 25, 35, and 45 cm placed horizontally from top to bottom; the top is located just below the 5 cm thick turf layer (Fig. 2; Right). Readings were logged using a data logger (Campbell Scientific Inc.) every 1 min. A soil-specific calibration was conducted in the laboratory, and a linear user-defined calibration equation was derived ($R^2 = 0.99$).

Ten-minute weather, air temperature, and rainfall data were collected from a weather station erected in February 2019 and operated by the Icelandic Meteorological Office [IMO] on behalf of the Gardabaer municipality (IMO, 2020a). The station is located approx. 70 m downstream from the study swale (Fig. 1). Daily snow depth was obtained from the Reykjavik No.1 weather station (64°07.648′, 21°54.166′; IMO, 2020b). The station is situated on a hilltop vegetated with grass (52 m a.s.l) at a central location in the city at a distance of approximately 6 km from the study site.

Pre/post surface cover conditions. In winter, snow cover depth and density were measured in the field prior to the experimental runs by extracting three snow cores from the side of the swale or the unused swale section. The average and standard deviation of the three measurements were determined. The overall accuracy of the snow depth measurements was determined to be 3–16% and for the snow density 1–13%. Snow height was re-estimated at the end of the consecutive experiments if the snow cover was not fully melted during the experiments. The presence of frost was investigated based on surface hardness, by inserting a blade into the soil and by visually noting the presence of ice crystals in the uppermost 5 cm (Orradottir et al., 2008). Surface and water temperature were measured using a handheld thermometer prior to the experimental run.

Hydrological monitoring during experiments: The inflow and outflow tanks were instrumented with pressure transducers (type Solinst 3001 Levelogger, accuracy ± 0.05% of full range). Water level measured at 10-s intervals was then converted into flow rates using the Kindsvater–Shen equation for V-notch weirs (Shen, 1981).

For the accuracy of the pressure transducer sensors (±3 mm) and the ranges of water level measurements, the overall accuracy of the flow measurements was estimated to be 1–6%. For quality purposes, inflow and outflow rates were also measured manually using a graduated cylinder as well as a stopwatch in case of a calibration error or a sensor malfunction. The effective width and depth of surface flow was measured manually at 1-m intervals along the length of the swale segment. In the presence of snow, the area of snow being wetted was also measured manually at 1-m intervals.

2.4. Derived data

2.4.1. Hydrological performance metrics

For each synthetic experiment, the volume of total flow, the lag time between inflow and outflow, and the peak flow reduction were determined from hydrographs, as shown on Fig. 3a. The relative peak flow reduction or flow attenuation was defined as the difference between the steady state inflow and outflow:

$$\Delta Q_{pkrel} = \frac{Q_{in} - Q_{out}}{Q_{in}} \quad (1)$$

The water balance components in the swale, and due to the limited duration of the experimental runs, can be defined as $V_{in} = V_{inf} + V_{out}$. The inflow volume includes the melt volume from the snowpack, V_{melt}. The total inflow and outflow volumes can be determined by integrating the flow rates, and the relative infiltrated volume or volume reduction, can be defined as

$$\Delta V_{infrel} = \frac{V_{in} - V_{out}}{V_{in}} \quad (2)$$

The lag time between the inflow and outflow, T_{lag}, is defined as the difference between the centroids of the two hydrographs as shown in Fig. 3a (Viessman and Lewis, 2002).

The fourth and final hydrological performance metric is the ratio of the wetted area to the total swale area. In absence of snow, the wetted width increases with the increase in inflow rate. In winter, however, snow cover can influence the effective area for infiltration, as schematically explained in Fig. 3. At the beginning of an event (Fig. 3a), runoff water wets the snow until it reaches its maximum water-holding capacity (wetting phase). This also marks the start of the process of wetting the soil (Fig. 3b and c). Afterwards, the runoff forms a flow path in the snowpack and the flow is concentrated within the resulting channel until it reaches the outflow end of the swale (runoff phase). At this time the soil reaches its maximum saturation and steady-state conditions prevail (Fig. 3b). When the inflow to the swale ceases, runoff continues for an average of 10 min. At this stage, the remaining runoff water exits the swale in the form of outflow and infiltrates the ground and the drainage phase starts. Drainage is a slower process, as

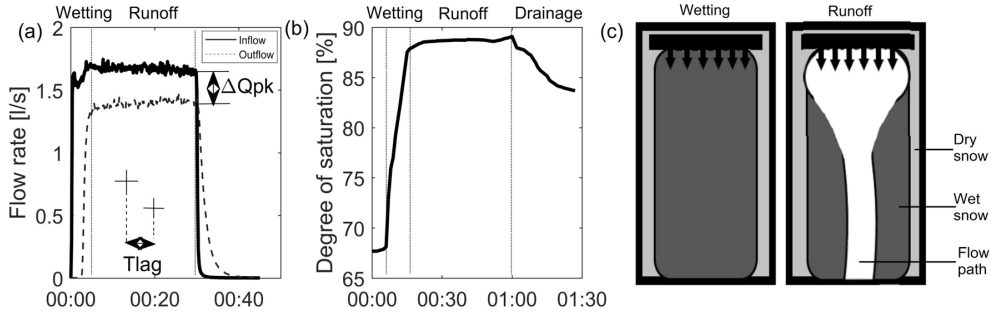

Fig. 3. Example of synthetic experiments data collection conducted on 22.02.2020. (a) Surface hydrological response, (b) subsurface response shown as the total degree of saturation, and (c) schematic of the changes in snow cover during the experimental runs. Dotted vertical lines indicate the different phases of wetting, runoff, and drainage.

can be seen in Fig. 3b as saturation remains almost unchanged following the end of the experiment for a longer period before drainage commences.

The fraction of the wetted area or the areal efficiency, *AE*, was estimated as the ratio of average overland flow width, W_{flow}, and total swale width, W_{total}, taken as the width of the bottom channel of the swale.

$$AE = \frac{W_{flow}}{W_{total}} \tag{3}$$

2.4.2. Soil performance metrics

The swale was divided volumetrically into 5 sections according to the depth at which each sensor was located with a volume of V_i (m^3) and the total moisture content in the swale at time *t*, $V_w(t)$ (m^3), was estimated as

$$V_w(t) = \sum_{i=1}^{5} \theta_i(t) V_i \tag{4}$$

where θ_i is the measured water content by sensor *i* at time *t*.

The degree of saturation in the swale at time *t*, *DS(t)* (%) was then estimated as the ratio of the total moisture volume in the swale V_w at time *t* and saturated moisture volume V_{sat} as

$$DS(t) = \frac{V_w(t)}{V_{sat}} \times 100 \tag{5}$$

The saturated moisture volume was determined as the sum of the available pore volume in each layer based on the measured porosity. Furthermore, an event maximum surface porosity was estimated as the ratio of the measured maximum water content at the surface during the experiment and the measured porosity in the same layer, i.e.

$$\text{Event max surface porosity} = \frac{\max[\theta_{i=1}(t)]}{\text{Porosity}_{\text{measured}}} \times 100 \tag{6}$$

The drainage capacity, *DC*, of the swale was estimated as the reduction in the degree of saturation 24 h after the last event on each experimental day (ΔDS_{24}). Drainage can take from one to two days, depending on the swale's *DC*. A 24-hour drainage period was chosen due to the frequent rain and snowmelt that could lead to the rewetting of the soil before reaching field capacity.

2.5. Data analyses

Winter was defined as the five-month period when air temperature started to descend below 0 °C (November) and lasted until the end of March. Spring was defined as the two months of April and May. Surface conditions during winter and spring were classified into four groups: Neutral, N when neither snow nor frost was present. Frozen, F, if frost was detected with hardness test manually before the experimental run when surface; or alternatively, when soil temperature was below or close to zero, and/or when volumetric water content at 5 cm or deeper remained constant during the synthetic experiment. Snow, S, and Snow on frost, SoF, when snow was present at the surface. Warm conditions, W, indicated the three summer months (June to August), during which surface or soil temperature exceeded 10 °C. The differences between the means of the different surface conditions and seasons for each performance metric were analyzed using analysis of variance (ANOVA), and multiple comparisons were performed using student's *t* test. Statistical analyses were performed using *JMP v. 14.0.0*.

The drivers for hydrological and soil performance metrics were quantified with a two-step linear regression analysis. In the first step, the correlation of performance with each external driver (i.e., inflow rate,

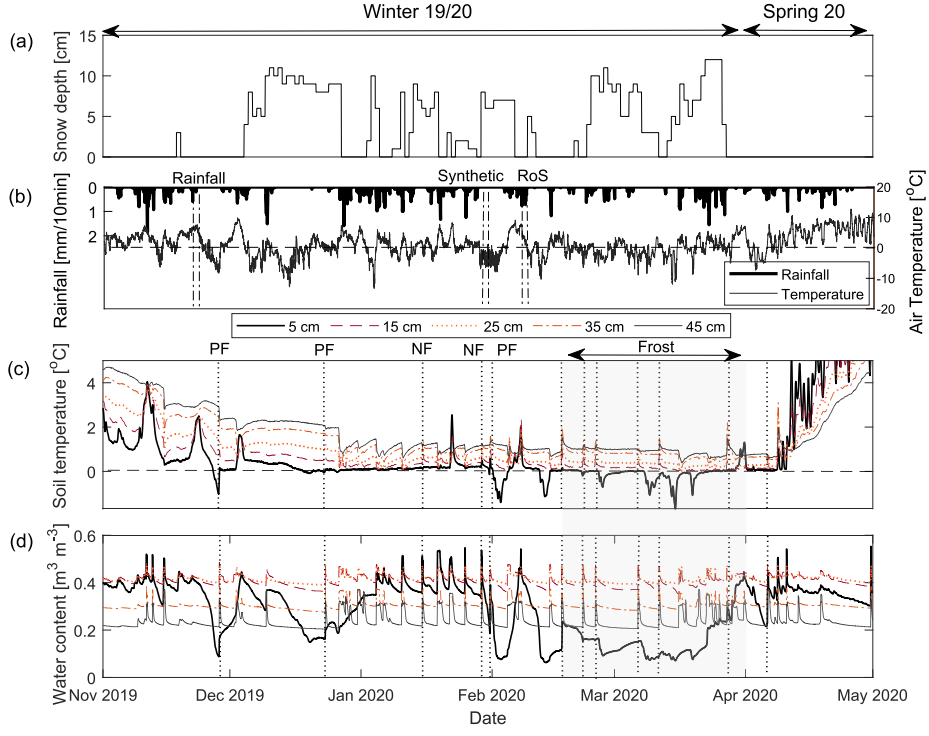

Fig. 4. Meteo-hydrological conditions during winter and spring 2019–2020. (a) Snow depth (Reykjavik Station No. 1), (b) precipitation and air temperature, (c) soil temperature, and (d) soil water content. Double dashed lines = rainfall, synthetic experiments, and RoS events leading to frost. Dotted lines = days at which the synthetic experiments were conducted; Partial frost "PF", no frost "NF", and gray shade highlights the longest soil frost period.

antecedent degree of saturation, surface and soil temperature, and snow depth) was considered. The drivers that had the highest correlation and level of significance were determined as primary drivers. In the second step, a multiple linear regression analysis was conducted first with the primary drivers. Single and multiple linear regression analyses were performed for the performance metrics using performance indicators such as inflow rate, surface and soil temperature, degree of saturation, and snow depth by adding one indicator at a time to each model. For each performance indicator the model with the best coefficient of determination was chosen. Parameters that did not enhance the model performance were eliminated from the analysis.

3. Results

3.1. Continuous monitoring results

The winter and spring 2019–2020 monitoring period was representative of average climatic conditions in Reykjavík (Arnardóttir, 2020): (1) 457 mm of precipitation fell during the six months starting in November; (2) Intermittent snow cover, with 12 snow cycles lasting from 1 to 25 days (Fig. 4a); (3) 21 days of sub-zero average air temperature, the longest cycle lasting for 10 consecutive days (Fig. 4b); (4) 15 soil freeze–thaw cycles, the longest period with sub-zero soil temperature lasted for 15 consecutive days (Fig. 4c). The maximum daily snow depth from Reykjavik Station No.1 was 12 cm, which was approximately half of the range measured in the study swale as the swale can accumulate more snow. During this period, the soil water content remained relatively constant at field capacity at each depth (Fig. 4d). Soil infiltration was noted by the momentary increases in water content at all depths during rain, RoS, and synthetic runoff experiments. Conversely, frost formation was reflected by the reduction in the measured soil water content at 5 cm depth corresponding to the phase change from liquid to solid. The presence of surface frost was identified when the soil moisture content at 5 cm depth did not reach full saturation during the synthetic experiments and/or when soil temperature was below 0 °C prior to the experiment. The most prolonged period of surface frost lasted from February 9 until March 29, 2020 (Fig. 4c and d; shaded area). The runoff experiments (dotted vertical lines; Fig. 4c and d) were timed to capture the range of the experimental conditions, i.e., frost and snow.

3.2. Swale performance indicators

The synthetic runoff experiments in the grass swale highlight hydrological impairment in winter, especially during frost (F) and snow on frost (SoF). With the exception of areal efficiency (*AE*), all performance metrics were statistically lower in presence of frost than when compared to warm ground conditions (Table 3; Fig. 5). Peak flow reduction dropped by a factor of 2.1 and 3.5, and volume reduction by a factor of 1.9 and 2.5 during frost in relation to neutral and warm conditions, respectively (Fig. 5a and b). Similarly, the outflow lag time (T_{lag}), representative of swale residence time, was 2.1 to 3.6 times lower during frost (F). This is consistent with the lower infiltration capacity and surface roughness of the grass cover. The drainage capacity (*DC*) was lowest in the presence of frost (SoF and to a lesser extent F; Fig. 5e). Although the average results for frost conditions were similar for the performance metrics tested (first two columns, Table 3), a greater variance was observed during F than SoF. Specifically, it should be noted that the maximum drainage capacity during frost matched the maximum during the warm period, which suggests that the type of frost or the extent to which the soil was frozen differed considerably.

A large variance was noted in the experimental runs during snow only conditions (S) suggesting that not only snow presence, but also snow characteristics such as depth and density, were influential factors. But on average, volume reduction was significantly higher in the presence of snow compared to frozen conditions (Table 3; Fig. 5b), indicating that a portion of the runoff volume was stored in the snowpack and was not released as outflow. The lag time was also longer, which can be explained by the initial wetting phase being longer in the presence of the snow (Fig. 5c). The *AE*, however, was on average lower during snow than frost conditions (Fig. 5d), consistent with the visual observation of the concentration of surface runoff (Fig. 3c).

The relative influence of surface versus soil conditions on the four hydrologic performance metrics was assessed by considering relationships with external experimental parameters. A single linear regression relationship, SLR, was performed to identify the key external drivers (i.e., inflow rate, antecedent moisture content, temperature, and snow depth), followed by a multiple linear regression analysis, MLR, to assess the relative importance of the top three to four co-acting drivers. Both single and multi-regression analyses highlighted the hydraulic loading

Table 3
Means (standard deviations) of the hydrological performance metrics for the different surface conditions and the level of significance for the comparison between the specific winter conditions i.e., frost (F), snow on frost (SoF), and snow (S) and neutral (N) and warm (W) conditions.

	Winter			Reference	
	F ($n = 10$)	SoF ($n = 9$)	S ($n = 7$)	N ($n = 9$)	W ($n = 24$)
ΔQ_{pk}	12 (7.3)	11 (3.6)	16 (8.5)	25 (8.0)	38 (10)
$_{rel}$	**/***	**/***	+/***		
ΔV_{inf}	19 (11)	20 (8.5) */***	39 (26) +/+	37 (11)	50 (14)
$_{rel}$	**/***				
T_{lag}	1.6 (0.8)	2.3 (1.2) +/*	7.4 (8.0) */+	3.3	5.7
	+/**			(2.2)	(3.0)
AE	58 (11) +/+	53 (8.6) +/*	43 (16) */***	58 (11)	63 (11)
DC	21 (5.3) +/*	20 (0.8)	23 (3.3) +/+	22 (3.0)	26 (1.5)
		+/***			

Notes: Significance in relation to N/W. $^{+}$ $p > 0.05$ * $p < 0.05$ ** $p < 0.01$ *** $p < 0.001$.

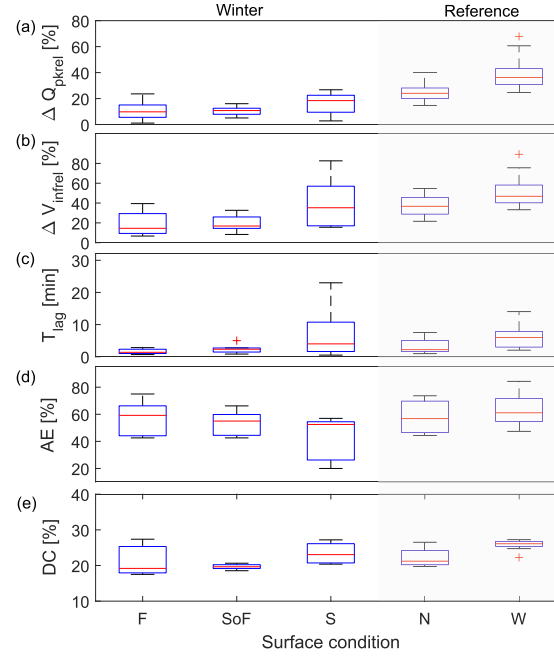

Fig. 5. Hydrological performance metrics in terms of surface conditions. (a) Relative peak flow reduction, (b) relative volume infiltrated, (c) runoff lag time, (d) areal efficiency, and (e) soil drainage capacity.

Table 4
Multiple and single regression for the performance metrics, regression coefficients, standards error, correlation coefficients, and models R^2. Not included parameters referred to as N/I.

Model		$\Delta Q_{pk\ rel}$		$\Delta V_{inf\ rel}$		*AE*		T_{lag}	
		B (SE)	*r*	*B (SE)*	*r*	*B (SE)*	*r*	*B (SE)*	*r*
1	Q_{in}	−2.95 (0.77)	−0.38**	−6.61 (1.33)	−0.47***	5.82 (0.96)	0.51***	−1.50 (0.27)	0.24***
	T_{sur}	1.41 (0.17)	0.76***	1.51 (0.27)	0.62***	N/I	N/I	0.19 (0.06)	0.06^{+}
	T_{soil}	N/I	N/I	N/I	N/I	0.96 (0.25)	0.36**	N/I	N/I
	R^2	0.66***		0.53***		0.47***		0.27***	
2	DS_{ini}	N/I	N/I	−0.24 (0.18)	−0.01^{+}	N/I	N/I	−0.05 (0.04)	0.00^{+}
	SD	−0.17 (0.15)	−0.34^{+}	0.38 (0.25)	−0.07^{+}	−0.37 (0.19)	−0.28^{+}	0.27 (0.05)	0.17**
	R^2	0.68***		0.57***		0.51***		0.58***	

Notes: B = regression coefficient for MLR. SE = std. error. r = correlation coefficient for SLR. $^{+}p > 0.05$ * $p < 0.05$ ** $p < 0.01$ *** $p < 0.001$. T_{sur} = surface temperature. T_{soil} = avg. soil temperature 5–45 cm depth. DS_{ini} = initial degree of saturation. SD = snow depth.

(presented as inflow rate, Q_{in}) and surface temperature as the primary performance drivers for the event-based performance metrics, followed by initial snow depth (Table 4). Because of the considerable intercorrelation between surface temperature and soil temperature, only the parameter with higher correlation was incorporated in the multi-regression models.

The MLR confirmed that higher hydraulic loading reduced the flow attenuation, on the one hand, while increasing *AE* on the other hand (note signs in Table 4). Low surface and soil temperatures and high snow depth reduced the performance. These three external drivers accounted for 68% and 57% of the natural variance of flow and volume reduction, and 51% for *AE*. T_{lag} was largely governed by the inflow rate and snow depth which contributed to delayed outflows. Surface temperature was not significantly correlated with T_{lag} in the SLR but was significant in the overall MLR model. The initial degree of saturation was not significant but did enhance the MLR model. *DC* differed vastly from the other performance metrics by being neither affected by surface conditions nor hydraulic loading (not shown, Table 4). Instead, the degree of saturation 24 h after the event was found to be mostly regulated by the maximum degree of saturation, DS_{max}, which was attained during the event, as well as the 24-hour average soil temperature after the event. These two soil-related parameters accounted for 64% of the variance.

Peak flow reduction was a measure of the steady state abstraction due to infiltration during the experiments using the constant flow rates

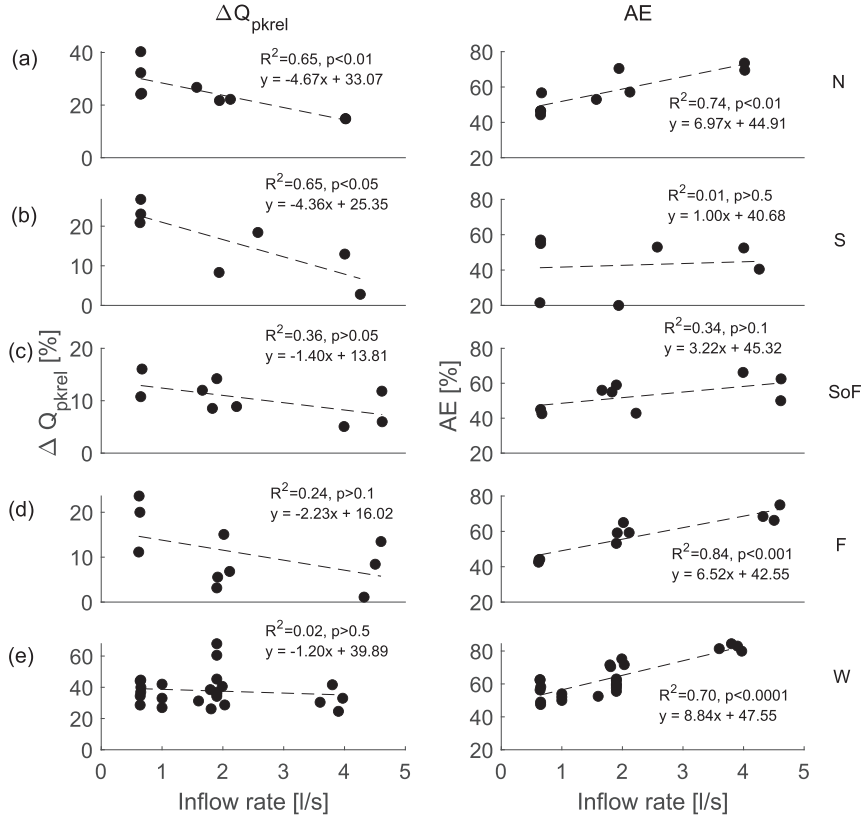

Fig. 6. Linear regression between hydrological inputs (Q_{in}) and peak flow reduction (left) and areal efficiency (right) for different surface conditions. (a) Neutral, (b) snow, (c) snow on frost, (d) frost, and (e) warm conditions.

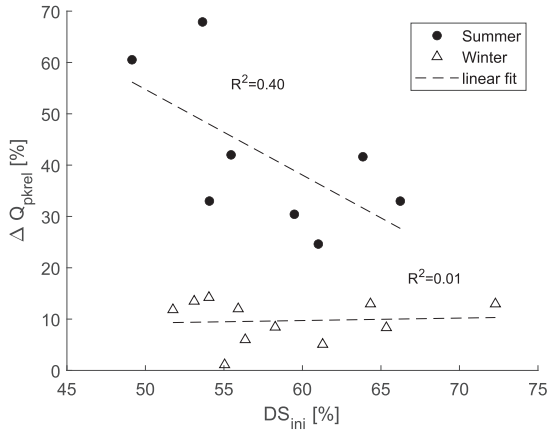

Fig. 7. Linear regression between the initial degree of saturation of the first events and peak flow reduction in summer (dot) and winter (triangle).

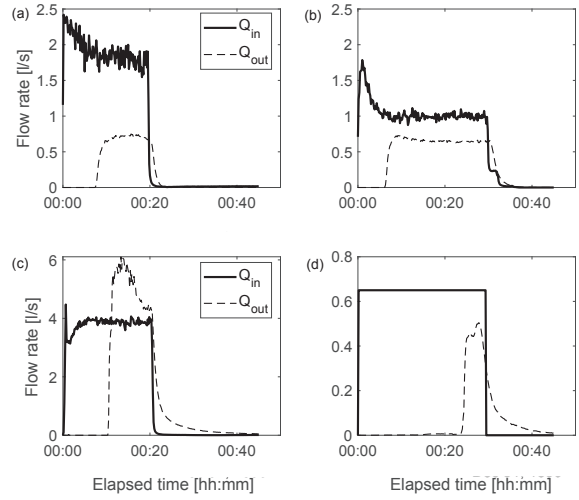

Fig. 8. Selected runoff events hydrographs. (a) Medium inflow with low degree of saturation, (b) low inflow with high degree of saturation, (c) high inflow with 30 cm of snow and frozen soil, and (d) low inflow with 30 cm of snow and unfrozen soil.

in this study. Upon reaching steady state, infiltration volume becomes independent of inflow rate. Hence, the flow attenuation decreased with the increase in inflow rate. This relationship was strongest in neutral winter conditions ($R^2 = 0.65$, $p < 0.01$; Fig. 6a). In snow conditions, the underlying soil was similar in nature to neutral conditions and consequently the relationship was just as strong (Fig. 6b). But as snow reduced *AE*, the flow and volume attenuation were lower than in neutral conditions. In the presence of frost (F and SoF), the relationship was less strong and more variations in infiltration capacity were observed (Fig. 6c and d; left panel). In frost only conditions, the relationship between inflow rate and *AE* was stronger than when snow was present on top of frost as expected (Fig. 6c and d; right panel). In warm conditions, however, the relationship between inflow rate and flow attenuation broke down (Fig. 6e). This suggests that another factor was influencing peak flow reduction, i.e., the initial degree of soil saturation, which, as previously mentioned, did not significantly influence the hydrologic performance metrics over the entire season ($p > 0.05$, Table 4). Nevertheless, the antecedent degree of saturation was found to be a major driver explaining the variability in flow attenuation in summer, albeit not statistically significant at the 5% level (Fig. 7). In winter, the degree of saturation did not exert a significant influence on peak flow reduction.

3.3. Hydrologic response of the swale

No significant correlation was found between hydrological performance of the swale and either snow depth or the initial degree of saturation over the entire study period (Table 4). However, a closer look at specific runoff experiments provides valuable insights into the processes that were not fully explained by statistical significance tests. To better understand the relationship between the hydrological response and the initial degree of saturation, the hydrographs of two consecutive experiments in summer 2019 were considered (Fig. 8a and b). Preceded by an abnormally long dry period of 2 weeks, the initial degree of saturation was at an absolute seasonal low (50%) prior to the former, medium flow experiment. The corresponding peak flow and volume reductions were the highest recorded throughout the study period for a medium flow (61 and 75%, respectively). The initial degree of saturation was much higher in the consecutive experiment (70%). A higher outflow rate was observed in the second experiment despite the much lower inflow rate used. Consequently, flow and volume reductions were reduced by a factor of 2 due to the increase in the initial water content (Fig. 8b).

Regression analyses indicated a negative relationship between snow depth and the swale performance metrics (Table 4), though not statistically significant. This confirmed that runoff events became more voluminous with the addition of meltwater. But this result is not generalizable, as noted from the hydrographs during two runoff experiments with 30 cm thick snow cover (Fig. 8c and d). When the soil was frozen and a high inflow rate was used, the water was initially stored in the snow to be suddenly released afterwards in a dam-burst- like manner, producing an outflow peak that exceeded the inflow rate. However, volume reduction was 23% due to the storage of runoff water in the snowpack. In contrast, when the soil was not frozen and a low inflow rate was used, the delay in outflow was 24 min which is the longest T_{lag} observed during the study period. The runoff peak did not surpass the inflow rate and the volume reduction was as high as 83%. This indicated that the presence of thick snow cover can either accentuate or severely attenuate runoff peaks, while providing considerable volume reduction.

3.4. Soil response during winter runoff events

Long-term measurements of soil and hydrological inputs provide valuable insights into the influential factors that contributed to frost formation. The first surface frost occurred after a rainfall event on November 22 (Fig. 4b; double dashed line) that was followed by a freezing cycle (min. −8.3 °C). The second soil frost period occurred in December due to a long period of surface cooling. The soil thawed in January, during which time the water content at 5 cm repeatedly peaked at 54% (corresponding to 99% degree of saturation). Two synthetic experiments on January 29 and 31 accompanied with subfreezing air temperature (min. −6.4 °C), led to frost formation at the 5 cm soil horizon, during this period the soil temperature dropped to a minimum of −1.3 °C. Frost was interrupted once again on February 7 as a result of a RoS event accompanied by an increase in air temperature (max. 8.1 °C). Following that, a sharp reduction in temperature was recorded (min. −10 °C), and with the absence of an insulating snow cover, surface water content dropped dramatically to 7%. These frost conditions were maintained for almost one and a half months, which was reflected in both an uncharacteristically low water content and limited response at 5 cm soil depth during the subsequent runoff events. The successive wetting of the soil during this period resulting from the multiple snowmelt events, as well as the synthetic runoff experiments led to the

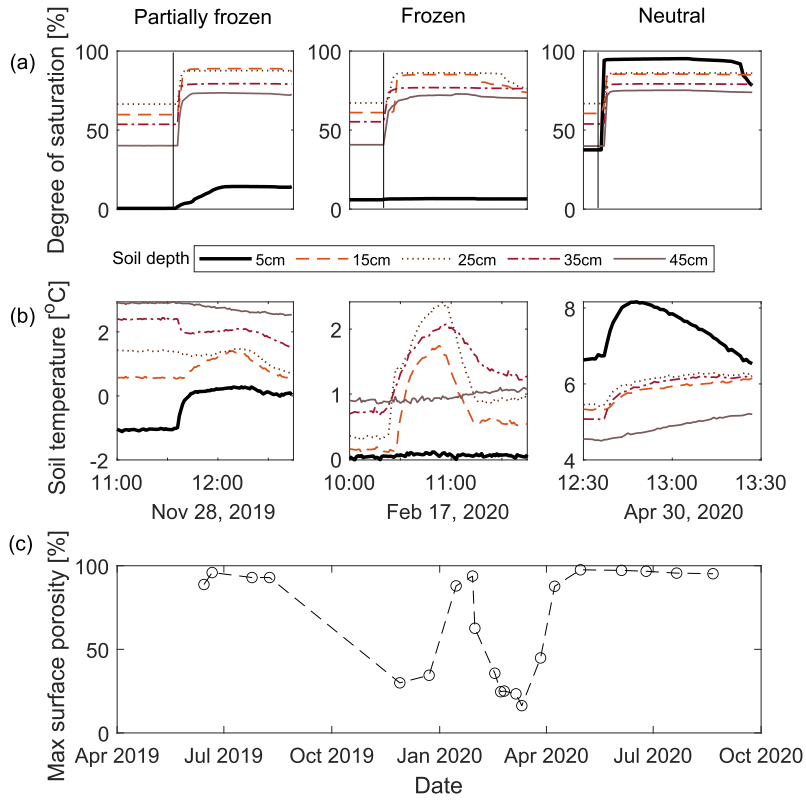

Fig. 9. Soil response during synthetic events with different soil conditions (from left to right = partially frozen, frozen, and neutral). (a) Degree of saturation, (b) soil temperature, and c) effective porosity within the first layer during synthetic experiments. Solid vertical line indicates the start of runoff.

extended period of frozen soil which lasted until the end of winter.

A closer look at the changes in soil saturation and temperature during specific events gives insights into the variations in frost type and infiltration capacity. When the soil was partially frozen (Fig. 9a; left panel), the water content in the deeper layers responded almost immediately to hydrological inputs while the top layer responded gradually peaking at 14% saturation at the end of the experiment. Hence, pore ice was present in the top 5 cm throughout the experiment, while, at the same time, allowing water to seep to the non-frozen ground below. Moreover, infiltrating water melted some of the frost in the topsoil during the experiment. This suggests that preferential flow paths and/or air-filled pores were present within the top frozen layer. During the most severe frost event (February 17; Fig. 9a; center), the deeper layers of the soil also responded to the runoff at the surface. However, the response was slightly delayed indicative of more resistance to the flow which might have resulted from frost penetration within the 5–15 cm soil horizon and thereafter thawing with the infiltrating water (Fig. 9a and b; center). It should be noted that the topsoil was frozen throughout the inflow period (i.e., soil saturation remained at 6%). In spite of this, downward water movement was still observed in the swale media. By the end of April (Fig. 9a; right), the soil returned to neutral conditions, as attested by the increase in saturation in the entire soil profile during the experiment on April 30. Lastly, the seasonal variations in soil porosity of the top layer throughout the study period showed two interrupted periods of low porosity. The first of these was during experiments in November and December and the second during experiments in February and March (Fig. 9c). Afterwards, the topsoil's porosity increased from 87% on April 8 to 98% on April 30 when the soil thawed completely. This suggested that the swale did not undergo a consistent reduction in infiltration capacity during winter but was subjected to repeated cycles of freezing and thawing as a result of the frequent rainfall events accompanied with an increase in air temperatures.

4. Discussion

4.1. Seasonal swale performance in cold maritime climate

The focus of this research was on the winter performance of grass swales, which are usually designed to infiltrate and treat small rainfall events and attenuate peak flow from large events (Woods Ballard et al., 2015). The 5.8 m long test section of the swale infiltrated on average 46% of the low flow rates (0.65–1 l/s) during the study period, which covered winter, spring, and summer. These low hydraulic loadings constituted almost half of the measured flows naturally entering the SuDS system. The infiltration was, on average, 7% and 32% for the higher flowrates during winter and summer, respectively. During extreme frozen conditions, a significant reduction in infiltration capacity was observed. Nevertheless, there were no indications that the swale capacity was exceeded. Overflowing of the side slopes was never observed in the swale, and the average flow depth was below 10 cm.

The winter hydrological performance decline observed in this study was consistent with previous research connecting reduced winter performance with vegetation dormancy and lower temperatures (Roseen et al., 2009). But more importantly, this study showed that the winter performance in a cold maritime climate fluctuated on a synoptic basis because of intermittent frost formation at the surface, and to a lesser extent, frequent snow cycles. The results of this study are best compared

with SuDS studies in cold coastal regions experiencing frequent freeze–thaw and RoS events, namely in the prairie environments in Canada and in Norway. Khan et al. (2012) observed an average peak flow reduction in bioretention cells of 92% for winter events with hydraulic loading of 25 cm/h. This was attributed to the water eventually infiltrating via preferential flow paths and reaching the underdrain without utilizing the entire media despite the presence of frost at a depth of 15 cm. Similarly, Paus et al. (2015) found that the total volume reduction achieved by three bioretention cells ranged between 55 and 100%. In contrast, the average flow attenuation in the swale in this study was only 13% for hydraulic loadings ranging between 19 and 131 cm/h. This comparison supports the findings of Roseen et al. (2009) that swales suffer the most noticeable performance decline in winter of SuDS elements. This can be attributed to the shorter retention time in a conveyance-based system such as swales compared to retention-based systems such as bioretention cells.

4.2. The interactions between runoff, snow, and soil frost

Muthanna et al. (2008) hypothesized that RoS played a role in frost formation based on the observation that the infiltrated stormwater refroze following both RoS and rainfall events. Roseen et al. (2009) also noted that frost resulting from freeze-thaw cycles was common and that soil freezing usually occurred before and after rain and snowmelt events. However, neither study quantified the effects of the frequent freeze–thaw cycles, the interactions between snow and frost, or their impact on subsequent events. In this study, however, synthetic runoff events were conducted in the presence of snow with the intention to simulate RoS events. Closely spaced water content and temperature measurements at different soil depths allowed for a continuous assessment of soil infiltration and frost formation in grass swales over an entire winter. The results clearly demonstrate that intermittent midwinter rain and RoS events led to high water contents and promoted frost formation. Specifically, during winter 19/20, three events (natural and synthetic) initiated separate freezing cycles which reduced soil porosity (Fig. 4c and d). The temporal wetting of the soil, which in some cases was combined with the removal of the snow cover, rendered the soil more susceptible to temperature fluctuations, as evidenced in the sharp reduction in soil temperature following these events (Fig. 4c). This is a common complication with the implementation of SuDS in coastal cold regions that experience repeated RoS and freeze–thaw cycles (Khan et al., 2012; Muthanna et al., 2008).

4.3. Key mechanisms affecting winter infiltration

The primary mechanism for hydrological performance deterioration was soil frost. Soil permeability in the presence of frost varied across experiments due to the heterogeneous nature of soils and frost formation, as well as the presence of cracks and preferential flow paths resulting from the frequent freeze–thaw cycles. Spatial variability was observed in six single-ring infiltration measurements conducted in an adjacent swale (Zaqout, unpublished data). On any given day, infiltration was impeded in certain locations while it was not affected in other locations. The formation of porous or granular frost with loose ice crystals may permit or even enhance infiltration (Flerchinger, 2013). A common factor that influences infiltration is frost depth (Fach et al., 2011). In this study, frost was only detected in the topmost layer at 5 cm soil depth (Fig. 4c and d). It is not clear how far the frost penetrated between 5 and 15 cm depth. Soil temperature at 5 cm intervals within the first 20 cm of the profile would have helped clearing this ambiguity on maximum frost depth. However, an excellent indication of soil infiltration and frost formation throughout the soil matrix was provided by water content probes spaced 10 cm apart (see Fig. 9 and discussion thereof).

The secondary mechanism that negatively affected winter performance was snow cover. Snow reduced the swale's surface area by concentrating surface runoff which would have otherwise been more evenly distributed in snow-free conditions. Moreover, the added snowmelt led to more voluminous runoff events and reduced water temperature, which negatively affects infiltration. Nevertheless, for the least intense runoff experiments (low flow), snow was also found to enhance the hydrological performance by storing significant amounts of runoff water and by delaying flow peaks. This storage function was dependent, however, on snow properties and the underlying soil conditions. Water stored in the snowpack was released instantaneously in a "dam-burst-like" release of water when thick snow was coupled with the presence of soil frost or dense snow layers. Such a burst was only observed once in this study, making further investigations necessary to verify the results. Lastly, the storage function of the snow becomes less important in longer duration events, as all of the snow will melt eventually and add to runoff. Most of the extreme winter flooding events recorded in Reykjavík involved >6 h of rainfall (Arnardóttir, 2020).

4.4. The importance of soil drainage in design

Previous studies have found that initial degree of saturation negatively influences the hydrological performance of SuDS (Rujner et al., 2018). This relationship was only detected during summer in this study, after dry periods lasting for weeks at a time (Fig. 7). Degree of saturation is highly linked with *DC*: Poorly drained soils tend to maintain a high degree of saturation, which in turn reduces their capacity to mitigate subsequent events. A *DC* in the range of only 20 to 26%, as in this study, might have exacerbated the impacts of winter conditions and promoted frost formation. Additionally, the high water content in the swale also affected the performance during non-frozen conditions by reducing the available volume for infiltration at the onset of runoff events. This was consistent with the previous findings from studies on infiltration-based systems (e.g., LeFevre et al., 2009; Muthanna et al., 2008) and emphasizes the importance of proper soil drainage, especially for winter operations.

We argue that *DC* is particularly important in a cold maritime climate, which frequently experiences precipitation in liquid form (as opposed to solely dry snow). The combination of liquid inputs and poor *DC* makes the soils more susceptible to freezing, even though air temperatures fluctuate only moderately around zero (the minimum daily temperature recorded in Reykjavík is −12 °C). Frost events particularly occurred 1–2 days following rainfall, simulated runoff, and RoS events which might not have been a long enough period to properly drain the swale media prior to the onset of freezing air temperatures. This was observed in the sharp drops in moisture content and soil temperature at 5 cm depth after the November 22, January 29 and 31, February 11 and 25, March 6 and 11 events (Fig. 4c and d). Frost formation was confirmed in the runoff experiments following those events and it was reflected in the deterioration in performance indicators.

To maintain a good soil drainage, and reduce the risk of frost formation, care must be taken in the design and operation of swales. Fine-textured soils such as clay and silt should be avoided in the filter media due to their low infiltration capacity and high water holding potential. Dust accumulation might occur when swales are located next to roads or parking lots with heavy traffic, especially in cold climates where studded tires that increase road erosion are used extensively (Barr, 2020). Filter strips are often used to capture road dust and sediments before entering the swale. In this study, the swale was adhering to best practices, but the swale filtering media laid on hard compacted clay. This might explain the low drainage capacity observed throughout the study period.

5. Conclusions

Maritime winter climate is both wet and mild, with air temperatures fluctuating around the freezing point and precipitation falling as rainfall, rain-on-snow and snow. This research assesses the impacts of co-acting winter conditions on the hydrological performance of grass

swales. To that goal, 63 synthetic runoff experiments were performed in a grass swale over 18 months. The swale hydrological performance was evaluated based on five metrics: the relative peak flow reduction, the relative infiltrated volume, runoff lag time, soil drainage capacity, and areal efficiency.

Results indicated a significant impairment in the hydrologic performance during winter. Peak flow attenuation was 13% in winter as compared to 20–40% in spring and summer. Similarly, the relative infiltrated volume was 22% in winter vs. 30–60% during the warm season. Poor flow attenuation was primarily associated with the reduction in soil porosity in the top 5 cm horizon because of the formation of ice lenses. However, macropores created by vegetation roots, biological activity, and the frequent freeze–thaw cycles allowed for infiltration to the deeper layers of the soil. Thus, no concrete frost fully blocking infiltration was observed during the study period. Runoff lag times where three times shorter in winter compared to summer reflecting a reduction in surface roughness. While the surface frost significantly reduced the overall performance of the swale, it did not compromise the swale overall function of attenuating small and medium events.

Snow cover provided both initial storage and resistance to overland flow resulting in longer lag times and high volume reduction during short-duration, low hydraulic loading events. But as an event progressed, overland flow formed in a concentrated path within the snowpack, effectively reducing the area of infiltration. The snow melted and added to the runoff volume. In the most severe case, the runoff initially stored in a thick snow was released instantaneously similar to a dam burst to the effect that the outflow exceeded inflow the swale. Hence, the combination of sudden snowmelt and low infiltration capacity can generate more intense rain-on-snow induced runoff events. However, this condition was observed only once in this study.

This study provided, to the authors' best knowledge, the first systematic assessment of the relative importance of hydraulic loading, surface and soil conditions on the seasonal performance of grassed swales in a cold climate. Single and multivariate regression analyses highlight that winter peak flow and volume reduction were primarily affected by surface temperature, followed by hydraulic loading and to a lesser extent snow depth. The moisture content of the underlying soil did not significantly affect the infiltration in winter but played a large role in explaining the variance in summer performance. The highest infiltration capacity observed in this study was when the soil was half saturated, which occurred in summer following a two-week dry period. Runoff lag times and areal efficiency were primarily affected by inflow rate and secondarily by surface conditions, such as snow depth. Soil drainage capacity was, however, governed by the 24-hour average swale media temperature following the event and the maximum soil saturation reached during the event.

In a maritime climate, with air temperature oscillating in the order of 15 times around the freezing point during winter, precipitation falls often in liquid form. Frequent rain and rain-on-snow infiltrates the ground which keeps the soil moist. In the absence of an insulating snow cover, the soil is more susceptible to freezing. Frost was observed to form within 1–2 days after runoff events, which negatively affected the swale's ability to infiltrate subsequent events. This combined with a soil drainage capacity of only 20–26% in 24 h, as found in this study, kept the soil highly saturated during winter and more susceptible to freezing.

With rising winter temperatures, regions that historically underwent a seasonal frost and snow period may now experience more frequent and intense mid-winter rain-on-snow followed by frost. This study confirms that SuDS may serve as a low impact, low-cost solution to reduce urban flooding in such cyclic climatic winter conditions. A special attention is, however, required in the design and operation of SuDS in relation to rain-on-snow and frost cycles. Proper soil drainage is instrumental in order to maintain the soil relatively dry and less susceptible to the frequent freezing. Limiting the presence of fine sediments that decrease infiltration is required both in the filter media during the construction phase and from surface loading during the operation lifetime of swales. The reduction in infiltration capacity during winter must also be taken into account when sizing SuDS. Therefore, incorporating site-specific considerations is recommended for the designing of infiltration-based components.

CRediT authorship contribution statement

Tarek Zaqout: Conceptualization, Methodology, Software, Validation, Formal analysis, Investigation, Resources, Data curation, Writing - original draft, Visualization. **Hrund Ólöf Andradóttir:** Conceptualization, Methodology, Resources, Supervision, Project administration, Funding acquisition.

Declaration of Competing Interest

The authors declare that they have no known competing financial interests or personal relationships that could have appeared to influence the work reported in this paper.

Acknowledgements

This research was funded by the Icelandic Research Fund (Icelandic: Rannís), grant number 185398-053. We thank the Garðabær Municipality, Iceland Meteorological Office, in particular, for operating the Urriðaholt weather station; Urriðaholt ehf, the Department of Water Supply in Garðabær, and the Fire Department in Hafnarfjörður for the help with running the field program. We also thank Halldóra Hreggviðsdóttir for her instrumental help with starting this research project. We are also grateful to Guðni Þorvaldsson and Berglind Orradóttir at The Agricultural University of Iceland for their help in setting up the soil monitoring program. A special thanks goes to our technician Vilhjálmur Sigurjónsson for his help with the experimental setup. The authors also thank the four anonymous reviewers for their thoughtful feedback on the manuscript.

Appendix A. Supplementary data

Supplementary data to this article can be found online at https://doi.org/10.1016/j.jhydrol.2021.126159.

References

Abu-Zreig, M., Rudra, R.P., Lalonde, M.N., Whiteley, H.R., Kaushik, N.K., 2004. Experimental investigation of runoff reduction and sediment removal by vegetated filter strips. Hydrol. Process. 18 (11), 2029–2037. https://doi.org/10.1002/hyp.1400.

Ahmed, F., Gulliver, J.S., Nieber, J.L., 2015. Field infiltration measurements in grassed roadside drainage ditches: Spatial and temporal variability. J. Hydrol. 530, 604–611. https://doi.org/10.1016/j.jhydrol.2015.10.012.

Arnardóttir, A. R. (2020). Winter Floods in Reykjavík: Coaction of Meteorological and Soil Conditions. Master thesis.

ASTM. (2009). D7263, Standard Test Methods for Laboratory Determination of Density (Unit Weight) of Soil Specimens. ASTM International, West Conshohocken, PA. https://www.astm.org/Standards/D7263.htm.

ASTM. (2017). D6913, Standard Test Methods for Particle-Size Distribution (Gradation) of Soils Using Sieve Analysis. ASTM International, West Conshohocken, PA. https://www.astm.org/Standards/D6913.htm.

ASTM. (2019). D2434, Standard Test Method for Permeability of Granular Soils (Constant Head). ASTM International, West Conshohocken, PA. https://www.astm.org/Standards/D2434.htm.

Bäckström, M., Viklander, M., 2000. Integrated stormwater management in cold climates. J. Environ. Sci. Health, Part A 35 (8), 1237–1249. https://doi.org/10.1080/10934520009377033.

Barr, B. (2020). Processes and Modeling of Non-Exhaust Vehicular Emissions in the Icelandic Capital Region. Master thesis.

Blecken, G.-T., Zinger, Y., Muthanna, T.M., Deletic, A., Fletcher, T.D., Viklander, M., 2007. The influence of temperature on nutrient treatment efficiency in stormwater biofilter systems. Water Sci. Technol.: J. Int. Assoc. Water Pollut. Res. 56 (10), 83–91. https://doi.org/10.2166/wst.2007.749.

Caldwell, T.G., Bongiovanni, T., Cosh, M.H., Halley, C., Young, M.H., 2018. Field and laboratory evaluation of the CS655 soil water content sensor. Vadose Zone J. 17 (1) https://doi.org/10.2136/vzj2017.12.0214.

Caraco, D., Claytor, R., 1997. Stormwater BMP Design: Supplement for Cold Climates. Center for Watershed Protection, Ellicott City, MD, pp. 1–96.
Davis, A.P., Stagge, J.H., Jamil, E., Kim, H., 2012. Hydraulic performance of grass swales for managing highway runoff. Water Res. 46 (20), 6775–6786. https://doi.org/10.1016/j.watres.2011.10.017.
Deletic, A., Fletcher, T.D., 2006. Performance of grass filters used for stormwater treatment – A field and modelling study. J. Hydrol. 317 (3–4), 261–275. https://doi.org/10.1016/j.jhydrol.2005.05.021.
Dietz, M.E., Clausen, J.C., 2008. Stormwater runoff and export changes with development in a traditional and low impact subdivision. J. Environ. Manage. 87 (4), 560–566. https://doi.org/10.1016/j.jenvman.2007.03.026.
Dong, C., Menzel, L., 2020. Recent snow cover changes over central European low mountain ranges. Hydrol. Process. 34 (2), 321–338. https://doi.org/10.1002/hyp.13586.
Fach, S., Engelhard, C., Wittke, N., Rauch, W., 2011. Performance of infiltration swales with regard to operation in winter times in an Alpine region. Water Sci. Technol. 63 (11), 2658–2665. https://doi.org/10.2166/wst.2011.153.
Flerchinger, G. N., Lehrsch, G. A., & McCool, D. K. (2013). Freezing and Thawing | Processes. In Reference Module in Earth Systems and Environmental Sciences (p. B9780124095489053000). Elsevier. 10.1016/B978-0-12-409548-9.05173-3.
García-Serrana, M., Gulliver, J.S., Nieber, J.L., 2017. Infiltration capacity of roadside filter strips with non-uniform overland flow. J. Hydrol. 545, 451–462. https://doi.org/10.1016/j.jhydrol.2016.12.031.
Garvelmann, J., Pohl, S., Weiler, M., 2015. Spatio-temporal controls of snowmelt and runoff generation during rain-on-snow events in a mid-latitude mountain catchment. Hydrol. Process. 29 (17), 3649–3664. https://doi.org/10.1002/hyp.10460.
Gavrić, S., Leonhardt, G., Marsalek, J., Viklander, M., 2019. Processes improving urban stormwater quality in grass swales and filter strips: A review of research findings. Sci. Total Environ. 669, 431–447. https://doi.org/10.1016/j.scitotenv.2019.03.072.
Khan, U.T., Valeo, C., Chu, A., van Duin, B., 2012. Bioretention cell efficacy in cold climates: Part 1 – Hydrologic performance. Can. J. Civ. Eng. 39 (11), 1210–1221. https://doi.org/10.1139/l2012-110.
Iceland Meteorological Office [IMO] (2020a). Ten-minute Weather and Rainfall Data at Gardabaer, Urridaholt Station No. 1474. Data delivery April 21, 2020.
Iceland Meteorological Office [IMO] (2020b). Daily Snow Depth at Reykjavík Manned Synoptic Station No. 1.
LeFevre, N.J., Davidson, J.D., Oberts, G.L., 2009. Bioretention of simulated snowmelt: Cold climate performance and design Criteria. Cold Regions Eng. 2009, 145–154. https://doi.org/10.1061/41072(359)17.
Liu, Y.-J., Hu, J.-M., Wang, T.-W., Cai, C.-F., Li, Z.-X., Zhang, Y., 2016. Effects of vegetation cover and road-concentrated flow on hillslope erosion in rainfall and scouring simulation tests in the Three Gorges Reservoir Area, China. Catena 136, 108–117. https://doi.org/10.1016/j.catena.2015.06.006.
Moghadas, S., Leonhardt, G., Marsalek, J., Viklander, M., 2018. Modeling urban runoff from rain-on-snow events with the U.S. EPA SWMM Model for Current and Future Climate Scenarios. J. Cold Reg. Eng. 32 (1), 04017021. https://doi.org/10.1061/(ASCE)CR.1943-5495.0000147.
Monrabal-Martinez, C., Aberle, J., Muthanna, T.M., Orts-Zamorano, M., 2018. Hydrological benefits of filtering swales for metal removal. Water Res. 145, 509–517. https://doi.org/10.1016/j.watres.2018.08.051.
Muthanna, T.M., Viklander, M., Thorolfsson, S.T., 2008. Seasonal climatic effects on the hydrology of a rain garden. Hydrol. Process. 22 (11), 1640–1649. https://doi.org/10.1002/hyp.6732.
Orradottir, B., Archer, S.R., Arnalds, O., Wilding, L.P., Thurow, T.L., 2008. Infiltration in Icelandic Andisols: The role of vegetation and soil frost. Arct. Antarct. Alp. Res. 40 (2), 412–421. https://doi.org/10.1657/1523-0430(06-076)[ORRADOTTIR]2.0.CO;2.
Paus, K.H., Muthanna, T.M., Braskerud, B.C., 2015. The hydrological performance of bioretention cells in regions with cold climates: Seasonal variation and implications for design. Hydrol. Res. nh2015084 https://doi.org/10.2166/nh.2015.084.
Roseen, R.M., Ballestero, T.P., Houle, J.J., Avellaneda, P., Briggs, J., Fowler, G., Wildey, R., 2009. Seasonal performance variations for storm-water management systems in cold climate conditions. J. Environ. Eng. 135 (3), 128–137. https://doi.org/10.1061/(ASCE)0733-9372(2009)135:3(128).
Rujner, H., Leonhardt, G., Marsalek, J., Perttu, A.-M., Viklander, M., 2018. The effects of initial soil moisture conditions on swale flow hydrographs. Hydrol. Process. 32 (5), 644–654. https://doi.org/10.1002/hyp.11446.
Shafique, M., Kim, R., Kyung-Ho, K., 2018. Evaluating the capability of grass swale for the rainfall runoff reduction from an urban parking Lot, Seoul, Korea. Int. J. Environ. Res. Public Health 15 (3), 537. https://doi.org/10.3390/ijerph15030537.
Shen, J. (1981). Discharge Characteristics of Triangular-notch Thin-plate Weirs. United States Department of the Interior, Geological Survey.
USDA. (1987). Soil Mechanics Level 1: Module 3—USDA Textural Soil Classification. Study Guide.
Valeo, C., Ho, C.L.I., 2004. Modelling urban snowmelt runoff. J. Hydrol. 299 (3), 237–251. https://doi.org/10.1016/j.jhydrol.2004.08.007.
Viessman, W., Lewis, G.L., 2002. Introduction to Hydrology, 5th edition. Prentice Hall.
Woods Ballard, B., Wilson, S., Udale-Clarke, H., Illman, S., Scott, T., Ashley, R., & Kellagher, R. (2015). The SUDS manual (C753). CIRIA: London, UK. ISBN 978-0-86017-759-3.

Paper II

Journal of Hydrology 607 (2022) 127495

Contents lists available at ScienceDirect

Journal of Hydrology

journal homepage: www.elsevier.com/locate/jhydrol

Research papers

Infiltration capacity in urban areas undergoing frequent snow and freeze–thaw cycles: Implications on sustainable urban drainage systems

Tarek Zaqout [a,*], Hrund Ólöf Andradóttir [a], Ólafur Arnalds [b]

[a] Faculty of Civil and Environmental Engineering, University of Iceland, Hjarðarhagi 6, 107 Reykjavik, Iceland
[b] Faculty of Agricultural and Environmental Sciences, Agricultural University of Iceland, Hvanneyri, Borgarnes, Iceland

ARTICLE INFO

This manuscript was handled by Corrado Corradini, Editor-in-Chief, with the assistance of Renato Morbidelli, Associate Editor

Keywords:
Grass swales
Infiltration
Frozen soil
SuDS
Runoff
Urban drainage

ABSTRACT

Sustainable Urban Drainage Systems (SuDS) promote environmental protection and climate resilience. SuDS implementation in cold climates faces concerns of impaired hydrological function due to infiltration-reducing frost. The goal of this research was to assess the seasonal variations in infiltration and how different surface covers prevalent in and near coastal cities respond to frequent rain-on-snow and freeze–thaw cycles. A total of 28 constant head infiltration measurements were conducted over a period of 28 months in Urridaholt in Gardabaer, Iceland (64° 4′18.46″ N, 21° 54′37.11″ W) in a grass swale, lupine, and barren terrains. All test locations exhibited infiltration-inhibiting frost in winter, whose severity increased with frequent snow and freeze–thaw cycles. The grass swale resisted structural deformations resulting from frost, which was attributed to the high near-surface porosity within the intertwined root layer and the high drainage capacity of the underlying soil. The sparsely vegetated lupine and the barren area experienced severe frost heaving and cracking, and soil structural collapse which led to bypass flow upon thawing. The non-vegetated site had 30 to 50 times lower infiltration during winter (19 mm h^{-1}) compared to the grass swale and lupine field (630- and 890-mm h^{-1}, respectively), and twenty times lower during summer and fall (45 mm h^{-1} vs. ~ 1000 mm h^{-1}). The study concludes that frequent warming and cooling renders soils particularly vulnerable to frost. Vegetation plays an instrumental role in maintaining the hydrological functions of SuDS in winter. Therefore, the greening of urban centers is an important step towards climate resiliency. Plant selection and SuDS design criteria need to account for cold climate hydrological performance. In that regard, plants that limit sunlight and fully shed their vegetation in winter, such as the invasive lupine, can potentially contribute to frost formation and increase runoff generation.

1. Introduction

Climate change and urbanization have motivated a shift in urban drainage policy from a single-purpose approach of reducing runoff to a multi-functional approach that provides social, economic, and health benefits (Davis et al., 2012; Deletic and Fletcher; Fletcher et al.; Wong and Brown, 2009). Decentralized, infiltration-based stormwater management using Sustainable Urban Drainage Systems (SuDS) has gained increased popularity in the recent decades (Barrett, 2008; Caraco and Claytor; Fletcher et al.; Wong and Brown, 2009). SuDS effectiveness in reducing and treating surface runoff largely relies on their infiltration capacity (Davis et al., 2012; García-Serrana et al.; Rujner et al., 2018). One of the key concerns with the wide adoption of SuDS in cold climates is the potential occurrence of infiltration-limiting frost (Fach et al., 2011; Khan et al., 2012; Muthanna et al., 2008; Paus et al., 2016; Zaqout and Andradóttir, 2021), which can render the normally permeable surfaces non-conductive (Bengtsson and Westerström, 1992; Westerström, 1984). Yet, there are also indications that bioretention systems can still perform well in freezing temperatures (>80% peak flow reduction; Khan et al., 2012; Roseen et al., 2009).

The conflicting reports on winter infiltration and frost formation are linked to a complex interplay between the soil, vegetation cover, and climatic conditions. Fine-textured, compacted, organic-rich soils hamper infiltration and drainage (Hillel, 1998; Rawls et al., 1983), while macropores and cracks formed by plant roots and freeze–thaw cycles aid it (Beven and Germann, 1982; Gray et al.). Densely vegetated surfaces (such as grass) tend to maintain a lower soil water content, higher infiltration rate and are less prone to frost formation than sparsely vegetated surfaces in rural areas (van der Kamp et al., 2003). Moreover, dense vegetation accompanied with deep roots such as in deciduous

* Corresponding author.
E-mail address: tarek@hi.is (T. Zaqout).

https://doi.org/10.1016/j.jhydrol.2022.127495
Received 28 September 2021; Received in revised form 14 January 2022; Accepted 17 January 2022
Available online 22 January 2022

forests allows for greater infiltration and less ice formation potential than dense vegetation or deep roots alone as exemplary of coniferous (evergreen) forests (Bormann and Klaassen, 2008; Orradottir et al., 2008). The type of frost and the hydraulic conductivity of frozen soils are, in turn, largely governed by the soil moisture content at the onset of freezing (Al-Houri et al., 2009; Fach et al.; Flerchinger et al., 2013), more so than the freezing temperature (Benoit, 1973): Relatively dry soils and dense vegetation promote granular and porous frost, while saturated soils and sparse vegetation are prone to concrete frost formation (Kane, 1980; Kane and Stein, 1983; Stoeckeler and Weitzman, 1960; Orradottir et al., 2008). Severe surface flooding occurs during sudden snowmelt events when all the filtering media pores are filled with ice or during saturated conditions (Bengtsson, 1985; Bengtsson and Westerström).

Frequent rain-on-snow and freeze–thaw is the key cause of urban flooding in cold maritime climate (Andradóttir et al., 2021). The repeated supply of cold liquid water from melting snow and the lack of thermal insulation from the atmospheric cooling provided by a continuous, seasonal snow cover render the soils wet for extended periods and susceptible to frequent freezing and thawing (Zaqout and Andradóttir, 2021; Flerchinger et al., 2013; Muthanna et al., 2008). Repeated freeze–thaw in dry soils enhances the formation of preferential flow paths and near-surface cracks (Fouli et al., 2013; Kane and Stein, 1983; Baratta, 2013; Flerchinger et al., 2013). Aggregate stability may increase after the first freeze–thaw cycle in wet soils, while decrease as more freezing cycles occur due to ice-lens and fractures formation (Arnalds, 2015; Flerchinger et al., 2013; Lehrsch, 1998). Considerable uncertainty remains on the role of freeze–thaw cycles on infiltration. For example, infiltration was observed to increase in clayey silt with the number of freeze thaw-cycles (Sterpi, 2015), while it remained unaffected, or decreased slightly, in loamy sand and clayey soils (Fouli et al., 2013).

As a result of climate change, more cities around the globe are predicted to experience frequent rain-on-snow and freeze–thaw cycles (Dong and Menzel, 2020; Garvelmann et al.). The performance of SuDS during frost is, however, still poorly understood and a limiting factor in their adoption in cold climates (Ekka et al., 2021; Fletcher et al.). Studies that evaluated infiltration capacity during winter freezing conditions are either based on laboratory soil columns without a vegetation cover (e.g., Fach et al., 2011; Moghadas et al., 2016); focused on sparse, large-rooted vegetation in bioretention cells with underdrains (e.g., Khan et al., 2012; Muthanna et al., 2008; Paus et al., 2016); or conducted in rural areas (e.g., Fouli et al., 2013; Gray et al.; Kane and Stein, 1983; Orradottir et al., 2008). Additionally, no studies have comprehensively investigated the efficiency of grass swales in cold climatic conditions (Ekka et al., 2021). Urban terrains differ from their rural counterparts because of soil compaction, clogging, and disruption, which results in inaccurate prediction of runoff volumes and peaks (Pitt et al., 2002). Therefore, to successfully transition to more climate-resilient cities, the response of different kinds of permeable urban surfaces to maritime winter conditions needs to be better understood, especially grass which constitutes a major share of green surfaces in the temperate and arctic regions (Kane and Stein, 1983).

The goal of this study was to quantify the changes in infiltration between summer and winter in three different surface covers in an urban area subject to the same hydro-climatological conditions. For this purpose, field infiltration experiments were conducted over 28 months in a grass swale specifically designed to infiltrate water and two adjacent terrains: a land covered with lupine (*Lupinus nootkatensis*) introduced for restoring deteriorated ecosystems (Vetter et al., 2018), and a bare soil (hereafter referred to as barren). Each surface cover has a different plant density and root characteristics and constitutes large areas in public or undeveloped urban areas. A particular focus was on relating infiltration capacity to surface frost and structural deformations as well as soil moisture content and soil drainage, the latter of which is relatively little discussed in previous infiltration experiments studies.

2. Materials and methods

2.1. Site description

The BREEAM (Building Research Establishment's Environmental Assessment Method) certified residential neighborhood of Urridaholt in Gardabaer, Iceland (64° 4′18.46″ N, 21° 54′37.11″ W) implemented SuDS to preserve the pre-development water cycle. The study site encompasses a grass swale and two nearby surface covers in a sloping landscape (Fig. 1a). The swale is approximately 3 m wide with a trapezoidal shape to infiltrate and convey excess runoff from private lots linearly to the downstream pond Urridavatn (Fig. 1b). The swale is separated into sections by check-dams to attenuate the flow. On one side of the swale is a lupine field (*Lupinus nootkatensis*), and on the other side, a gravelly path that was paved with asphalt in February 2019. The lupine was introduced from Alaska during the last century and has been used to facilitate the reclamation of degraded surfaces. Further uphill, an area of barren soils can be found (Fig. 1a). The three surfaces at this site represent varying plant densities and different root structures and depths (Table 1). Being located close to one another, the different surfaces develop a similar thick snow cover in winter and of similar density (Andradóttir and Zaqout, unpublished data).

The grass swale was constructed without specific layering or an underdrain. A 50 cm thick soil overlies a natural clay layer and basaltic rock. The dominant soil texture class in the three tested sections of the swale was sandy loam according to USDA Soil Textural Classification (USDA, 1987). The soil in the swale consisted of 15–20% gravel, 75–82% sand, and 2.5–4% fines in accordance with ASTM D6913 (ASTM, 2017). The soil in the lupine field was also classified as sandy loam but contained a higher portion of fines (16.5%), while the sand portion was similar to the one in the swale (72%). The soil bulk density and porosity were measured in the laboratory as intact soil cores were extracted at 10-cm intervals from the 30-cm soil horizon, which showed a higher porosity in the grass swale than in the lupine field (Table 1).

2.2. Experimental approach

Many studies on soil freeze–thaw cycles have been conducted in controlled incubators or growth chambers using repacked soil columns or intact mesocosms (Henry, 2007). While providing valuable information, laboratory tests underestimate field infiltration because of the artificial packing of the soil and lack of naturally formed cracks and pores due to vegetation (Ding et al., 2019). The small volumes of the collected soils also lead to a rapid equilibrium with ambient air temperatures, which causes unrealistically severe freezing and large temperature fluctuations (Henry, 2007). Field experiments, in turn, can account for the spatial variability of a heterogeneous terrain over different seasons. Ring infiltrometers are thin-walled (single or double), open-ended cylinders that are inserted in the ground and can be used to estimate the cumulative infiltration rate and the field saturated hydraulic conductivity (Elrick et al., 1995; Reynolds and Elrick, 1990; Dane et al., 2002).

The approach taken in this study was to use single ring infiltrometers to assess water infiltration at the top 20 cm of soil that is prone to frost formation in a cold maritime climate. The perceived advantage of using double-ring infiltrometers is questionable during freezing conditions, as the effectiveness of the outer ring in eliminating lateral flows is not proven except for shallow ponded depths and impractically large diameters (Swartzendruber and Olson, 1961; Youngs, 1987). Shallow ponded water depth is not appropriate in subfreezing temperature, as it increases the risk of water freezing within the ring during the experiment. Additionally, in seasonally wet soils with high water holding capacity (Zaqout and Andradóttir, 2021), such as in this study, an overestimation of the infiltration capacity due to lateral flow resulting from the capillarity of the surrounding unsaturated soil (Reynolds and Elrick, 1990), is less of a concern. The small set of single infiltrometers

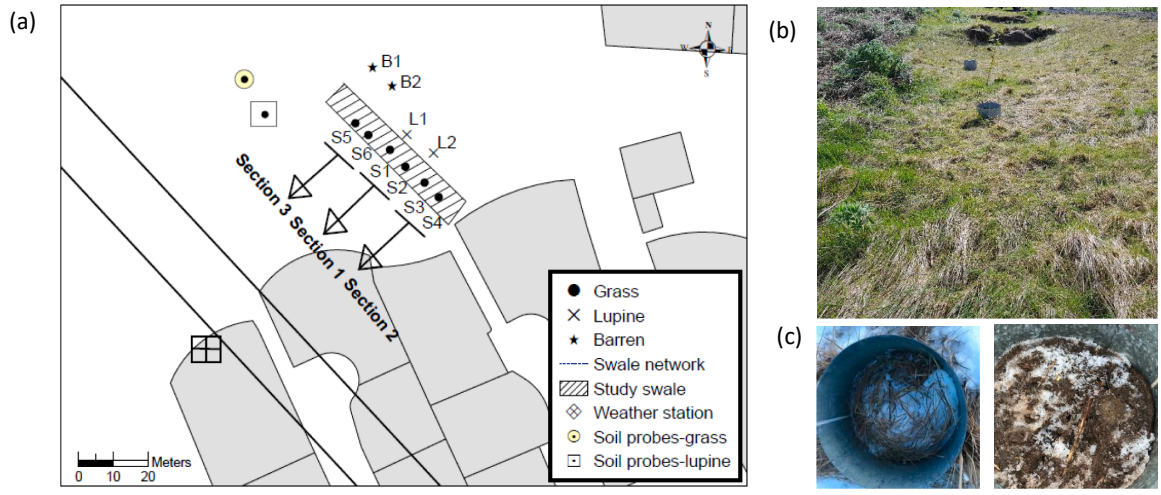

Fig. 1. a) Study site and locations of the single-ring infiltration measurements at the swale (S1–S6), lupine field (L1 and L2), and barren area (B1 and B2), b) the grass swale during summer, c) examples of freezing conditions in the grass swale (bottom left), and in barren soil (bottom right).

Table 1
Characteristics of soil in the terrains at the Urridaholt study site (Gimingham, 1969; Hanslin and Kollmann; Riege and Sigurgeirsson, 2009), and measured onsite soil characteristics.

Plant species	Description	Shoot	Roots	Soil*		
				Porosity (%)	Bulk density (g cm^{-3})	Soil texture
Grass	Herbaceous species with soil-binding root structure.	Dense (6–10 blades/cm^2) Uniform (mat-like) Height: 2–15 cm.	Density: high. Fibrous and shallow (5–10 cm).	28–52	1.46–1.93	Sandy loam
Lupine (*Lupinus nootkatensis)*	Hardy plant with nitrogen fixating root system.	Sparse (0.6–1 m between plants) Height: 30–90 cm Leaves: Palmately, <6 cm long.	Density: low. Thick, deep (1–2 m) taproot, with a few secondary or tertiary lateral roots.	27–45	1.27–1.90	Sandy loam

Notes: * Range represents variation in depth below surface. Highest porosity and lowest bulk density were measured within first 10 cm of soil. Lowest porosity and highest bulk density were measured at 30 cm.

may serve as a good indicator of whether and to which degree infiltration is reduced in winter.

2.3. Experimental design and procedure

A total of 8 infiltration rings were installed at the study site in the summer of 2018. The infiltrometers were placed close to one another, with easy access to water supply along a walking path (Fig. 1a). The rings were 22.5 cm in diameter and 40 cm in height. The infiltrometers were gently hammered to establish good contact with the soil and to minimize disturbances down to 15–17 cm depths perpendicular to the slope of the soil surface. A drainage hole was drilled at the bottom of each ring to prevent the accumulation of water inside in between measurements, which is plugged before the commencement of a measurement. Four infiltration rings were added in the summer of 2019 in order to get a better representative sample in the grass swale.

A mesh was placed within the infiltration ring to ensure that the water poured into the ring uniformly spread over the surface. An initial volume of water was added instantly at time $t = 0$ until the water level within the ring stabilized, and using a stopwatch, the recording of time was started. The water level or ponded depth (H) was maintained at approximately 5 cm by adding water continuously using graduated cylinders with volumes of 1 and 2 L. The added volume was recorded every 5 min and timed using a timer. The experiment was discontinued when the added volume remained constant for three consecutive iterations, which occurred after approximately 45–60 min during summer and 30–45 min during winter. The measurements were conducted once every 3–4 weeks to minimize the disturbance of the study site prior to each measurement.

Before each infiltration measurement, the surface, water, and air temperatures were measured using a handheld thermometer. Pictures were taken of the terrain surface within the rings. The presence of surface frost was noted by visually observing the presence of ice lenses (see Fig. 1c). Soil structural changes and frost heave were evaluated by measuring the distance between the pre-set soil surface elevation and the surface elevation on the measurement day using a hand-held measuring tape.

2.4. Continuous data monitoring

Soil conditions. Soil water content and temperature were measured at a grass swale located 50 m downhill of the study locations at depths from 5 to 45 cm at 10-cm intervals. Readings were logged using a data logger (type CS650, Campbell Scientific, Inc., accuracy ± 1%, Caldwell et al.,

2018) every 1 min. Similarly, the adjacent lupine field was instrumented with the same instruments at 5, 15, and 25 cm depths starting September 2019. A soil-specific calibration was conducted in the laboratory, and a linear user-defined calibration equation was derived for volcanic soils e.g., Icelandic Andosols (described in Campbell Scientific Inc, 2021). Soil temperature measured by the local utility Veitur ehf at the Heiðmörk station located 10 km inland from the study site was obtained for reference (Veitur, 2021). The measurements were made at 5, 10, 15, 20, and 50 cm depths from December 12, 2018, to October 31, 2020.

Meteorology. Ten-minute weather, air temperature, and rainfall data were collected from a weather station installed in February 2019 and operated by the Icelandic Meteorological Office [IMO] on behalf of the Gardabaer municipality (IMO, 2020a). The station is located approx. 100 m downstream from the location of the measurements. Hourly temperature, snow depth, and rainfall were also collected from the Reykjavik No. 1 station located on a hilltop 6 km away from the study site (IMO, 2020b) for reference purposes.

2.5. Data analyses

Winter climate and soil conditions. The seasonal number of air freeze–thaw cycles and the freezing and thawing indices were calculated to assess the intensity of these air temperature variations using the degree-day method (Andersland and Ladanyi, 1994; Zwissler et al., 2016). The air freezing degree days (FDD) were estimated as the sum of the daily average temperatures below zero ($T_{avg} < 0$ °C) during winter (November to March), and the thawing degree days (TDD) were estimated as the sum of the daily average temperatures above freezing ($T_{avg} > 0$ °C):

$$Degree\ day = T_{avg} - 0^{\circ}\mathrm{C} \tag{1}$$

$$Cumulative\ Degree\ day = \sum (T_{avg} - 0^{\circ}\mathrm{C}) \tag{2}$$

Similarly, a soil frost cycle was derived based on the average daily temperature at 5 cm depth so that if the soil temperature dropped below zero for one day would be counted as a cycle. Maximum frost penetration was derived as the maximum soil depth at which the average daily temperature was below zero. A rain-on-snow (RoS) event was defined as a day with precipitation concurrent with a reduction in snow depth. A snow cycle was defined as 24-hours with a snow depth of >1 cm measured at 9 AM.

Saturated hydraulic conductivity (K_{sat}) was estimated with two significant digits from the measured steady-state flow rate (Q_s in m^3/s) following the analytical expression of Reynolds and Elrick (1990) for the one-ponding-depth approach

$$K_{sat} = (\alpha\gamma Q_s)/T \tag{3}$$

where

$$T = \left[a(\alpha H + 1) + \gamma\alpha\pi a^2\right], \tag{4}$$

and

$$\gamma = Ge = 0.316\left(\frac{d}{a}\right) + 0.184 \tag{5}$$

where α in m^{-1} is a parameter defined by soil texture taken as 12 for loam soils (Gardner, 1958), G_e is a shape factor, T is a function of the soil texture, ponding depth, and the radius, a is the ring radius in meters (0.04 m^2), d is the depth of ring insertion in the ground in meters (0.15 m), and H is the ponded water level in meters (0.05 m).

The relationships between K_{sat} and soil and water temperature were then compared with the theoretical relationship describing the variations in water density and viscosity (Hillel, 1998).

$$K_{sat} = k\,\frac{\rho \bullet g}{\mu} \tag{6}$$

where k is the intrinsic soil permeability (cm^2), ρ is the water density (g/cm^3), g is the gravitational acceleration (cm/s^2), and μ is the water dynamic viscosity in poise units (dyn sec/cm^2).

Statistical analyses. The similarity in temporal evolution of infiltration amongst different testing locations within the same terrain was tested with linear regression analyses. Similarly, the relationship between infiltration and weather conditions was tested with linear regression. Inter-and between terrain variability were assessed using one-way analysis of variance (ANOVA) where the different terrains (grass swale, lupine, barren) were treated as main effects. The differences between terrains were analyzed by performing multiple comparisons using the student's t test to look for significant differences. Data used for analysis was transformed where required in order to account for the assumptions of normality. The normality of the data was tested using the Kolmogorov-Smirnov test (K-S) and Shapiro-Wilk test. The normality is accepted at $p > 0.05$. The spatial variation within the swale was assessed by comparing the arithmetic mean of the infiltration rates from each of the six infiltrometers. Statistical difference was based on the 5% significance level unless otherwise stated.

3. Results

3.1. Meteorological conditions

An overview of the weather during the 28-month study period is presented in Fig. 2. In the first winter, the snow season started unusually late in the middle of January with a 32-day long snow cycle with a maximum 31 cm depth (Fig. 2a). This corresponds to one of the longest snow cycles ever recorded in Reykjavík (Andradóttir et al., 2021; Arnardóttir, 2020). At the same time, the air temperature fluctuated around the freezing point (Fig. 2b), reflected in a balance between freezing and thawing days (FDD and TDD; Fig. 2c). The second winter, however, was representative of average maritime cold climate conditions with 21 freeze–thaw cycles, intermittent snow cover (13 snow cycles, longest lasting 23 days) starting November 18, and moderate snow depth (max. 12 cm; Table 2). The subsurface also experienced more days of frost, more intense and deeper frost penetration, as well as more thaw cycles. The spring and summer conditions were equally warm, but summer 2019 was drier with total precipitation of 307 mm compared to a 409-mm total rainfall during summer 2020.

3.2. Seasonal evolution of infiltration

Tested locations within each terrain exhibited a similar seasonal evolution during the 28 field campaigns (Fig. 3, top panels), reflected in good correlation coefficients and low *p-values* (Fig. 3, bottom panels). In winter 2018/2019, with the long-standing snow cover (Fig. 2a), the infiltration in the grass swale's sections was not impeded or slightly increased, however insignificantly ($p > 0.05$; Fig. 3a), compared to summer. This is in stark contrast to the less dense vegetation cover lupine (Fig. 3c) and bare ground (Fig. 3e), where the winter infiltration dropped to half that of the antecedent summer. During the following winter, characterized by intermittent snow and frequent freeze–thaw, infiltration-inhibiting frost formed in all terrains. The sites covered with the dense grass turf remained infiltrative during the freezing period. The sparsely vegetated areas exhibited both a reduction and a subsequent increase in infiltration around mid-winter in the lupine field (Fig. 3c), and late winter in the barren soil terrain (Fig. 3e). The high infiltration rates coincided with structural deformations observed at the surface (discussed in section 3.3 to follow). It is interesting to note that after the structural deformations in the latter part of winter, the infiltration rates did not return to the same values as the summer before. Thus, suggesting

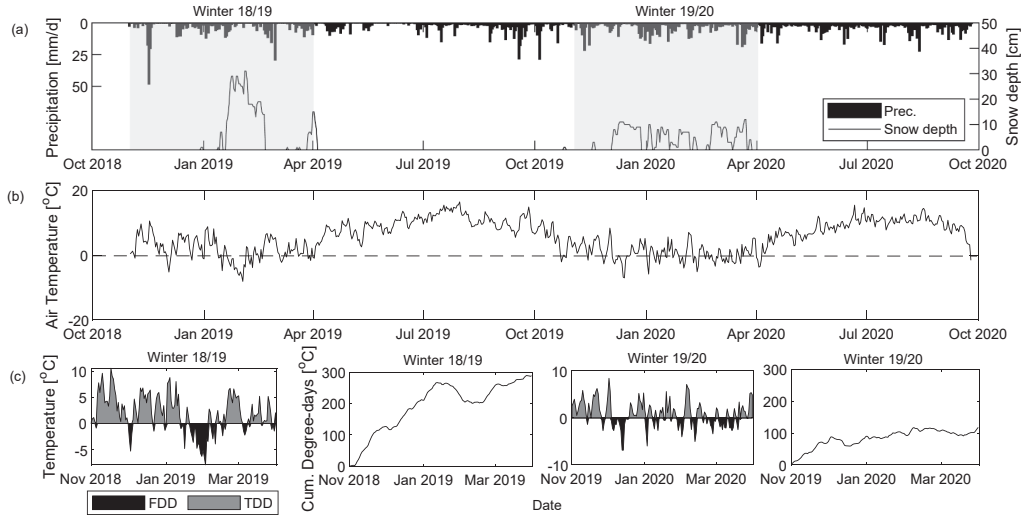

Fig. 2. a) Daily precipitation and snow depth data from Reykjavik No. 1 station, b) daily average air temperature data from Reykjavik station No. 1 for the period of November 2018 to September 2020, c) freezing and thawing degree-days during winter 2018/2019 and the cumulative degree-days (left), and winter 2019/2020 and the cumulative degree-days (right).

Table 2
Characteristics of the winter seasons 2018/2019 and 2019/2020 in Urridaholt, Gardabaer.

Physical domain	Indicator	Winter 2018/2019	Winter 2019/2020
Precipitiation[1]	No. of snow cycles	3	13
	Maximum snow depth (cm)	31	12
	Max duration (day)	32	23
	Cum. Precipitation (mm)	428	528
	RoS (days)	13	35
Air[1]	No. FDD	44	64
	No. TDD	107	88
	Cum. FDD (°C)	−104	−111
	Cum. TDD (°C)	392	229
	Freeze-thaw cycles	13	21
Soil[2]	Soil frost cycles	5	12
	Max frost depth (cm)	5	15
	Min soil temperature (°C)	−0.98	−3.68
	No. of days with soil frost	113	167

Notes: Winter is defined as the five months of November to March. FDD = freezing degree-days. TDD = thawing degree-days. [1]Reykjavik station No. 1, [2] Rural, unforested Heiðmörk at 5 cm depth (Veitur, 2021).

that the soil structure was rearranged as a result of intense freeze–thaw cycles.

The linear regression between the tested locations (Fig. 3; bottom panels) indicates that despite the differences in absolute values, each terrain exhibited a similar response to seasonal and event-based changes. Except for the test location S1, which behaved differently during the testing period, infiltration measurement pairs were well correlated within each location (R^2 = 0.32–0.65), and statistically significant at the 95% level ($p < 0.05$). The less vegetated sites that were susceptible to structural changes, i.e., the lupine and barren fields, also showed consistent patterns in infiltration during frost, freezing and thawing behavior, and soil deformation as well as when returned to normal conditions in spring. This high similarity between test sites within the same terrain supports the use of a small number of infiltrometers to assess the potential formation of infiltration-inhibiting frost during frequent freeze–thaw cycles.

3.3. Frost heave observations

The areas with sparse or absent vegetation cover (i.e., lupine and barren) were vulnerable to freezing and thawing and frost heave, while the grass swale exhibited no signs of frost related surface cracks or heave (Fig. 4a). Specifically, during the second winter, which was representative of maritime climate. Frost heave was physically observed on both test locations in the lupine field after 3 FTCs on December 18, 2019 (Fig. 4a; middle column), concurrent with a 58% reduction in infiltration capacity (Fig. 3c). A month later, after 5 FTCs, the soil structure at the lupine location (L2) had collapsed inward within the ring when thawed, forming large cracks and a separation between the infiltration ring and the soil. Concurrent with the observed soil surface collapse, abnormally rapid water infiltration rate was observed on January 17, 2020, which is interpreted as bypass flow along the side walls of the infiltration ring. Lupine location (L1) followed after 7 FTCs a month later. The soil recovered in spring, but the average infiltration rates in the lupine terrain were 34% lower than summer averages.

In the barren sites, the infiltration dropped by 34% after only one FTC, plunging to only 4 mm h^{-1} after 3 FTCs on December 18 when frost heave was physically observed (Fig. 4a; rightmost). Concurrent with such low infiltration was low drainage that maintained the soil wet and ultimately resulted in the formation of an ice layer on the surface, which impeded infiltration throughout winter 2019/2020. During the spring thaw, the barren soil became supersaturated. The infiltration ring moved vertically upwards by 8 cm (Fig. 4a; bottom panel), and water seeped from underneath the ring during an infiltration experiment, indicative that the soil was still frozen underneath, blocking infiltration. Hence, these physical observations suggest deep frost formation in the barren ground, which was neither observed in the lupine nor grass. The structural changes in the barren were accompanied with an increase in measured infiltration rates as high as 1753% corresponding to 685 mm h^{-1}.

During the milder winter, frost related deformations were also observed but only towards the end of winter and beginning of spring thaw (Fig. 4b). Frost heave was physically observed not only within, but

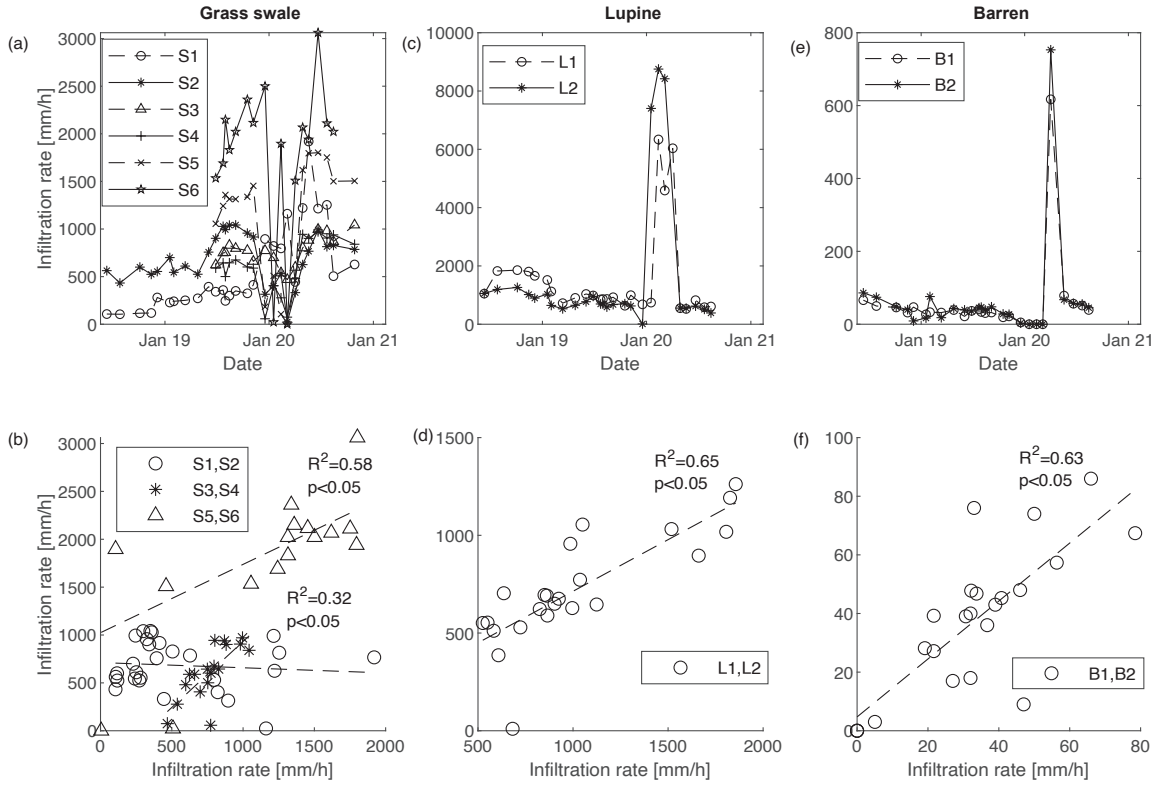

Fig. 3. Infiltration rates for each point measurement at the a) swale (S1, S2, S3, S4, S5, and S6), b) linear regression between S1 and S2, S3 and S4, and S5 and S6, c) lupine (L1 and L2), d) linear regression between L1 and L2, e) barren (B1 and B2), and f) linear regression between B1 and B2.

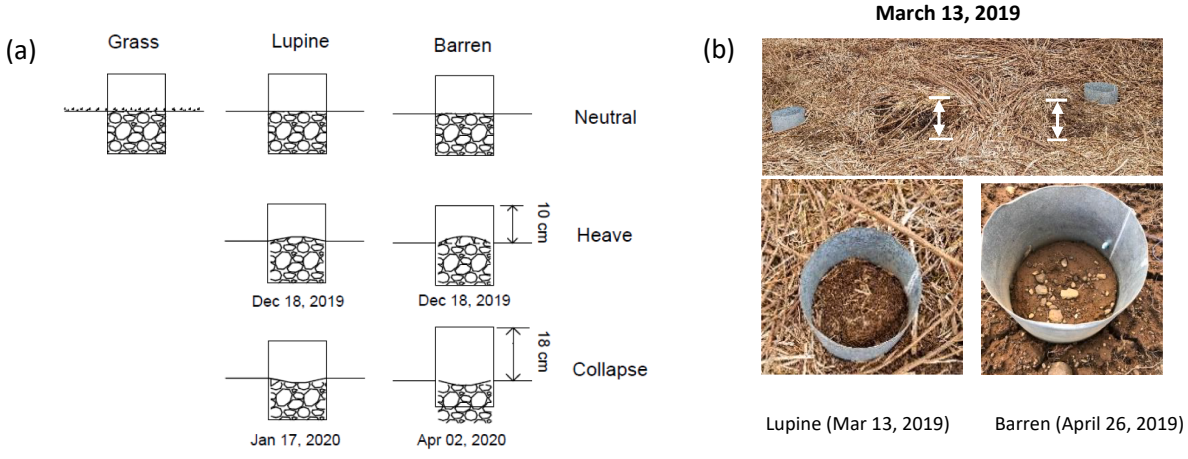

Fig. 4. a) Schematic of the soil structural changes in the different terrain during winter 2019/2020 compared to the swale (left) at the lupine (center), and at the barren (right), and b) visual observation of frost heave in the lupine and surface cracks in lupine and barren.

also between, the two tested locations in the lupine terrain (Fig. 4b; top and bottom left). In addition, large cracks were observed outside the test rings in the barren area (Fig. 4b; bottom right). Frost heave, large cracks, and subsequent collapse, that contributed to observed bypass flow during the second winter with frequent freeze–thaw cycles (Fig. 2a), were not bound to the location of the metal infiltration rings, but a prevalent phenomenon in the lupine and barren terrains. In the following analyses, the primary focus is on the infiltration measurements representing porous media flow. Therefore, the high infiltration rates related to the occurrence of bypass flow are not included in the analyses.

3.4. Underlying soil conditions

Continuous water content and temperature data in the lupine and swale fields give insights into the susceptibility of the soil in the lupine terrain to frost. The soil at 5 cm depth started to freeze one month earlier under the sparsely vegetated terrain (lupine) than in the more permanently vegetated grass swale in winter 2019/2020 (Fig. 5a). But more importantly, the drainage capacity of the soil in the swale was much higher than in the lupine (the 24-hour average reduction in saturation was 14% in the swale compared to only 4% in lupine during winter runoff events; Fig. 5b). As expected under such conditions, the degree of saturation in the lupine field was on average higher than in the grass (85% vs. 80%, respectively), consistent with a higher field capacity. Moreover, the soil in the grass swale repeatedly reached high saturation levels (88–100%) in response to rainfall and/or snowmelt but never reached saturation (max 92%) in the lupine. This indicates that the near-surface porosity in the grass was higher due to the interlinked roots system beyond the grass cover. This could also be explained by the presence of more fine materials (silt and clay) in the lupine terrain than in the manmade grass swale. Consistent with high water holding capacity and poor drainage, the soil under lupine reached supersaturation during spring thaw on March 20 (Fig. 5b). However, the soil at 5 cm depth in the grass swale seems to form porous near-surface frost more easily than lupine, which was observed in the sharp reductions in water content following three natural snowmelt/RoS events due to a phase change from water to ice (Fig. 5d). The type of frost seemed to permit vertical water movement, which was confirmed during the synthetic runoff experiments conducted by Zaqout and Andradóttir (2021) in the same swale section. Lastly, the seasonal evolution of the temperature of the deep soils at 25 cm is statistically similar in winter, with frost never reaching this depth for both lupine and grass (Fig. 5c). The lupine, however, provided sun shading in summer, as reflected in 0.6 °C lower soil temperature than in the grass swale.

3.5. Temperature dependence

Water and surface temperature contribute to changes in infiltration rates. As temperature decreases, the infiltration capacity drops because of the increased water viscosity (Equations 3–6). The average water temperature used in the infiltration experiments during summer and fall experiments were 13 and 11 °C, respectively. The average water temperature was significantly lower during winter (3 °C). Similarly, the surface temperature measured next to each infiltration ring was lowest during winter with an average of −0.42 °C compared to an average surface temperature during summer of 12.5 °C. The theoretical relationship of increasing hydraulic conductivity with water temperature is confirmed with a linear regression analyses of measured infiltration rates in the grass swale (Fig. 6a). The correlation is weak but significant at the 95% confidence level ($R^2 = 0.27$). The relationship between infiltration capacity and ground surface temperature was stronger than that between infiltration and water temperature ($R^2 = 0.42$; Fig. 6b), supporting that the temperature of the soil medium exerts a control on the infiltration rate. The large residuals between the observed rates and the theoretical relationship reflect the importance of other seasonal processes than the effect of temperature variations on infiltration capacity: During summer, biological activity and root growth contribute to enhancing infiltration, whereas the formation of pore ice and structural changes reduces permeability in winter (García-Serrana et al., 2017). However, no statistically significant correlation between temperature and infiltration was found for lupine and barren soil (Fig. 6c and d). This suggests that the antecedent moisture and frost formation processes play a more influential role than water viscosity in these terrains.

3.6. Impact of snow cycles on infiltration

The two studied winter seasons exhibited different meteorological conditions, which reflected on frost formation and infiltration capacity. To identify which meteorological driver influenced infiltration capacity the most, the temporal evolution of infiltration during winter was analyzed with respect to representatives, readily available hydroclimatic factors: (1) No. of FDD to represent seasonal cooling; (2) No. of snow cycles (snow depth > 1 cm) to represent the fluctuations in surface/soil conditions in a maritime climate. The number of freezing degree days did not explain the temporal evolution of infiltration in winter

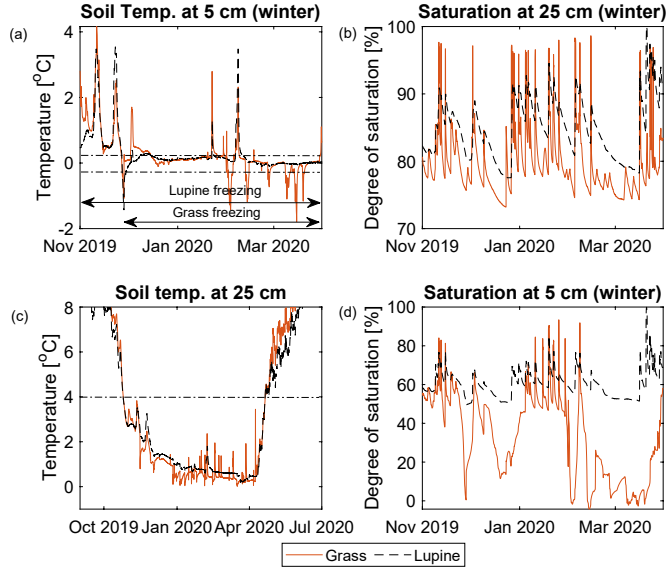

Fig. 5. Comparison between soil temperature and degree of saturation in the densely vegetated terrain (grass) and the sparsely vegetated terrain (lupine): a) soil temperature at 5 cm depth in the swale (solid line) and lupine (dashed line), b) degree of saturation at 25 cm depth in the swale and lupine, c) soil temperature at 25 cm depth, and d) degree of saturation at 5 cm.

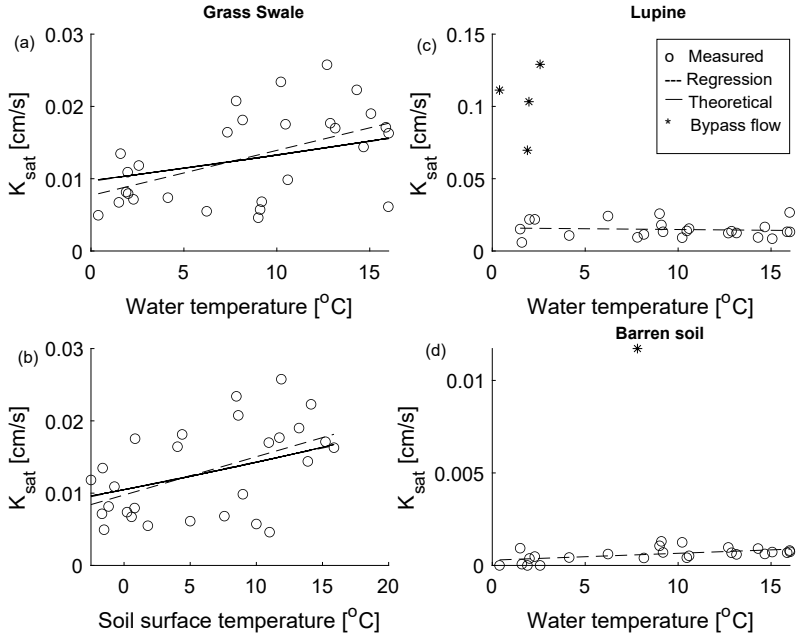

Fig. 6. Linear regression between water (or soil surface) temperature (dashed line) and measured (o) and theoretical K_{sat} values (solid line) in a)-b) grass, c) lupine, and d) barren. Asterisk (*) denote unrealistically high values due to soil deformation.

and between winters. In general, the response of each terrain was consistent between years when plotted against the number of snow cycles (Fig. 7). The infiltration rate dropped with increasing snow cycles in the grass and barren (Fig. 7a, c). The lupine started to show deformations after 2–4 snow cycles (Fig. 7b). This supports the interpretation that structural changes due to frost heave, and the potential formation of macropores, are related to the frequency of freeze–thaw more than the severity of cooling.

3.7. Variability within and across terrains

While the primary focus of this study was to resolve the effects of frequent freeze thaw on infiltration in the different terrains, the experiments also provided insights into spatial variability. A summary of all measurements conducted within each test site during the two-year monitoring program is presented in Fig. 8. The variability, shown as boxes representing the median, 25th, and 75th percentiles, and the extreme data points (whiskers) represent both seasonal variability and variability between the two winters with different frost intensity, as discussed in sections 3.1 and 3.6. Of the six test sites in the grass swale, three (S2 to S4) did not significantly differ ($p > 0.05$). S5 and S6 were both statistically different from the remaining test locations ($p < 0.05$). The unusually high infiltration in S6 (Fig. 8a) was attributed to the presence of large rocks at the bottom of the infiltration ring. Despite some statistical differences, consistent drops were recorded in winter across all the test locations within the grass swale. The two lupine test sites were statistically different but within the same range (Fig. 8b). The infiltration capacity in the two barren sites did not significantly differ (Fig. 8c). While acknowledging the spatial variability, the infiltration in each location can be compared on an order of magnitude basis. The comparison suggests that infiltration in the vegetated terrains was on the same order of magnitude during the two-year study period. The infiltration in the non-vegetated terrain was, however, an order to two magnitudes lower (Table 3).

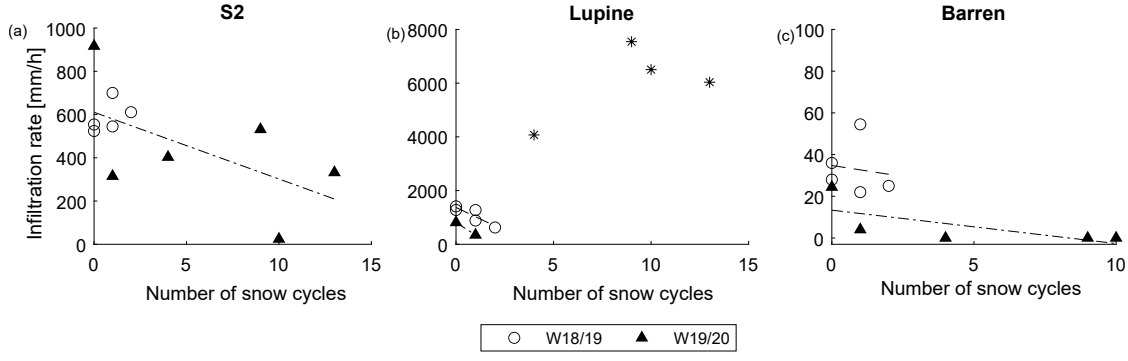

Fig. 7. Relationship between the number of snow cycles prior to each experiment and infiltration capacity during winter 2018/2019 and winter 2019/2020 at: a) grass location No. 2, b) lupine, and c) barren. Outliers resulting from structural deformation marked as asterisk (*).

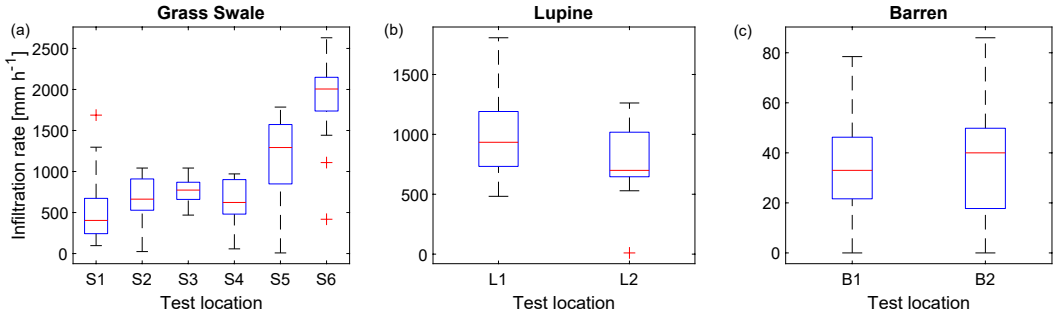

Fig. 8. Median and range of infiltration rates measured during the study period in each terrain. a) Grass Swale, b) lupine, and c) barren. Note the scale differs between the graphs. The central marks represent the median, the bottom and top edges represent the 25th and 75th percentiles, respectively. The whiskers extend to the maximum and minimum data points, and the outliers are plotted individually using the '+' symbol.

Table 3
Statistical analyses of seasonal mean and standard deviation of infiltration in mm hr^{-1} (and number of measurements) in three terrains during 28-month study period.

Season	Grass	Lupine	Barren
Summer & fall	$980^{a} \pm 560$ (67)	$890^{a} \pm 330$ (26)	$45^{b} \pm 15$ (26)
Winter	$630^{a} \pm 530$ (40)	$890^{b} \pm 370$ (15)	$19^{c} \pm 20$ (20)

Notes: Means connected with the same letter are not statistically different from each other, statistically significant for *p-value* < 0.05.

4. Discussion

4.1. Role of SuDS in a cold maritime climate

SuDS aim to reduce urban flooding via infiltration and flow retardance by replacing traditionally impervious areas with permeable, green areas. Besides the known hydrological benefits, reducing and treating runoff of harmful pollutants, SuDS also enhance biodiversity and the aesthetical value of urban areas. This study provides new insights into the potential role of infiltration-based solutions in strengthening the resilience of urban areas against winter flooding in a maritime climate characterized by frequent freeze–thaw cycles. Infiltration experiments, physical observations, and continuous monitoring (Table 4) demonstrated that an engineered grass swale, with a continuous and finely woven root mat and more porous underlying soils, drained faster, developed less frost, resisted soil deformations due to frost in comparison with two undisturbed terrains (lupine and barren) during frequent freeze–thaw (winter 2019/2020). These surface and soil properties resulted in a sustained infiltration throughout repeated freeze–thaw.

The non-vegetated terrain (i.e., barren) was prone to frost formation and infiltration-inhibiting concrete frost. The sparsely vegetated field (i.e., lupine) maintained high saturation during winter, which led to a singular occurrence of concrete frost formation, frost heave during both winters, and bypass flow following a structural collapse upon thawing in the second winter. While macropores might be beneficial in alleviating urban flood risks by increasing infiltration during winter, flow through large preferential paths reduces the pollutant removal efficiency associated with water movement through porous media. This contradicts the integral function of SuDS which ultimately aim to preserve the integrity of receiving waters and can be particularly dangerous in cold regions, where snow that accumulates more pollutants than rainfall-induced runoff is often cleared from streets and deposited in roadside swales (Andradóttir and Vollertsen, 2015; Gavrić et al.). Bypass flow through cracks and fissures has been observed to severely limit solute removal within the top 1 m of soils (Flury et al., 1994). While the water quality of

Table 4
Summary of physical observations in urban Reykjavik during frequent freeze thaw cycles (winter 2019/2020).

Physical domain	Observations	Plant/root density		
		High Grass	Low Lupine	None Barren
Surface	Surface frost	Yes	Yes	Yes
	Surface cracks	Not visible	Some	Very large
	Frost heave	Not visible	High	Very large
Topsoil (≤5 cm)	No. days w/ frost	167	170	–
	Avg. winter temperature (°C)	1.07	0.97	–
	Max. porosity [1] (%)	52/52	39/45	–
Soil (≤25 cm)	Avg. water content (%)	31	35	
	Drainage capacity (% per 24 h)	14	4	–
	Max. saturation	No	Yes	–
Winter infiltration	Min. K_{sat} (mm h^{-1}) [2]	8	10	0
	Bypass flow	No	Yes	Yes
	K_{sat} temperature dependence	Yes	No	No

[1] Onsite soil porosity inferred from water content probes/measured at testing locations.
[2] Minimum measured hydraulic conductivity within a single test site.

infiltration was not a focus in this study, the rapid water seepage observed following the severe structural deformation in the lupine and barren suggests a potential water quality risk. Structural changes due to freezing and thawing resulted in a semi-permanent decrease of 29% and 26%, in the lupine and barren, respectively, between summer 2019 and 2020, while the grass swale increased infiltration by 50%. In summary, this study highlights that surface vegetation plays an essential role in improving infiltration in summer and winter. Bare soils had a significantly lower infiltration capacity than the vegetated surfaces during the two-year study period, which can amplify runoff peaks and volumes in urban areas making such non-vegetated areas undesirable for sustainable urban development.

This research also shows that repeated freeze–thaw, characteristic of cold maritime climate, is detrimental to infiltration in manufactured and undisturbed terrains. By studying two distinct winters, one with a 32-day long snow cycle together with a few short-lived ones, the other with intermittent snow cover over five months, soil freezing, and reduced infiltration were linked to repeated cycles of snow rather than cumulative degree-days of cooling, represented by FDD (Table 2). This confirms previous hypotheses (e.g., Muthanna et al., 2008; Roseen et al., 2009) and observations (Zaqout and Andradóttir, 2021) that repeated

melting and refreezing of meltwater within the soil media is an influential factor for the formation of frost and deeper frost (15 cm compared to 5 cm in the first winter). Previous research conducted in cold coastal regions (e.g., Khan et al., 2012; Muthanna et al., 2008; Paus et al., 2016) also emphasized the need for good drainage capacity to minimize the adverse effects of freeze–thaw cycles. This research, however, also suggests that vegetation cover can enhance the near-surface soil porosity that is repeatedly exposed to freezing air temperature in cold maritime climates, which in return improves the drainage capacity and minimizes the potential for frost formation.

4.2. Practical implications for urban landscapes

SuDS are usually designed based on local experience using available residual material onsite (Rujner et al., 2018). This study supports the importance of re-manufacturing local soils that are poorly draining for usage in infiltration-based urban drainage systems to avoid high water contents that can form impermeable frost (LeFevre et al., 2009; Muthanna et al., 2008). The grass swale's good performance is attributed to the fact that the swale's media was man-made and contained coarser material than the local soils present in the undisturbed terrains (i.e., barren/lupine) and because of the vegetation cover. Common complications resulting from cold climate conditions are altered surface roughness, increased runoff peaks and volumes, reduced or impeded infiltration capacity due to frost, dormant vegetation, and infiltration of de-icing salts (Roseen et al., 2009). However, such complications can be partially avoided by including a gravel-based drainage layer and/or underdrains to promote faster drainage (LeFevre et al., 2009). Maintenance practices might need to also be reconsidered, which can include regular inspections following melt events to remove residual sand and sediments, and prepare damages to vegetation, and mulching to restore the moisture capacity and soil structure in spring (Caraco and Claytor, 1997).

Secondly, large areas of bare soils should be avoided because of their significantly worse seasonal infiltration potential and concrete frost potential in winter. Bare grounds within the built environment also tend to be more affected by human activity and increased compaction than vegetated terrains due to the lack of a root system that can sustain porosity (Barbosa et al., 2020). Leaving robust vegetated terrains undisturbed with native plants may be a cost-effective solution for peak flow and volume reduction during extreme summer rainfall events.

Lastly, the SuDS literature focuses on selecting plants that can tolerate highly variable soil moisture conditions, the local soil pH and texture, and pollutant loading (Prince George's County, 1999). This study highlights that plant selection criteria need to be expanded to ensure optimal cold climate hydrological performance. Sparsely vegetated, e.g., *Lupinus nootkatensis* that fully shed their vegetation in winter, and bare surfaces might not be a recommended practice because their susceptibility to the formation of cracks and macropore structures can lead to the bypassing of infiltrating water, therefore, jeopardizing the quality of groundwater. Lupine also tends to limit sun penetration to lower vegetation, leaving the ground similar to bare soil and frost-sensitive than the densely vegetated surfaces.

4.3. Data strengths and limitations

Assessing winter infiltration during frequent frost and snow cycles is not an easy task and difficult to optimize due to practical considerations (time, resources, sunshine duration, frost). The approach taken in this study was to conduct single ring infiltrometer experiments within the first 20 cm of soils that are prone to frost formation as a robust, time-efficient method that minimally disturbed the soil. The measured seasonal evolution of infiltration exhibited high similarity between the test points within the same terrain, which supports the use of this technique to assess the impacts of frequent freeze and thaw infiltration within the same site (Fig. 3). Overall, the measured infiltration in non-vegetated terrain in this study conforms well with measurements in sandy loam soils, which varied from 1 to 87 mm h^{-1} in frozen and nonfrozen conditions in a laboratory setting (Al-Houri et al., 2009). The grass swale and lupine exhibited slightly higher summer and winter infiltration than a bioretention cell (450 mm h^{-1} and 5–10 mm h^{-1} in summer vs. winter; Paus et al., 2016), which can be attributed to the high porosity and low bulk density of Icelandic Andosols (Arnalds, 2015; Table 1). The study also confirms that spatial variability can be considerable even within small distances due to the heterogeneous nature of soils and frost formation. Infiltration rates measured in the field using ring infiltrometers are always higher than rainfall-induced infiltration observed in real events due to the larger ponding depth (Hillel, 1998; Rawls et al., 1983). The saturated hydraulic conductivity measured using ring infiltrometer was 2 to 5 times higher in this study compared to synthetic runoff experiments at the same site (Zaqout and Andradóttir, 2021), consistent with observations in bioretention cells made by Paus et al. (2016).

Bypass flow was observed in sparsely vegetated terrains undergoing frequent freeze thaw but not quantified in this study. The use of intrusive metal rings may exacerbate the occurrence of macropore flow associated with frost heave and soil collapse, as the wall of the metal infiltration ring was observed to separate from surrounding soil. The inclusion of an outer ring (dual ring infiltrometer) is also expected to be vulnerable to bypass flow amplification as the surface area of the metal in contact with the soil would be larger. To quantify the increased infiltration due to frost-induced macropore formation, non-intrusive methods such as synthetic runoff events over a larger area (e.g., Bäckström; Davis et al., 2012; Rujner et al., 2018; Zaqout and Andradóttir, 2021), would be preferred. Such methods, however, are not suitable for resolving spatial variability, require large amounts of running water and have a greater potential of generating synthetic freezing at the surface, as discussed in section 2.2. Lastly, the performance of infiltration-based systems can change considerably over extended periods (years) due to clogging, vegetation/roots growth, and structural changes, both natural due to soil deformations and intentional due to compaction, and management practices. Therefore, the findings, presented in this study, cannot be extrapolated to longer time periods.

5. Conclusions

Observations made over 28 months in this study provide insights into the hydrological performance of grass swales, urban runoff generation, the design, and implementation of green infrastructure in cold maritime climates. The field measurements were conducted in a grass swale with a permanent vegetation cover, a lupine field, and a barren terrain. The results indicate that the grass swale was more resilient to the developing infiltration-inhibiting frost, compared to the other less vegetated terrains. The swale's infiltration capacity was maintained throughout the study period despite the significant reduction in infiltration rates in winter compared to the summer and fall averages (630 vs. 980 mm h^{-1}). The sparsely/non-vegetated surfaces (i.e., lupine and barren), however, were more susceptible to frost formation and frost heave than the grass swale, which resulted in pronounced structural changes due to freeze–thaw cycles and led to a structural breakdown in the two terrains. The vegetated terrains were also considerably more infiltrative than the barren area throughout the study period, suggesting that the bare ground can generate higher runoff rates and volumes and can lead to a higher flooding risk, especially when soil frost is present. In addition, the structural deformation in those terrains, which may lead to the formation of large cracks, can result in groundwater contamination as the soil ceases to function as a filter, and crack flow may carry organic soil particles to groundwater systems.

The findings of this research suggest that the stormwater control measures that provide sustainable urban drainage solutions in cold maritime areas should aim to minimize non-vegetated or impermeable areas and promote the integration of green surfaces for flood mitigation. Because of frequent rain-on-snow and intermittent snowmelt, the soils

tend to be more saturated in cold maritime climates than in continental areas, and thus, well-drained and vegetated soils are preferred to avoid media freezing and regular maintenance is required to sustain the functionality of SuDS.

Declaration of Competing Interest

The authors declare that they have no known competing financial interests or personal relationships that could have appeared to influence the work reported in this paper.

Acknowledgements

This research was funded by the Icelandic Research Fund (Icelandic: Rannís), grant number 185398-053. We thank the Gardabaer Municipality, Iceland Meteorological Office, and Urridaholt ehf for onsite research facilities. We are also grateful to Guðni Þorvaldsson, Jón Guðmundsson, and Berglind Orradottir at The Agricultural University of Iceland for their help in setting up the soil monitoring program. We thank Veitur ehf for access to reference soil data. Thanks also to Johanna Sörensen at Lund University for her contribution to the interpretation and visualization of the results and reviewing the early writing of the manuscript. A special thanks to Halldóra Hreggvidsdottir for motivating and facilitating SuDS research in Iceland.

Data availability

The data used in this study were collected from the field by the researchers, acquired from the Icelandic Meteorological Office (IMO) and Veitur ehf, and presented herein. Any additional data is available upon request from the aforementioned rightful owners.

References

Al-Houri, Z.M., Barber, M.E., Yonge, D.R., Ullman, J.L., Beutel, M.W., 2009. Impacts of frozen soils on the performance of infiltration treatment facilities. Cold Regions Sci. Technol. 59 (1), 51–57. https://doi.org/10.1016/j.coldregions.2009.06.002.

Andersland, O.B., Ladanyi, B., 1994. An Introduction to Frozen Ground Engineering. Springer US, 10.1007/978-1-4757-2290-1.

Andradóttir, H.Ó., Vollertsen, G.E., 2015. Temporal variability of heavy metals in suburban road runoff in rainy cold climate. J. Environ. Eng. ASCE 141 (3), 04014068. https://doi.org/10.1061/(ASCE)EE.1943-7870.0000894.

Andradóttir, H.Ó., Arnardóttir, A.R., Zaqout, T., 2021. Rain on snow induced urban floods in cold Maritime Climate: risk, indicators and trends. Hydrol. Processes 35 (9), e14298. https://doi.org/10.1002/hyp.14298.

Arnalds, O., 2015. The Soils of Iceland. Springer, Netherlands, 10.1007/978-94-017-9621-7.

Arnardóttir, A.R., 2020. Winter Floods in Reykjavík: Coaction of Meteorological and Soil Conditions (Master's Thesis). http://hdl.handle.net/1946/34938.

ASTM, 2017. D6913, Standard Test Methods for Particle-Size Distribution (Gradation) of Soils Using Sieve Analysis. ASTM International, West Conshohocken, PA https://www.astm.org/Standards/D6913.htm.

Bäckström, M., 2002. Sediment transport in grassed swales during simulated runoff events. Water Sci. Technol. 45 (7), 41–49. https://doi.org/10.2166/wst.2002.0115.

Baratta, V.M., 2013. The Effects of Freeze-Thaw Cycles on the Infiltration Rates of Three Bioretention Cell Soil Mixtures [Master of Science, University of Iowa]. 10.17077/etd.s85qb45x.

Barbosa, L.A.P., Munkholm, L.J., Obour, P.B., Keller, T., 2020. Impact of compaction and post-compaction vegetation management on aggregate properties, Weibull modulus, and interactions with intra-aggregate pore structure. Geoderma 374, 114430. https://doi.org/10.1016/j.geoderma.2020.114430.

Barrett, M.E., 2008. Comparison of BMP performance using the international BMP database. J. Irrigation Drainage Eng. 134 (5), 556–561. https://doi.org/10.1061/(ASCE)0733-9437(2008)134:5(556).

Bengtsson, L., 1985. Characteristics of Snowmelt Induced Peak Flows in a Small Northern Basin. Hydrol. Res. 16, 137–156. https://doi.org/10.2166/nh.1985.0011.

Bengtsson, L., Westerström, G., 1992. Urban snowmelt and runoff in northern Sweden. Hydrol. Sci. J. 37 (3), 263–275. https://doi.org/10.1080/02626669209492586.

Benoit, G.R., 1973. Effect of freeze-thaw cycles on aggregate stability and hydraulic conductivity of three soil aggregate sizes. Soil Sci. Soc. Am. J. 37 (1), 3–5. https://doi.org/10.2136/sssaj1973.03615995003700010007x.

Beven, K., Germann, P., 1982. Macropores and water flow in soils. Water Resour. Res. 18, 1311–1325. https://doi.org/10.1029/WR018i005p01311.

Bormann, H., Klaassen, K., 2008. Seasonal and land use dependent variability of soil hydraulic and soil hydrological properties of two Northern German soils. Geoderma 145 (3), 295–302. https://doi.org/10.1016/j.geoderma.2008.03.017.

Caldwell, T.G., Bongiovanni, T., Cosh, M.H., Halley, C., Young, M.H., 2018. Field and laboratory evaluation of the CS655 soil water content sensor. Vadose Zone J. 17 (1), 170214. https://doi.org/10.2136/vzj2017.12.0214.

Campbell Scientific Inc., 2021. CS650 and CS655 Water Content Reflectometers, Instruction Manual, Revision: 08/2021, 2011-2021, Campbell Scientific Inc. 26 pp.

Caraco, D., Claytor, R., 1997. Stormwater BMP Design: Supplement for Cold Climates. U. S. Environmental Protection Agency.

Dane, J.H., Topp, G.C., Campbell, G.S., Soil Science Society of America (Eds.), 2002. Methods of soil analysis. Part 4: Physical methods. Soil Science Society of America.

Davis, A.P., Stagge, J.H., Jamil, E., Kim, H., 2012. Hydraulic performance of grass swales for managing highway runoff. Water Res. 46 (20), 6775–6786. https://doi.org/10.1016/j.watres.2011.10.017.

Deletic, A., Fletcher, T.D., 2006. Performance of grass filters used for stormwater treatment—A field and modelling study. J. Hydrol. 317 (3–4), 261–275. https://doi.org/10.1016/j.jhydrol.2005.05.021.

Ding, B., Rezanezhad, F., Gharedaghloo, B., Van Cappellen, P., Passeport, E., 2019. Bioretention cells under cold climate conditions: effects of freezing and thawing on water infiltration, soil structure, and nutrient removal. Sci. Total Environ. 649, 749–759. https://doi.org/10.1016/j.scitotenv.2018.08.366.

Dong, C., Menzel, L., 2020. Recent snow cover changes over central European low mountain ranges. Hydrol. Process. 34 (2), 321–338. https://doi.org/10.1002/hyp.13586.

Ekka, S.A., Rujner, H., Leonhardt, G., Blecken, G.-T., Viklander, M., Hunt, W.F., 2021. Next generation swale design for stormwater runoff treatment: a comprehensive approach. J. Environ. Manage. 279, 111756. https://doi.org/10.1016/j.jenvman.2020.111756.

Elrick, D.E., Parkin, G.W., Reynolds, W.D., Fallow, D.J., 1995. Analysis of early-time and steady state single-ring infiltration under falling head conditions. Water Resour. Res. 31 (8), 1883–1893. https://doi.org/10.1029/95WR01139.

Fach, S., Engelhard, C., Wittke, N., Rauch, W., 2011. Performance of infiltration swales with regard to operation in winter times in an Alpine region. Water Sci. Technol. 63 (11), 2658–2665. https://doi.org/10.2166/wst.2011.153.

Flerchinger, G.N., Lehrsch, G.A., McCool, D.K., 2013. Freezing and Thawing|Processes. In: Reference Module in Earth Systems and Environmental Sciences (p. B9780124095489053000). Elsevier. 10.1016/B978-0-12-409548-9.05173-3.

Fletcher, T.D., Andrieu, H., Hamel, P., 2013. Understanding, management and modelling of urban hydrology and its consequences for receiving waters: a state of the art. Adv. Water Resour. 51, 261–279. https://doi.org/10.1016/j.advwatres.2012.09.001.

Fletcher, T.D., Shuster, W., Hunt, W.F., Ashley, R., Butler, D., Arthur, S., Trowsdale, S., Barraud, S., Semadeni-Davies, A., Bertrand-Krajewski, J.-L., Mikkelsen, P.S., Rivard, G., Uhl, M., Dagenais, D., Viklander, M., 2015. SUDS, LID, BMPs, WSUD and more – The evolution and application of terminology surrounding urban drainage. Urban Water J. 12 (7), 525–542. https://doi.org/10.1080/1573062X.2014.916314.

Flury, M., Flühler, H., Jury, W.A., Leuenberger, J., 1994. Susceptibility of soils to preferential flow of water: a field study. Water Resour. Res. 30 (7), 1945–1954. https://doi.org/10.1029/94WR00871.

Fouli, Y., Cade-Menun, B.J., Cutforth, H.W., 2013. Freeze–thaw cycles and soil water content effects on infiltration rate of three Saskatchewan soils. Canadian J. Soil Sci. 93 (4), 485–496. https://doi.org/10.4141/cjss2012-060.

García-Serrana, M., Gulliver, J.S., Nieber, J.L., 2017. Non-uniform overland flow-infiltration model for roadside swales. J. Hydrol. 552, 586–599. https://doi.org/10.1016/j.jhydrol.2017.07.014.

Gardner, W.R., 1958. Some steady-state solutions of the unsaturated moisture flow equation with application to evaporation from a water table. Soil Sci. 85 (4), 228.

Garvelmann, J., Pohl, S., Weiler, M., 2015. Spatio-temporal controls of snowmelt and runoff generation during rain-on-snow events in a mid-latitude mountain catchment. Hydrol. Process. 29 (17), 3649–3664. https://doi.org/10.1002/hyp.10460.

Gavrić, S., Leonhardt, G., Österlund, H., Marsalek, J., Viklander, M., 2021. Metal enrichment of soils in three urban drainage grass swales used for seasonal snow storage. Sci. Total Environ. 760, 144136. https://doi.org/10.1016/j.scitotenv.2020.144136.

Gimingham, C.H., 1969. The interpretation of variation in North-European Dwarf-Shrub heath communities. Vegetatio 17 (1), 89–108. https://www.jstor.org/stable/20035430.

Gray, D.M., Landine, P.G., Granger, R.J., 1985. Simulating infiltration into frozen Prairie soils in streamflow models. Canadian J. Earth Sci. https://doi.org/10.1139/e85-045.

Hanslin, H.M., Kollmann, J., 2016. Positive responses of coastal dune plants to soil conditioning by the invasive Lupinus nootkatensis. Acta Oecol. 77, 1–9. https://doi.org/10.1016/j.actao.2016.08.007.

Henry, H.A.L., 2007. Soil freeze–thaw cycle experiments: trends, methodological weaknesses and suggested improvements. Soil Biol. Biochem. 39 (5), 977–986. https://doi.org/10.1016/j.soilbio.2006.11.017.

Hillel, D., 1998. Environmental soil physics: Fundamentals, applications, and environmental considerations. Elsevier.

Iceland Meteorological Office [IMO], 2020a. Ten-minute Weather and Rainfall Data at Gardabaer, Urridaholt Station No. 1474. Data delivery April 21, 2020.

Iceland Meteorological Office [IMO], 2020b. Daily Snow Depth at Reykjavík Manned Synoptic Station No. 1.

Kane, D.L., 1980. Snowmelt infiltration into seasonally frozen soils. Cold Regions Sci. Technol. 3 (2–3), 153–161. https://doi.org/10.1016/0165-232X(80)90020-8.

Kane, D.L., Stein, J., 1983. Water movement into seasonally frozen soils. Water Resour. Res. 19 (6), 1547–1557. https://doi.org/10.1029/WR019i006p01547.

Khan, U.T., Valeo, C., Chu, A., van Duin, B., 2012. Bioretention cell efficacy in cold climates: Part 1 — hydrologic performance. Canadian J. Civil Eng. 39 (11), 1210–1221. https://doi.org/10.1139/l2012-110.

LeFevre, N.J., Davidson, J.D., Oberts, G.L., 2009. Bioretention of simulated snowmelt: cold climate performance and design criteria. Cold Regions Eng. 2009, 145–154. https://doi.org/10.1061/41072(359)17.
Lehrsch, G.A., 1998. Freeze-thaw cycles increase near-surface aggregate stability. Soil Sci. 163 (1), 63–70. Scopus. 10.1097/00010694-199801000-00009.
Moghadas, S., Gustafsson, A.-M., Viklander, P., Marsalek, J., Viklander, M., 2016. Laboratory study of infiltration into two frozen engineered (sandy) soils recommended for bioretention: laboratory study of infiltration into frozen engineered soil. Hydrol. Process. 30 (8), 1251–1264. https://doi.org/10.1002/hyp.10711.
Muthanna, T.M., Viklander, M., Thorolfsson, S.T., 2008. Seasonal climatic effects on the hydrology of a rain garden. Hydrol. Process. 22 (11), 1640–1649. https://doi.org/10.1002/hyp.6732.
Orradottir, B., Archer, S.R., Arnalds, O., Wilding, L.P., Thurow, T.L., 2008. Infiltration in icelandic andisols: the role of vegetation and soil frost. Arctic Antarctic Alpine Res. 40 (2), 412–421. https://doi.org/10.1657/1523-0430(06-076)[ORRADOTTIR]2.0.CO;2.
Paus, K.H., Muthanna, T.M., Braskerud, B.C., 2016. The hydrological performance of bioretention cells in regions with cold climates: Seasonal variation and implications for design. Hydrol. Res. 47 (2), 291–304. https://doi.org/10.2166/nh.2015.084.
Pitt, R., Chen, S., Clark, S., 2002. Compacted urban soils effects on infiltration and bioretention stormwater control designs. Global Solutions Urban Drainage. https://doi.org/10.1061/40644(2002)14.
Prince George's County, 1999. Low-impact Development: An Integrated Design Approach. MD Department of Environmental Resources.
Rawls, W.J., Brakensiek, D.L., Miller, N., 1983. Green-ampt infiltration parameters from soils data. J. Hydraulic Eng. 109 (1), 62–70. https://doi.org/10.1061/(ASCE)0733-9429(1983)109:1(62).
Reynolds, W.D., Elrick, D.E., 1990. Ponded infiltration from a single ring: I. Analysis of steady flow. Soil Sci. Soc. Am. J. 54 (5), 1233–1241. https://doi.org/10.2136/sssaj1990.03615995005400050006x.
Riege, D.A., Sigurgeirsson, A., 2009. Facilitation of afforestation by Lupinus nootkatensis and by black plastic mulch in south-west Iceland. Scand. J. Forest Res. 24 (5), 384–393. https://doi.org/10.1080/02827580903117404.
Roseen, R.M., Ballestero, T.P., Houle, J.J., Avellaneda, P., Briggs, J., Fowler, G., Wildey, R., 2009. Seasonal performance variations for storm-water management systems in cold climate conditions. J. Environ. Eng. 135 (3), 128–137. https://doi.org/10.1061/(ASCE)0733-9372(2009)135:3(128).
Rujner, H., Leonhardt, G., Marsalek, J., Perttu, A.-M., Viklander, M., 2018. The effects of initial soil moisture conditions on swale flow hydrographs. Hydrol. Process. 32 (5), 644–654.
Sterpi, D., 2015. Effect of freeze–thaw cycles on the hydraulic conductivity of a compacted clayey silt and influence of the compaction energy. Soils Found. 55 (5), 1326–1332. https://doi.org/10.1016/j.sandf.2015.09.030.
Stoeckeler, J.H., Weitzman, S., 1960. Infiltration rates in frozen soils in Northern Minnesota. Soil Sci. Soc. Am. J. 24 (2), 137–139. https://doi.org/10.2136/sssaj1960.03615995002400020020x.
Swartzendruber, D., Olson, T.C., 1961. Sand-model study of buffer effects in the double-ring infiltrometer. Soil Sci. Soc. Am. J. 25 (1), 5–8. https://doi.org/10.2136/sssaj1961.03615995002500010009x.
USDA, 1987. Soil Mechanics Level 1: Module 3—USDA Textural Soil Classification. *Study Guide*.
van der Kamp, G., Hayashi, M., Gallén, D., 2003. Comparing the hydrology of grassed and cultivated catchments in the semi-arid Canadian prairies. Hydrol. Process. 17 (3), 559–575. https://doi.org/10.1002/hyp.1157.
Veitur, 2021. Soil temperature measured at Heiðmörk by station in unforested area. Data delivery April 20, 2021. Reykjavik: Veitur ehf.
Vetter, V.M.S., Tjaden, N.B., Jaeschke, A., Buhk, C., Wahl, V., Wasowicz, P., Jentsch, A., 2018. Invasion of a legume ecosystem engineer in a cold biome alters plant biodiversity. Front. Plant Sci. https://doi.org/10.3389/fpls.2018.00715.
Westerström, G., 1984. Snowmelt runoff from Porsön residential area, Luleå. 4, 315–323. http://urn.kb.se/resolve?urn=urn:nbn:se:ltu:diva-38161.
Wong, T.H.F., Brown, R.R., 2009. The water sensitive city: principles for practice. Water Sci. Technol. 60 (3), 673–682. https://doi.org/10.2166/wst.2009.436.
Youngs, E.G., 1987. Estimating hydraulic conductivity values from ring infiltrometer measurements. J. Soil Sci. 38 (4), 623–632. https://doi.org/10.1111/j.1365-2389.1987.tb02159.x.
Zaqout, T., Andradóttir, H.Ó., 2021. Hydrologic performance of grass swales in cold maritime climates: impacts of frost, rain-on-snow and snow cover on flow and volume reduction. J .Hydrol. 597, 126159. https://doi.org/10.1016/j.jhydrol.2021.126159.
Zwissler, B., Oommen, T., Vitton, S., 2016. Method to quantify freeze-thaw effects on temperate climate soils: Calvert Cliffs. J. Cold Regions Eng. 30, 06016002. https://doi.org/10.1061/(ASCE)CR.1943-5495.0000103.

Paper III

Trends in soil frost formation in a warming maritime climate and the impacts on urban flood risk

Tarek Zaqout [1,*], Hrund Ólöf Andradóttir[1], Johanna Sörensen[2]

[1] Faculty of Civil and Environmental Engineering, University of Iceland, Hjarðarhagi 6, 107 Reykjavík, Iceland, tarek@hi.is, hrund@hi.is

[2] Division of Water Resources Engineering, Lund University, John Ericssons Väg 1, V-Hus, Lund, Sweden, johanna.sorensen@tvrl.lth.se

Abstract

The most severe urban flooding in cold maritime climates is due to the co-action of long-duration rainfall, snowmelt, and soil frost. Increasing winter air temperature due to climate change is projected to change the magnitude and frequency of rain-on-snow (RoS) events and increase the number of freeze-thaw cycles and midwinter snowmelt. While daily rainfall records are readily available, less is known about the infiltration and frost formation within urban soils. Thus, there is uncertainty on how warming winter conditions may affect urban flood risk and the climate resilience of cities. The aim of this study was, therefore, to assess soil frost formation in the past 70 years in the maritime city of Reykjavík, Iceland (64° N, 21° W), and its co-action with runoff generation, and the potential implications on urban flood risk. To that end, the daily thermal and hydraulic conditions of the soil were simulated using the SHAW model dating back to 1949, calibrated based on hourly observations from 2007. Model simulations indicated that the minimum soil temperature at 10 cm depth has been warming at a rate of 0.015 °C/year in the past seven decades. Climate warming is also noted in a steady decline in frost depth and the duration of soil

frost each winter (p-value < 0.05). However, the freezing season has shortened so that the timing of maximum frost coincides more with the timing of maximum RoS and snowmelt events. Furthermore, RoS events during frost have the capacity to produce larger runoff volumes than rainfall or snowmelt alone based on the joint frequency analysis of winter events using the copula method. This, combined with increasing volume during RoS events, suggests that winter floods may intensify in the next decades, which urges re-thinking urban stormwater management in cold climates.

Keywords: Climate change, flooding, rain on snow, snowmelt, frost, SHAW model.

1. Introduction

Soil frost is a widespread phenomenon affecting about 35% of the earth's surface (Williams & Smith, 1989). Soil frost significantly alters the hydrological cycle, and surface and subsurface exchanges of water and energy (Shanley & Chalmers, 1999; Wang et al., 2009). Infiltration into frozen and partially frozen soils is reduced due to the presence of ice lenses (Granger et al., 2011; Khan et al., 2012; Slater et al., 1998; Wang et al., 2009). Soil frost paired with rain-on-snow (RoS) generated the greatest number of flooded properties in a cold maritime climate (Andradóttir et al., 2021). Additionally, frost formation is a key performance indicator for the hydrological performance of sustainable urban drainage systems (SUDS), which are increasingly adopted to integrate separate stormwater systems and increase cities' resilience to climate change (Zaqout et al., 2022; Zaqout & Andradóttir, 2021). Water infiltration into frozen soil is essential for understanding and managing the biological activity and nutrients in soils (Watanabe et al., 2013). Severe frost action can impair the development and even the existence of plants and, as such, is known to severely contribute to soil erosion and compromise land restoration efforts (Arnalds, 2015; Benninghoff, 1952).

The atmospheric-soil exchanges of heat and water, and hence soil frost formation, are governed by the surface conditions (snow and vegetation) and the physical properties of the underlying soil. Plant foliage influences the albedo and wind velocity profile near the soil surface, and hence the shortwave and turbulent heat exchanges; plant roots affect the soil porosity and stability (Flerchinger & Pierson, 1991; Zaqout et al., 2022). Snow is an effective insulator, and the absence of or late-developing snowpacks leads to deeper and more persistent soil frost (Shanley & Chalmers, 1999; Stadler et al., 2000). The conductance of heat and water through the soil is

affected by the grain size distribution, porosity, organic content, the presence of macropores and cracks, and the water content of the soil at the onset of freezing (Stähli et al., 1999). Specifically, dry soils have been found to maintain infiltration even when frozen, while saturated soils promote concrete frost formation (Granger et al., 2011; Kane, 1980).

Coastal cold regions are subjected to intermittent midwinter snowmelt, RoS events, and freeze-thaw cycles (Andradóttir et al., 2021; Muthanna et al., 2008). The repeated supply of near-freezing meltwater, together with the lack of the thermal insulation provided by a continuous snow cover, results in an excessive wetting of the soil, rendering it susceptible to frequent freezing and thawing (Zaqout et al., 2022; Zaqout & Andradóttir, 2021). Frequent freeze-thaw cycles (FTCs) negatively affect soil ecosystem diversity and productivity because they cause changes in soil physical properties, lead to soil deformation, and affect water movement (Fouli et al., 2013). Liquid-solid phase changes alter the soil's hydraulic and thermal properties significantly (Lundin, 1990; Watanabe & Kugisaki, 2017; Zheng et al., 2021). Thus, to fully understand frost formation in a cold maritime climate undergoing frequent freeze-thaw requires either the monitoring of water content and soil temperature; Alternatively, the coupled modeling of heat and water transfer through the snow, vegetation, and soil strata. Several numerical models of soil freezing and thawing have been developed for agricultural, forestry, ecological, and civil engineering applications (e.g., Flerchinger & Saxton, 1989; Guymon & Luthin, 1974; Hansson et al., 2004; Jansson & Karlberg, 2004; Šimůnek et al., 2016). However, most studies on soil freezing and thawing used data from laboratory experiments to calibrate and validate the models (He et al., 2015; Zheng et al., 2021), which may not be representative of the temporal and spatial variations in atmospheric forcing, soil layering, vegetation covers in the field (Zheng et al., 2021).

Assessing flood risks in urban areas is difficult due to the heterogeneous nature of urban catchments and the complex interactions between rain, snow, and soil frost (Andradóttir et al., 2021; Moghadas et al., 2018). In recent years, joint probability theories have been adopted to analyze flood risk resulting from two or more hydrologic variables (Lian et al., 2013; Sörensen & Bengtsson, 2014; Zellou & Rahali, 2019), the most famous of which is the copula model (Chen, 2019; Nelsen, 2007). Introduced by Sklar (1959), the method involves expressing a multivariate joint cumulative distribution function in terms of univariate marginal distribution functions and describing the dependence between the variables with copula functions (Salvadori & De Michele, 2007).

With more wet and warm winters, precipitation falls more in liquid form. Midwinter melt and RoS events have been found to become more frequent (Garvelmann et al., 2015; Surfleet & Tullos, 2013; Wever et al., 2014; Würzer & Jonas, 2018) and RoS events more voluminous (Andradóttir et al., 2021). Moreover, the number of freeze-thaw cycles has been increasing in mountainous regions (Garvelmann et al., 2015; Würzer et al., 2016). Frequent RoS, snowmelt, frost formation, and infiltration in frozen ground are highly interlinked processes and less understood than during continuous snow cover (Wever et al., 2014). While soil frost is a key indicator of urban flooding, it is rarely considered when planning urban drainage systems (Bengtsson & Westerström, 1992; Caraco & Claytor, 1997; Maksimovic et al., 2000). The lack of routine monitoring of soil is also a limiting factor for understanding urban flood risk and how the urban flood risk may change with climate change. Therefore, the goal of this research was, on the one hand, to improve the understanding of soil frost formation in an area undergoing frequent freeze-thaw cycles and RoS events by means of numerical modeling. On the other hand, to analyze the joint probability and

timing of winter flood indicators (i.e., rainfall, snowmelt, and RoS events) during frost. Lastly, the implications of the research findings on urban flood risk and stormwater management are discussed in the context of the need for more climate-resilient cities, as stipulated by the United Nations (Sustainable Development Goal No. 11).

2. Materials and Methods

2.1.Numerical model

Three coupled, one-dimensional numerical models were preliminarily assessed: Hydrus 1-D (Šimůnek et al., 2016), SWAT (Neitsch et al., 2011), and the Simultaneous Heat and Water (SHAW) model (Flerchinger & Saxton, 1989a, 1989b). The SHAW model, which is widely applied to in situ soil freezing and thawing events, performed best in the preliminary tests and was chosen for this study.

The SHAW model is a physically-based, finite-difference, coupled heat, water, and solute transfer model in the atmosphere–plant–snow–residue–soil systems (Fig. 1). It requires knowledge of soil physical and hydraulic properties, i.e., soil texture, bulk density, saturated water content, and saturated hydraulic conductivity, as well as meteorological conditions. The water balance is expressed as (Flerchinger & Saxton, 1989a):

$$\frac{\partial \theta_l}{\partial t} + \frac{\rho_i}{\rho_l}\frac{\partial \theta_i}{\partial t} = \frac{\partial}{\partial Z}\left[K\left(\frac{\partial \Psi}{\partial Z}\right) + 1\right] + \frac{1}{\rho_l}\frac{\partial q_v}{\partial Z} \quad (1)$$

where t is the time (s), θ_l is the liquid volumetric water content ($m^3\ m^{-3}$), θ_i is the frozen volumetric water content ($m^3\ m^{-3}$), ρ_l is the liquid water density (kg m^{-3}), ρ_i is the ice density (kg m^{-3}), K is the hydraulic conductivity (m s^{-1}), Ψ is the soil water matric potential (m H_2O), q_v is the vapor water flux (m s^{-1}), and Z is the depth (m).

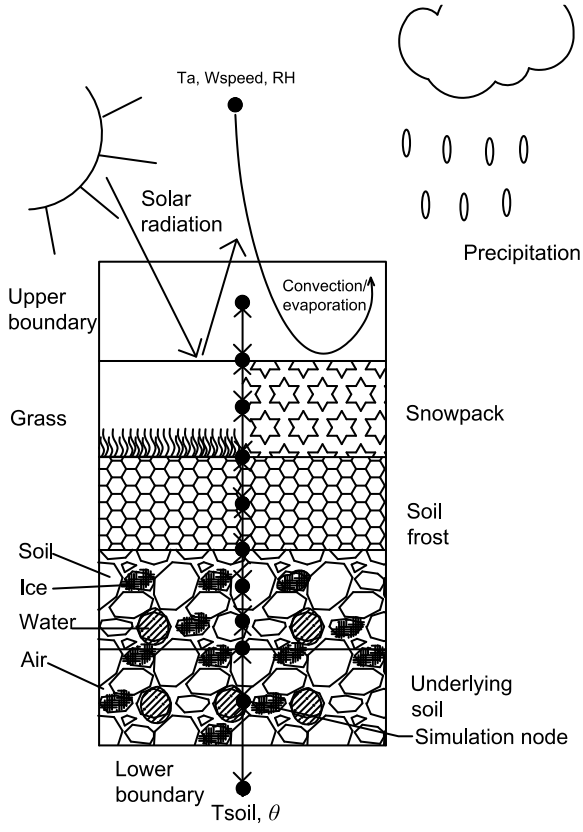

Figure 1 Physical system described by the SHAW model showing the upper (energy budget at the surface) and lower boundary, snowpack and soil frost on the right, the vegetation cover, and the underlying soil constituents on the left.

The relationship between matric potential, Ψ, liquid water content, θ_l, and hydraulic conductivity, K, is expressed by a set of equations that govern the water movement in the soil (Campbell, 1974).

$$\Psi = \Psi_e \left(\frac{\theta_l}{\theta_s}\right)^{-b} \tag{2}$$

$$K = K_s \left(\frac{\Psi_e}{\Psi}\right)^{2+(\frac{3}{b})} = K_s \left(\frac{\theta_l}{\theta_s}\right)^{2b+3} \tag{3}$$

Here, θ_s is the saturated water content ($m^3\ m^{-3}$), Ψ_e is the air entry potential (m H_2O), and b is the pore size distribution index, K_s is the saturated hydraulic conductivity (m s^{-1}). Once frost is developed, the capillary suction acts to pull water from the unfrozen soil upwards towards the freezing front. This equation describing the relationship between matric potential Ψ, and soil temperature T (°C) is as follows (Fuchs et al., 1978):

$$\Psi = \frac{L_f}{g}\left(\frac{T}{T + 273.16}\right) \tag{4}$$

Where g is the gravitational acceleration (m s^{-2}), L_f is the latent heat of fusion (J m^{-3}). The ice content θ_i can be determined as the difference between the total water content and the maximum liquid water content.

The governing one-dimensional energy equation, which includes soil temperature, freezing and thawing, and conductive and convective heat transfer of liquid and vapor, is described by Flerchinger & Saxton (1989a)

$$C_s \frac{\partial T}{\partial t} - \rho_i L_f \frac{\partial \theta_i}{\partial t} = \frac{\partial}{\partial Z}\left(\lambda_s \frac{\partial T}{\partial Z}\right) - \rho_l c_l \frac{\partial (q_l T)}{\partial Z} - L_v \left(\frac{\partial q_v}{\partial Z} + \frac{\partial \rho_v}{\partial t}\right) \quad (5)$$

where C_s is the volumetric heat capacity of the soil (J m^{-3} °C^{-1}), λ_s is the soil thermal conductivity (W m^{-1} °C^{-1}), and c_l is the specific heat of liquid water (J kg^{-1} °C^{-1}). The thermal conductivity and heat capacity of the soil is based on summing the different soil constituents (minerals, organic matter, water, ice, and air) following the method developed by de Vries (1963) and modified for frozen soils by Penner (1970)

$$\lambda_s = \frac{\sum m_j \lambda_j \theta_j}{\sum m_j \theta_j} \quad (6)$$

$$C_s = \sum \rho_j C_j \theta_j \quad (7)$$

where m is a weighing factor, and j denotes the different soil constituents. Moist soil with a water content of 0.05 m^3 m^{-3} or higher for sand, and 0.15 m^3 m^{-3} or higher for clay, is a continuum of liquid water, soil granules, ice, and air.

The surface boundary condition is determined by the energy balance on the surface as follows:

$$R_n + H_{sf} + L_v E_{sf} + G = 0 \quad (8)$$

where R_n is the net radiation (W m^{-2}), H_{sf} is sensible heat flux (W m^{-2}), E_{sf} is the evaporation rate (m s^{-1}), and G is the ground conduction flux (W m^{-2}).

2.2.Study site

The capital region of Reykjavík (230,000; 1000 km^2) includes six municipalities sited within a few kilometers from the coastline in the southwestern corner of Iceland (Fig. 2). The local climate is heavily influenced by the Gulf Stream, with cool summers and mild winters with temperatures fluctuating around the freezing point (Einarsson, 1984). Soil frost rarely extends beyond 20 cm depth (Petersen, 2018). Precipitation tends to be frequent and mild (213 rainy days totaling approx. 1000 mm per annum; Ólafsson et al. (2007)). Precipitation falls mostly at high winds with the forward passage of cyclones from the southwest, which prevail especially in winter (Einarsson, 1984). The most severe urban flood events in Reykjavík were associated with the co-action of rain, snow, and soil frost (Andradóttir et al., 2021).

Figure 2 Greater capital area of Reykjavík Iceland. Road infrastructure marked as grey lines, the Atlantic Ocean and freshwater bodies in light blue, and the study sites as squares. The smaller map shows location of Reykjavík capital area in Iceland.

2.3.Input data and calibration

Data from two sites located 6 km apart were obtained for the purpose of the study (Fig. 2). Both sites were located in open grass-covered areas, 40–50 (m a.s.l.) and at less than 3 km distance from the ocean (Table 1).

Table 1 Summary of sites soil physical properties and high-resolution weather and soil monitoring.

		Urriðaholt	**Reykjavík**
Site	**Elevation**	42 m a.s.l.	52 m a.s.l.
	km to sea	2.8	2.5
	Land slope	3.3%	0%
	Surface cover	Grass	Grass
Soil	**Soil type**	Sandy loam	N/A
	Bulk density	1.46–1.93 g cm^{-3}	N/A
Monitoring	**Parameters**	T_s & WC	T_s
	Depths (cm)	5, 15, 25, 35, 45	10, 20, 50, 100
	Period	Nov 2018–2022	Sep 2007–2019
	Resolution	10 min	1 hour
Weather	**Parameters**	T_a, RH, Ps, W_s, W_d, P	T_a, RH, Ps, W_s, W_d, P, LW, SW
	Period	Feb 2019–2022	Sep 2007–2019
	Resolution	10 min	1 hour

Notes: T_s = soil temperature (°C), WC = water content, RH = relative humidity (%), P_s = atmospheric pressure (hPa), W_s = wind speed (m/s), W_d = wind direction, P = Precipitation, L/SW = long/short wave radiation.

Urriðaholt site

For the purpose of calibrating and testing the model, hourly weather and soil temperature data were compiled from the high resolution (10 minutes) monitoring program in the residential neighborhood Urriðaholt in Garðabær, Iceland (64° 4'18.46" N, 21° 54'37.11" W) as described in (Zaqout et al., 2022). The neighborhood was built with a large network of sustainable urban

drainage systems (SUDS) to safeguard the quantity and quality of water entering Urriðavatn pond. Soil temperature and water content were monitored at 5 cm depths within a grass swale starting November 2018. For model simulations, hourly incoming shortwave radiation was used from Reykjavík station (IMO, 2022a).

Measured soil temperature and moisture content in the grass swale at the Urriðaholt site was used as the initial values at each depth for the start of the simulation period in 2018. Soil physical characteristics at different horizons, such as particle size distribution and bulk density, were measured in the laboratory. The soil was sandy loam with 15–20% gravel, 75–82% sand, and 2.5–4% silt and clay. Saturated soil water content and field capacity were estimated from observed soil water content measured using water content reflectometers. Saturated hydraulic conductivity was estimated based on typical values for the corresponding soil textural class, cross-checked with single-ring infiltration measurements at the study site. More details on the soil monitoring program are available in Zaqout & Andradóttir (2021) and Zaqout et al. (2022).

Reykjavík site

Long-term soil frost formation in the capital was simulated using historical weather data from the IMO headquarters in Bústaðavegur 7, Reykjavík (64° 07'39.1" N, 21° 54'08.5" W). The model was first calibrated against hourly soil temperature using the automatic meteorological monitoring record over 12 years (Table 1). Soil physical and hydraulic characteristics were manually adjusted by trial-and-error, starting with measured soil properties in Urriðaholt as basis (Table 1 in supplements). The model was then run using 24-hour average air temperature, relative humidity, precipitation, and wind speed measured from midnight to midnight (IMO, 2020b). Daily solar radiation prior to 2007 was estimated based on the potential extraterrestrial solar radiation (S_o, W

m^{-2}) that is largely depicted by latitude, and measured diurnal cloud cover, *N*. Following the approach outlined in Bras (1990), the clear sky solar radiation, S_c, was estimated as:

$$\frac{S_c}{S_o} = \exp\left(-n\,\alpha 1\,m\right) \tag{9}$$

where a turbidity factor of $n = 3$ was chosen to represent the clean urban area, α_1 is the molecular scattering coefficient, and the optical air mass, *m*, approximated by the cosecant ($1/\sin\alpha$) of the solar altitude α. Cloud cover in oktas was converted to a ratio from 0 to 1, and the net radiation incoming radiation was estimated as:

$$\frac{S_s'}{S_c} = 1 - 0.65N^2 \tag{10}$$

The accuracy of the shortwave radiation estimation was determined by comparing it with observed solar radiation from 2007 to 2018 and found to highly agree with the observed values (R^2=0.9, RMSE=33 W/m^2; Fig. A.1).

2.4.Data analyses

Model performance evaluation

The model prediction ability was primarily assessed based on soil temperature and secondarily on the basis of soil water content. Two performance metrics were used. The linear correlation coefficient (R^2) was calculated to test how well seasonal and synoptic changes were represented in the model. In addition, the root mean square error (RMSE) was calculated to assess the average deviation between the observed and simulated value at each time step.

Soil frost statistics and trends

The most relevant model outputs to soil frost were soil frost depth, soil temperature, and ice content for each soil layer ($m^3\ m^{-3}$). SHAW model calculates frost depth via linear interpolation of ice content in the deepest layer with frost. A soil layer can have a sub-freezing temperature but will not be considered frozen unless ice is present. For each calendar year, the number of frost days and days with continuous frost were determined. A freeze-thaw cycle (FTC) was determined based on the presence of frost in the form of ice content.

Trends were assessed using the Mann-Kendall test (Kendall, 1948; Mann, 1945) and the significance of the slope using the Theil-Sen method (Sen, 1968; Theil, 1950). These methods were chosen due to their simplicity because they are non-parametric (the data does not need to conform with any particular distribution), they allow for missing data, and can be used for small datasets ($n < 40$; Gilbert, 1987). A significant trend is considered for a 95% confidence level ($\alpha = 0.05$).

Co-probability of liquid water and frost

The approach to understanding the co-action of hydrological inputs and soil frost was to estimate the joint probability of occurrence of two winter hydrological events. The combined daily precipitation and snow depth measurements at 9 A.M., annual maximum rainfall, snowmelt, and rain on snow in the presence of soil frost were calculated. Rainfall was distinguished from snowfall based on a temperature threshold, T_{RH} (°C), that incorporated relative humidity, RH (%), following the method presented by Feiccabrino et al. (2015).

$$T_{RH} = 0.75 + 0.085(100 - RH) \tag{11}$$

With this definition, daily precipitation was classified either as dry or wet, when in some instances, it can take both forms. Snowmelt was defined based on the reduction of snow depth, ΔSD, converted to snow water equivalents assuming a snow density, ρ_s, of 200 kg m^{-3}, in relation to a water density, ρ_w, of 1000 kg m^{-3}. If precipitation was recorded together with a reduction in snow depth, the precipitation was assumed to be rainfall. The magnitude of RoS was taken as the sum of the rain and liquid snowmelt volume (mm) estimated from measured snow depth (in cm) as presented in Andradóttir et al. (2021).

$$RoS = P + snowmelt = P + (\frac{\rho_s}{\rho_w} \times \Delta SD \times 10) \tag{12}$$

Each of the annual daily maximum datasets was fitted to a distribution using the maximum likelihood method, and the goodness of fit was assessed using the Kolmogorov-Smirnov, Cramer-von Mises, and Anderson-Darling tests. Then, the distribution with the lowest Akaike (AIC) and Bayesian Information Criteria (BIC) was chosen. As such, maximum snowmelt during frost was fitted to the lognormal distribution, maximum frost during snowmelt to the Weibull distribution, maximum rainfall during frost to the lognormal distribution, and maximum frost during rainfall to the Weibull distribution. Maximum RoS during frost and maximum frost during RoS were both fitted to the Weibull distribution (Table 2 in supplements). The return periods were then derived for each of the co-acting hydrological variables (Chow et al., 1988).

The copula method was used to estimate the joint distribution C ($F_x(x)$, $F_y(y)$) = C (u_1, u_2) of two dependent variables based on their marginal distributions of the annual maximum values fitted to a theoretical distribution $F_x(x) = u_1$ and $F_y(y) = u_2$ (Chen, 2019; Lian et al., 2013; Zellou & Rahali, 2019). The four Archimedean copulas most widely used for hydrological analyses due to their simplicity (Nelsen, 2007) were tested (Table 2). The three pairs of winter flood-inducing hydrological variables (i.e., maximum snowmelt during frost, rainfall during frost, and RoS during frost) were then fitted to one of the bivariate Archimedean copulas (i.e., Joe, Clayton, Gumbel, and Frank) using the maximum likelihood method. The bivariate copula family that best fits the pair was chosen based on the highest log-likelihood and lowest AIC and BIC (Zellou & Rahali, 2019). Two sets were modeled using the Clayton copula, and RoS during frost was fitted using the Frank copula (Table A.1).

The probabilities of the joint occurrence of annual maxima for the period of 1949 to 2018 were estimated based on the joint cumulative distribution function (CDF). Furthermore, the bivariate

joint return periods for the annual maxima were derived as the inverse of the probability of both events occurring simultaneously, defined as the AND operator. The joint probability of exceedance for two hydrological events was calculated following Lian et al. (2013) and Zellou & Rahali (2019) as:

$$P\big((X > x) \cap (Y > y)\big) = 1 - F(x) - F(y) + F(x, y) \quad (13)$$

where P ((X > x) ∩ (Y > y)) is the probability of both X and Y exceeding a certain threshold.

Table 2 Bivariate Archimedean copula families and their functions and generators. The marginal (univariate) distributions are u1 and u2, and θ is the estimated bivariate copula parameter

Copula	C (u_1, u_2)	Generator	Parameter
Joe (1997)	$1 - \left[(1-u_1)^\theta + (1-u_2)^\theta - (1-u_1)^\theta(1-u_2)^\theta\right]^{\frac{1}{\theta}}$	$\varphi(t) = -ln\left[1-(1-t)^\theta\right]$	$\theta \in [1, \infty)$
Clayton (1978)	$(u_1^{-\theta} + u_2^{-\theta} - 1)^{-\frac{1}{\theta}}$	$\varphi(t) = t^{-\theta} - 1$	$\theta \in (0, \infty)$
Gumbel (1960)	$exp\left\{-\left[(-ln(u_1))^\theta + (-ln(u_2))^\theta\right]^{\frac{1}{\theta}}\right\}$	$\varphi(t) = (-lnt)^\theta$	$\theta \in [1, \infty)$
Frank (1979)	$-\frac{1}{\theta} ln\left[1 + \frac{(e^{-\theta u1} - 1)(e^{-\theta u2} - 1)}{e^{-\theta} - 1}\right]$	$-ln\left(\frac{e^{-\theta t} - 1}{e^{-\theta} - 1}\right)$	$\theta \in R \backslash \{0\}$

3. Results

3.1.Model simulation performance

Soil temperature

The SHAW model accurately predicted the hourly, daily, and seasonal changes in soil temperature at various depths within the top 1 m of soil at both sites during all seasons, as reflected in $R^2 > 0.91$ and RMSE = 0.66–1.6 °C (Table 3). The model performed slightly better at Urriðaholt, where soil properties were tested in the laboratory and the field, than at the Reykjavík site, where the soil properties were not measured. In the Urriðaholt site, the model performed equally well during the calibration period (until August 3, 2020) and validation period (starting August 4, 2020). While the model performance dropped during winters at both sites (lower R^2 and RMSE, Table 3), the timing of frost formation and thawing was well captured within the top 25 cm of the soil that is most susceptible to frost (Fig. 3a, b, and c). Hence, for urban hydrology applications, the model predicts very well repeated freeze-thaw in the top 25 cm of soil. The model performance was slightly lower in the bottom layers. Lastly, as expected, the model was less reliable in capturing temperature peaks during the second winter of 2019/2020, when synthetic runoff experiments were conducted in the grass swales (Zaqout & Andradóttir, 2021). The experiments led to artificially-induced peaks in temperature caused by the infiltration of warmer water, and that winter was excluded.

Table 3 The SHAW model prediction performance of hourly soil temperature and water content in the grass swale in Urriðaholt 2018–2022 and Reykjavík 2007–2018. The range represents varying soil depth or variations between winters.

			Calibration		Validation	
Site			R^2	RMSE	R^2	RMSE
Reykjavík	T_s	All seasons	0.91–0.92	0.98–1.64	-	-
		Winters	0.30*–0.94	0.82–2.53*		
Urriðaholt	T_s	All seasons	0.98–0.99	0.66–0.89	0.97–0.98	0.71–0.93
	T_s	Winter 1, 2	0.71–0.94	0.40–1.08	-	-
	T_s	Winter 3, 4	-	-	0.66–0.88	0.66–0.99
	WC	All seasons	0.1–0.43	0.02–0.06	0.2–0.44	0.01–0.06

Notes: * Greater deviations were found for the last three years. Winter 1, 2, 3, and 4 refer to the four winters between 2018 and 2022.

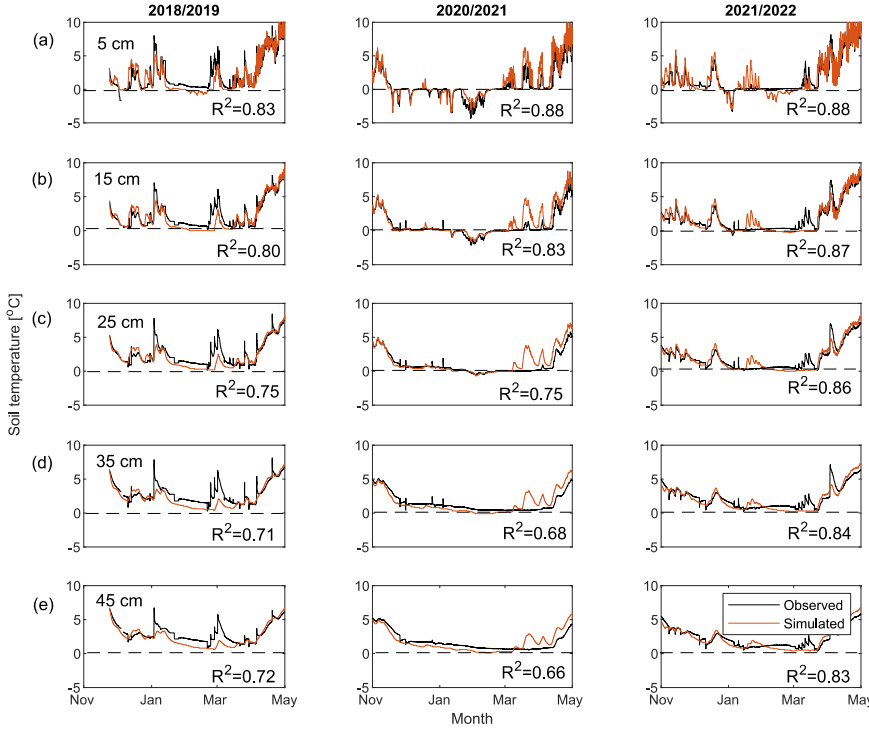

Figure 3 Observed and simulated soil temperature in the grass swale in Urriðaholt during winter 1 (2018/2019; left panels), winter 3 (2020/2021; middle panels), and winter 4 (2021/2022; right panels) at a) 5 cm depth, b) 15 cm, c) 25 cm, d) 35 cm, and e) 45 cm.

Soil liquid moisture content and frost depth

The simulated moisture content deviated considerably from observed values at Urriðaholt (Table 3). For the entire monitoring period, the model's performance was relatively more accurate for the validation period than the calibration (R^2 = 0.1–0.43 vs. 0.2–0.44). The simulated values were worse during winter when the model failed to capture sharp increases during rainfall. It did,

however, capture relatively well the reduction in liquid moisture content resulting from soil freezing. Moreover, the model confirms observations that that soil in Urriðaholt in winter is permanently wet (Zaqout et al., 2022; Zaqout & Andradóttir, 2021), so sub-freezing temperatures might develop frost. The model accurately predicted soil frost formation and frost depth during four winters with very different frost conditions (Fig. 4). In the winter of 2018/2019, frost was only observed at the topsoil horizon (5 cm), represented by negative soil temperature and a reduction in the liquid moisture content due to the phase change (heavy horizontal line in Fig. 4). The model, however, predicted the frost depth to have reached down to a 12 cm depth. This was also shown in the simulated ice content by the model as ice developed at the 5-cm simulation depth (θ_i = 0.24) and slightly at 15 cm depth (θ_i = 0.07). The second winter, in contrast, showed more occurrences of soil frost compared to the first winter with longer persistence (Fig. 4). Still, the maximum frost depth similarly did not extend beyond the 15-cm soil horizon, which was also consistent with the field observations. However, the ice content was almost double of that during the preceding winter at the same depth (θ_i = 0.41), which indicates that the topsoil horizon was almost completely frozen with few soil pores available for infiltration (θ_{max} = 0.54 at 5 cm depth). During the winter of 2020/2021, the soil experienced severe freezing reaching down to 31 cm depth, while the observed soil frost was only at 25 cm due to the 10-cm spacing between sensors. The maximum ice content at 5 cm was similar to the one during the preceding winter (θ_i = 0.43). All the layers, except the one at 45 cm, developed frost represented in the predicted ice content (θ_i = 0.26, 0.15, and 0.02) for the second, third, and fourth layers, respectively. In the winter of 2021/2022, the soil was frozen down to a maximum of 20 cm, and the maximum ice content was 0.22 at 5 cm depth as well as 15 cm. During the last winter, the maximum frost depth was observed to reach 15 cm, while the model estimated frost at a 20 cm depth.

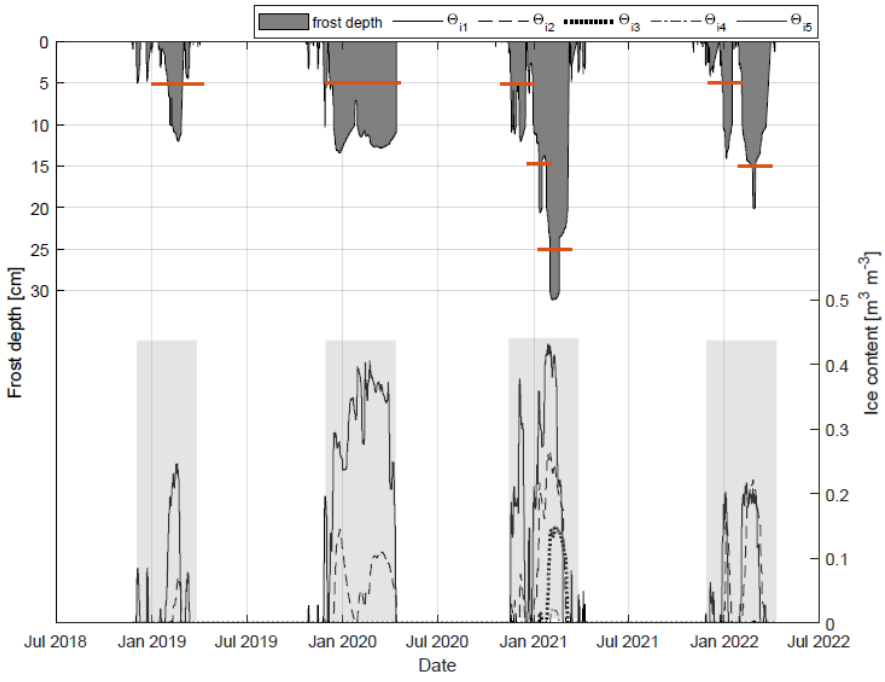

Figure 4 Total simulated frost depth and ice content at 5, 15, 25, 35, and 45 cm depths (θ_{i1}–θ_{i5}) in the grass swale in Urriðaholt in winters between 2018 and 2022. Solid orange horizontal lines are the observed maximum frost depth (measured at 5, 15, 25, 35, and 45 cm depth).

3.2.Soil frost predictions and sensitivity analysis

Daily soil temperature and moisture content at 10, 20, and 50 cm depths, frost, and snow depth were simulated using the calibrated SHAW model and historical weather data at Reykjavík dating back to 1949. Selected time series are presented in Figure 5, and top-level statistics are summarized in Table 4. The model predicts some increase in winter soil temperature (Fig. 5a). The lowest soil temperature at the surface (-3.7 °C) and 10 cm (-2.6 °C) was simulated for the winter of 1949. However, the model overestimated the measured soil temperature in the last three winters (2015–

2018; RMSE=0.82–2.5, R^2=0.3–0.94) while correctly identifying the timing of frost. A consistent decrease in frost depth and ice content from 39 cm in 1949 was seen over 70 years (Fig. 5b and Table 4). The maximum number of days with soil frost in any given calendar year was 153 days, which was in 1951. Meanwhile, the minimum number of frost days was 26 days in 1987 and the shortest period of continuous frost lasted for only 4 days, also in 1987. The average number of freeze-thaw cycles in a year is 3.65, and the maximum was 8 cycles, occurring both in 1965 and 1971.

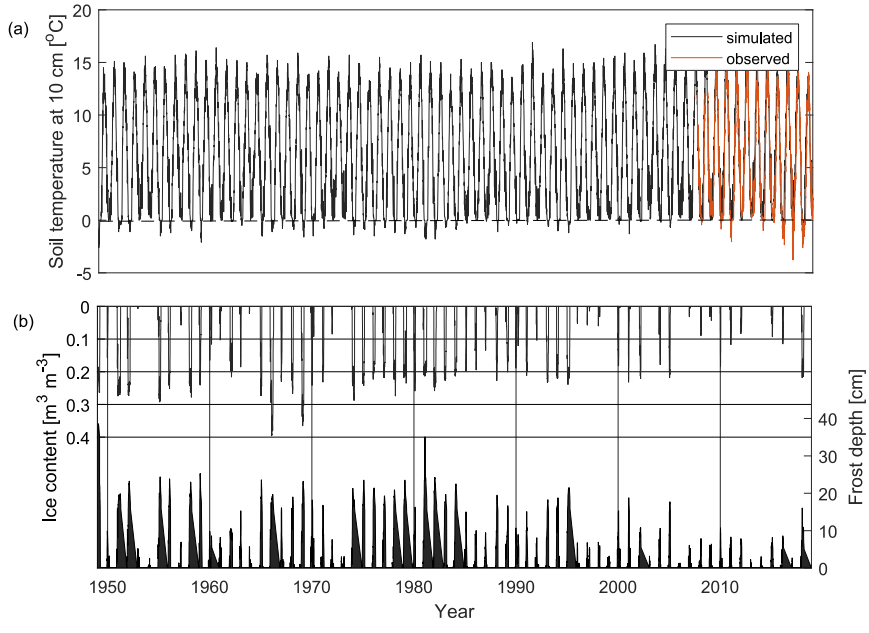

Figure 5 a) Simulated diurnal soil temperature in Reykjavík from 1949 to 2018 and observed (2007–2018) at 10 cm, b) time evolution of soil frost depth and ice content (θi) at 10 cm depth in Reykjavík from simulations from 1949 to 2018.

Table 4 Summary of long-term surface and subsurface winter conditions in Reykjavík for 1949–2018.

	Max.	Min.	Avg. ± Std.
T_{soil} [°C] at 10 cm	17.5	-2.6	6.1 ± 5.2
Snow depth [cm]*	48.0	1.0	7.0 ± 6.7
Frost depth [cm]	39	0.1	9.9 ± 8.1
No. days with soil frost	153	26	85.8 ± 29.7
No. days with continuous frost	158	4.0	65.6 ± 40.8
No. of soil FTC	8.0	1.0	3.65 ± 1.95

Notes: * Observed snow depth values from the Reykjavík station no. 1.

A sensitivity analysis was conducted using several selected parameters, both at the surface and within the soil profile, as well as selected meteorological inputs (Table 5). Common soil textural classes according to the USDA (1987) and saturated hydraulic conductivity were tested. Uncertainty regarding precipitation depth in dry form (snowfall) was also tested using corrected snowfall depth following the method presented by Crochet et al. (2007). The model predictions were consistent in terms of maximum predicted frost depth, no. of frost days, and FTCs, as well as soil temperature (RMSE = 1.51–2.11; R^2 = 0.91–0.93). The model was most sensitive to changes in surface cover as it was found that if the ground was considered bare, the RMSE increased significantly (2.11 °C). Moreover, the prediction for the winter seasons of 2015/2016, 2016/2017, and 2017/2018 was not improved for any of the tested parameters.

Table 5 Sensitivity analysis of selected soil and meteorological parameters.

Parameter	Properties	Soil temp.[1] [°C]	Max. frost depth [cm]	No. of days with frost	No. of FTCs
		RMSE, R^2	Max., Min, Avg. ± Std. Dev.		
Calibrated model run	**Sandy loam, 10 cm grass**	1.64, 0.92	39, 2.9, 15 ± 7	153, 26, 85 ± 30	8, 1, 4 ± 2
Soil texture	Loamy sand	1.60, 0.92	40, 1.7, 16 ± 9	147, 11, 78 ± 30	8, 1, 4 ± 2
	Loam	1.53, 0.93	38, 1.0, 13 ± 8	144, 9, 73 ± 31	9, 1, 4 ± 2
	Sandy clay loam	1.51, 0.93	38, 1.0, 12 ± 7	143, 9, 71 ± 31	9, 1, 4 ± 2
Vegetation cover	Bare ground	2.11, 0.91	38, 2, 16 ± 8	156, 27, 87 ± 31	9, 1, 4 ± 2
	5 cm	1.56, 0.92	38, 2, 15 ± 8	156, 25, 87 ± 30	8, 1, 4 ± 2
Hydraulic conductivity	1 cm/h	1.66, 0.92	37, 2, 15 ± 7	155, 26, 87 ± 30	8, 1, 4 ± 2
	10 cm/h	1.70, 0.92	37, 3, 16 ± 7	156, 30, 90 ± 30	9, 1, 4 ± 2
Precipitation corrected[2]	Snowfall	1.62, 0.92	37, 2, 15 ± 7	155, 23, 85 ± 30	8, 1, 4 ± 2

Notes: [1] Soil temperature simulated at 10 cm depth and compared with observations from 2007 to 2018 at the same depth. [2] Precipitation (snowfall) corrected for underestimated depth with wind speed.

3.3.Soil frost trends

The Mann-Kendall and Sen's slope tests showed that soil frost depth decreased significantly (p-value < 0.05) in the 70 years analyzed in this study (Fig. 6a and Table 6). Similarly, the total number of days with soil frost near the surface has decreased by almost half during these seven

decades, from 108 to 62 days (Fig. 6b). This trend is even greater when considering the number of days of the median annual maximum frost depth (return period of 2 years) at 15 cm depth (Table 6). Projecting the simulations forward, soil frost may rarely reach 15 cm in another two decades. Soil frost has also become less persistent, as the number of days with continuous soil frost decreased significantly (p-value < 0.05; Fig. 6c and Table 6). This suggests that the instances of intermittent formation of soil frost have increased during winter, which was reflected in the increase, however insignificantly, in the number of freeze-thaw cycles over the studied 70 years. The increase in the frequency of intermittent frost can also be seen in the significant increase in the minimum soil temperature at 10 cm depth in Reykjavík for the simulation period of 1949 to 2018 (Fig. 6d).

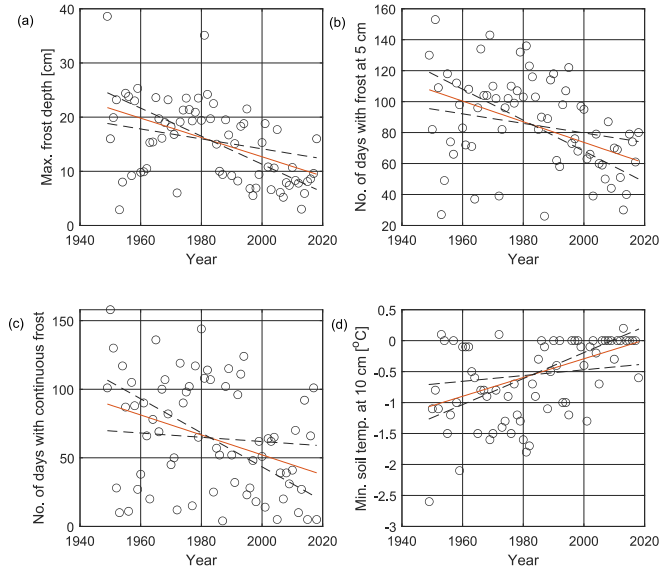

Figure 6 a) Maximum soil frost depth, b) number of days with soil frost at 5 cm depth, c) number of days with continuous frost, and d) minimum soil temperature at 10 cm depth in Reykjavík for the period of (1949–2018). The solid line represents Sen's slope, and the dashed lines represent the trend for the upper and lower 95% confidence intervals of the slope.

Table 6 Median, trends and goodness-of-fit of simulated soil conditions in Reykjavík 1949–2018.

Hydrological variable	Unit	Median	Sen's slope (unit/year)	R^2
Max. frost depth	cm	15.7	-0.18	0.24^{*}
Soil frost at 5 cm depth	days	85.0	-0.67	0.15^{*}
Soil frost at 15 cm depth	days	49.0	-0.84	0.18^{*}
Continuous soil frost	days	64.5	-0.73	0.11^{+}
Min. soil temperature	°C	-0.55	0.015	0.23^{*}

Notes: * $p < 0.001$, $^{+}$ $p < 0.01$

3.4.Co-probability of soil frost and runoff generation

The maximum RoS volume during frost and maximum frost during RoS were both found to fit the Weibull distribution. The univariate return period and event depth (i.e., RoS in mm, and frost in cm) were derived (Table 7). The joint cumulative distribution function of RoS and frost was then calculated using the Frank copula (Table 2). The probability of simultaneous occurrence was obtained using Eq. 15. The probability of two hydrological events occurring simultaneously is considerably lower than the probability of only one occurring at a time. That can be seen in the 2- and 5-year return periods corresponding to 20 and 30 mm of RoS coinciding with frost depths of 11 and 20 cm (Table 7). For instance, a 5-year RoS event (30 mm) occurring simultaneously with a 2-year frost depth (11 cm) has a bivariate return period of approximately 9 years, which can result in repetitive flooding. Furthermore, a 2-year RoS event (20 mm) and a 2-year frost depth (11 cm) have a probability of co-occurring with a return period of less than 4 years (27%), which can be considered a frequent event.

Table 7 Joint probability of occurrence during one year for the maximum RoS volume during the maximum frost depth for different return periods (T) during winter.

		Max. frost depth during RoS [cm]						
		0.7	11.2	19.5	25	29.4	35.1	39.1
Max. RoS volume during frost [mm]	T [years]	1	2	5	10	20	50	100
3.0	1	**0.977**	0.491	0.197	0.095	0.049	0.020	0.010
20.1	2	0.492	**0.266**	0.111	0.054	0.028	0.011	0.006
30.0	5	0.195	0.110	**0.047**	0.023	0.012	0.005	
35.4	10	0.099	0.056	0.024	**0.012**	0.006		
40.1	20	0.050	0.028	0.012	0.006			
45.5	50	0.020	0.011	0.005				
49.2	100	0.010	0.006					

Among the three tested sets (i.e., snowmelt & frost, rainfall & frost, and RoS & frost), the RoS volume during frost was found to be the highest, especially compared with snowmelt and rainfall alone during frost (Fig. 7). Extreme snowmelt events resulting in more than 40–50 mm of meltwater release (T=50–100 years) when the soil is frozen at least at the surface (T=1–2 years) have a probability of only 1–2% (Fig. 7; Table A.2). That said, the probability of a 2-year frost depth (> 10 cm), co-occurring with a 2-year snowmelt event (> 10 mm/d) or a 5-year snowmelt event (20 mm/d) is relatively high (joint probability of 28% and 12%). In contrast, rainfall during frost was found to have slightly larger event depths than those for snowmelt during frost, as well as marginally higher joint probabilities (joint probability of 30% for a 2-year vs. 2-year events; Fig. 7; Table A.2).

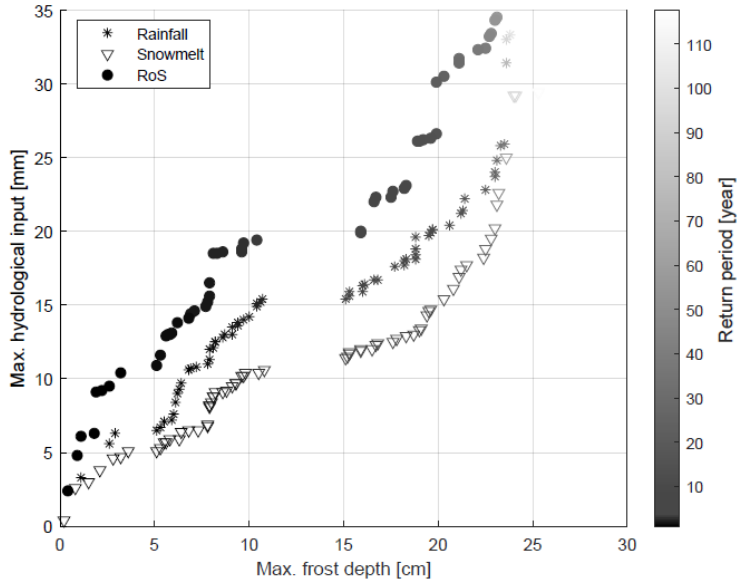

Figure 7 The bivariate return periods for the hydrological inputs during frost are represented as snowmelt during frost, rainfall during frost, and RoS during frost.

3.5.Timing of worst soil frost and runoff generation

Soil frost was most frequently simulated during peak winter months, from December to March (Fig. 8a). The 24-hour maximum frost depth in January and February was significantly higher than in the rest of the winter months (p-value < 0.05), with an average of 12.6 and 12.3 cm, respectively (Fig. 8b). This timing of maximum frost coincides very well with the largest RoS volume, averaging at 8.5, 9, and 11 mm in January, February, and March (Fig. 8c). The largest snowmelt depths also occurred in January and February (an average of 9.7 and 9.5 mm, respectively, Fig. 8d). Total precipitation and rainfall depth were highest during October, November, and December (not shown). The SHAW model predicts that the soil frost season has shortened significantly in the past 70 years, both with a delayed start (p-value > 0.05) and earlier end (p-value < 0.05; Fig.

9a and b, respectively). So, while the frost season is shortening, it is not affecting the likelihood of maximum frost co-occurring with maximum RoS. The fact that the last day of frost is no longer occurring as late as April and May suggests that the likelihood of maximum frost and maximum RoS or snowmelt occurring simultaneously may increase in the next few decades under continuous climate warming.

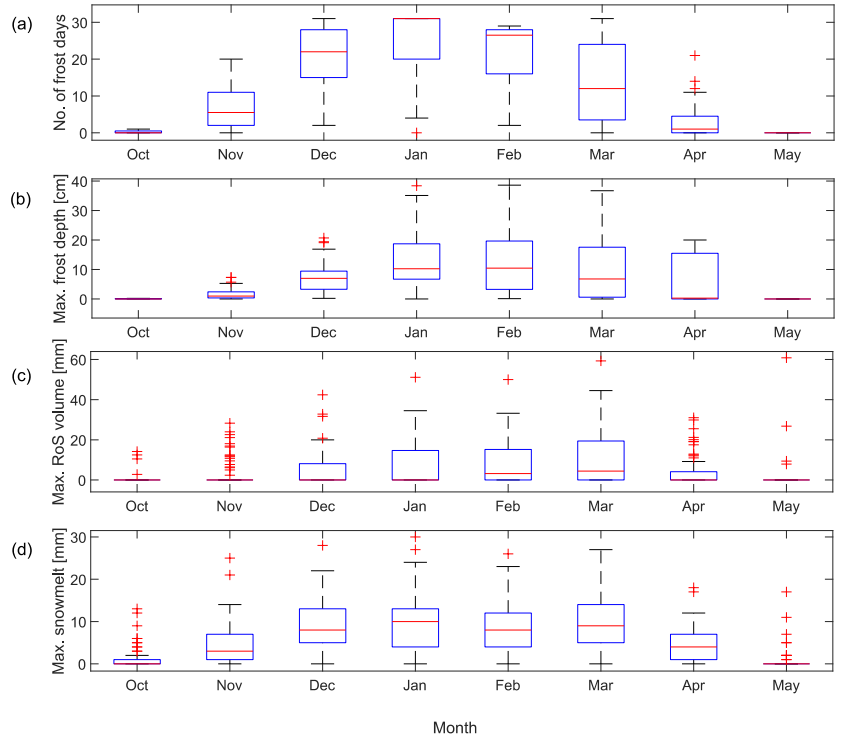

Figure 8 A summary of the maximums of winter hydrological flood indicators per month for Reykjavík (1949–2018): a) no. of frost days, b) frost depth, c) RoS volume, and d) snowmelt. The whiskers extend to the maximum and minimum data points. Outliers are plotted individually as red crosses.

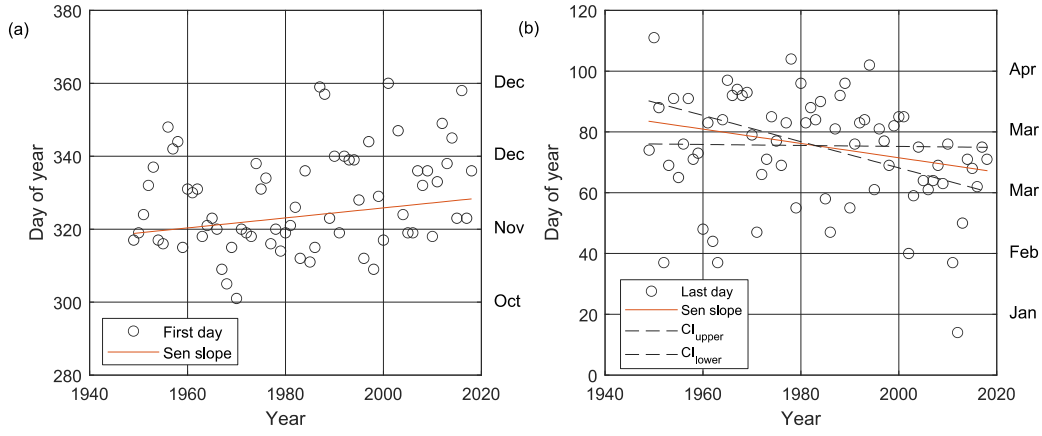

Figure 9 Timing of beginning and end of soil freezing from 1949 to 2018 represented as a) trend in the first day of soil frost formation at the beginning of winter and b) trend in the last day of frost formation at the end of winter. The solid line represents Sen's slope, and the dashed lines represent the upper and lower 95% confidence intervals of the significant slope.

4. Discussion

4.1.Intensifying winter floods

Climate change has been found to cause an increase in air temperature, precipitation, midwinter snowmelt, and RoS event volume in cold climate regions (Andradóttir et al., 2021; Dong & Menzel, 2020; Garvelmann et al., 2015; Nygren et al., 2021; Wever et al., 2014; Würzer et al., 2016). An annual RoS event was found to generate five times greater runoff than a 10-year summer rainfall event in urban Kiruna, Sweden (Moghadas et al., 2018). RoS was responsible for all large floods (T > 5 years) in a rural river catchment in Oregon in the United States (Surfleet & Tullos, 2013). The transition from snowmelt-only runoff in spring to a rain-forced runoff has been found to increase extreme flow peaks and flooding (e.g., Gellens & Roulin, 1998; Middelkoop et al.,

2001). Moreover, climate modeling, e.g., in a high-altitude Alpine catchment, predicted that the magnitude of extreme RoS-induced flooding would continue to increase in the 21st century (Sezen et al., 2020).

This study focused on resolving the trends in soil frost and co-action with rain and snowmelt in a maritime climate undergoing historically frequent freeze-thaw cycles. With the help of a numerical, physically-based model, frost depth was found to decrease over the last 70 years under maritime climatic conditions, consistent with previous research (e.g., Nygren et al., 2021). The total number of frost days and duration of continuous frost decreased, suggesting shorter frost cycles, consistent with more intermittent frost. The number of freeze-thaw cycles was, however, not found to increase at a significant level. This study confirms previous research about the importance of RoS in generating urban floods: 24-hour RoS events were found to be on the order of 5 and 10 mm more voluminous than maximum rainfall and snowmelt events with the same return period (Table 7). However, the research adds to previous knowledge by highlighting that RoS-induced flood risk is connected to a high co-occurrence with soil frost. For example, moderate winter events ($T < 2$ years) occurred simultaneously with moderate frost depths (> 10 cm) relatively frequently ($T < 4$ years). Mild rainfall and snowmelt events are known to result in significant damages if combined with deep frost formation, which can render the normally pervious soils during summer not conductive in winter (Bengtsson & Westerström, 1992; Westerström, 1984). At the studied site, even frost as shallow as 5 cm reduced the infiltration to a third of its summer rate in grassed surfaces and more in sparsely and non-vegetated areas (Zaqout et al., 2022). Almost all significant winter flooding events in the metropolitan area of Reykjavík have previously been associated with RoS combined with soil frost (Andradóttir et al., 2021).

While soil frost depth and duration were found to decrease in this study, which may ultimately suggest it is becoming a less relevant driver for urban flooding, there are no clear indications that winter floods will become more benign in the next decades. Conversely, the timing of maximum soil frost was found to shift so that it coincides more with the largest RoS and snowmelt events in the months of January–March. This, combined with a greater RoS volume, suggests that winter floods may intensify, at least in the next decades, while frost is still present. Urban areas shifting from a cold to a temperate climate may be severely affected as the magnitude and frequency of runoff caused by RoS and frost-induced runoff increases. The repeated snowmelt during winter due to frequent freeze-thaw cycles is known to reduce soil insulation provided by an intact snow cover. Consequently, deep frost formation that might be impervious until the thawing process is completed is expected to increase (Moghadas et al., 2018). Under a consistently warming climate, an increase in winter infiltration can be expected in the long term (Clilverd et al., 2011; Jyrkama & Sykes, 2007), and other studies even went as far as arguing that frost will cease to exist and thus will not affect future runoff processes at certain latitudes (Ford et al., 2020).

4.2 Re-thinking urban stormwater management in cold climates

Winter conditions are often overlooked when designing drainage systems (Butler et al., 2018; Thorolfsson, 2012), as high-intensity, short-duration heavy summer rainfall is usually considered the largest cause of urban flooding (Bengtsson & Westerström, 1992; Hammond et al., 2015). Additionally, freeze-thaw cycles are often not taken into account in hydrological modeling (Qi et al., 2019), leading to an underestimation of runoff prediction. This study, however, indicates that winter floods involving rain, snowmelt, and soil frost, are not likely to decrease in the near term.

Therefore, the impact of frost on infiltration and urban runoff generation is still relevant and needs to be considered short-to-midterm in the planning design and operation of urban stormwater management systems (Nygren et al., 2021).

Achieving climate resilience requires overcoming current and future vulnerabilities amplified by population growth and a changing climate. United Nations Sustainable Development Goal No. 11 emphasizes safe and healthy urban environments, accessible green spaces, and adaptation to climate change. In the past few decades, single-purpose, pipe-based drainage networks have been shifting towards sustainable urban drainage systems (SUDS) that take into account ecological aspects and preserve biodiversity, as well as human wellbeing (Fletcher et al., 2015; Wong & Brown, 2009). SUDS involve local source-control solutions such as green roofs, raingardens, and rainwater harvesting techniques, and larger downstream site and regional controls such as grass swales, detention ponds, and wetlands (Woods Ballard et al., 2015). Such measures can mitigate the impacts of climate change and reduce urban flood risks by storing, attenuating, and reducing surface water close to where it falls. However, SUDS performance in cold climates is vulnerable to soil frost, which particularly form following RoS and rainfall events (Zaqout & Andradóttir, 2021; Muthanna et al., 2008). SUDS elements are known to maintain functionality throughout winter if care is taken in their design and implementation (Khan et al., 2012; Paus et al., 2016; Roseen et al., 2009). In that regard, it is important to ensure good hydraulic conductivity of the underlying soil, e.g., by avoiding fine-textured soils that are more susceptible to frost and incorporating an effective, gravel-based drainage layer with an underdrain to avoid media freezing (LeFevre et al., 2009; Muthanna et al., 2008; Roseen et al., 2009). The presence of a thick vegetation cover and dense root system in the topsoil significantly decreases the thermal

conductivity and heat capacity of the underlying soil and can also improve the winter efficiency of SUDS (Yang et al., 2005; Zaqout et al., 2022). The consensus is that SUDS can help transform cities and increase their resilience to flooding by accommodating large volumes of runoff water even during winter, especially in light of climate change. This involves cooperation between private property owners, who implement on-site control, and municipalities that provide conveyance and storage systems to accommodate excess runoff.

5. Conclusions

In this paper, soil temperature, liquid and ice moisture content, and frost depth were simulated for two study areas in the greater capital region of Iceland using the Simultaneous Heat and Water (SHAW) model. A good agreement between the simulated and the observed soil temperature was found at the two tested sites ($R^2 > 0.91$), which provided valuable insights into the freezing and thawing processes. The numerical model proved particularly helpful in overcoming the lack of long-term soil observations needed for frequency and trend analyses and resolving very shallow frost that is difficult to measure (within the top 5 cm). The results show that the rise in air temperatures and liquid precipitation in winter due to climate change resulted in a significant reduction in frost depth over the last 70 years. However, a shift in the timing of maximum frost depth occurred and started to coincide with the largest winter events, which might pose a higher urban flood risk in the future if the trend continues. This study highlights the importance of analyzing the co-acting hydrologic variables, which is specifically needed in a cold climate, as severe events can result from two mundane events happening simultaneously, especially in the presence of soil frost that is often overlooked in the design of urban drainage systems. In particular,

rain-on-snow events during frost were found to pose the greatest flood risk, being more voluminous than rainfall or snowmelt alone. The changing winter patterns and hydrological processes require a reconsideration of the planning and design of urban drainage systems, specifically due to the increase in the number, frequency, and magnitude of rain-on-snow events in the last decades. Therefore, a shift towards more sustainable approaches for stormwater management and re-thinking urban runoff generation and drainage systems from a singular focus to a multipurpose approach is urged.

Acknowledgments

This research was funded by the Icelandic Research Fund (Icelandic: Rannís), grant number 185398-053. We thank the Garðabær Municipality, Iceland Meteorological Office, and Urriðaholt ehf for on-site research facilities. The Agricultural University of Iceland, especially to Prof. Ólafur Arnalds for his valuable soil insights. Viðar Guðmundsson, professor in Physics at the University of Iceland, is thanked for his help with programming. A special thanks goes to Halldóra Hreggviðsdóttir for motivating and facilitating SUDS research in Iceland.

Data availability

The data used in this study were collected from the field by the researchers and acquired from the Icelandic Meteorological Office (IMO). Any additional data is available upon request from the aforementioned rightful owners.

Appendix

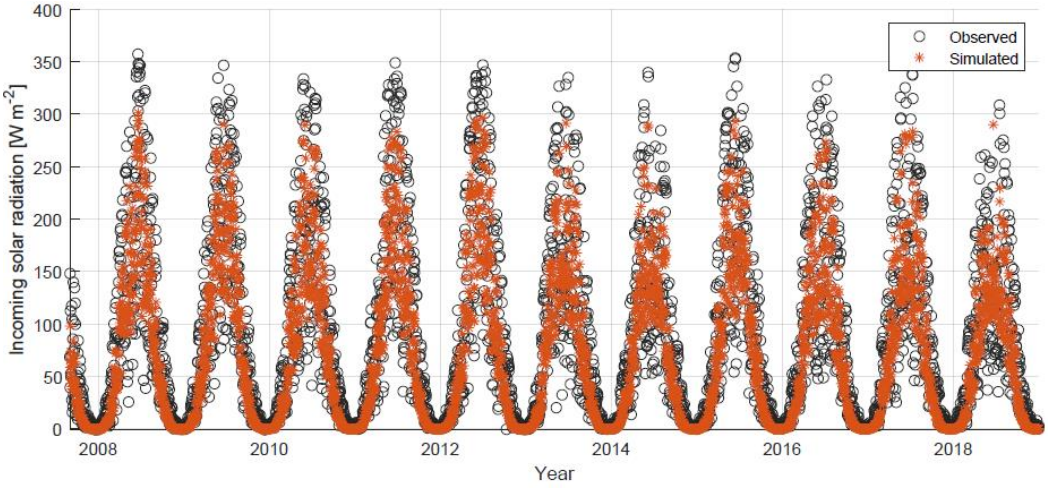

Fig. A. 1 Measured and simulated incoming daily solar radiation in Reykjavík for the period of 2007–2018.

The bivariate Archimedean copula family fitted to each pair of annual maximum hydrological variables (i.e., snowmelt & frost, rainfall & frost, and RoS & frost) was chosen based on the highest log-likelihood and lowest AIC and BIC, which are highlighted in Table A.1. The parameter of each bivariate copula was estimated using the maximum likelihood method (Table A.1).

Table A. 1 Copula parameter estimation and selection criteria of copula model.

				Selection criteria		
	Family	θ	Kendall's tau	Log-Likelihood	AIC	BIC
Snowmelt during frost	Clayton	0.33	0.14	**1.92**	**-1.85**	**0.40**
	Gumbel	1.13	0.11	0.84	0.32	2.57
	Joe	1.13	0.07	0.38	1.25	3.50
	Frank	1.08	0.12	1.04	-0.09	2.16
Rainfall during frost	Clayton	0.52	0.21	**4.47**	**-6.94**	**4.69**
	Gumbel	1.18	0.15	1.50	-0.99	1.25
	Joe	1.14	0.07	0.33	1.34	3.59
	Frank	1.85	0.20	3.11	-4.22	-1.97
RoS during frost	Clayton	0	0	0	2.00	4.01
	Gumbel	1.04	0.04	0.06	1.87	3.88
	Joe	1.06	0.03	0.06	1.88	3.89
	Frank	0.62	0.07	**0.27**	**1.46**	**3.47**

The joint probability of maximum snowmelt occurring with maximum frost and the maximum rainfall occurring with maximum frost are shown in Table A.2. The highlighted joint probabilities indicate the events of interest for return periods $1 < T < 100$ years.

Table A. 2 Joint probability of occurrence for the annual maxima of the hydrological variables for different return periods during winter.

		Max. frost depth during snowmelt [cm]						
		1.1	12.3	20.3	25.2	29.3	34.3	37.8
Max. snowmelt during frost [mm]	T [years]	1	2	5	10	20	50	100
2.0	1	**0.981**	0.498	0.198	0.098	0.050	0.020	0.010
10.4	2	0.498	**0.284**	0.117	0.058	0.030	0.012	0.006
18.8	5	0.199	0.118	**0.050**	0.025	0.013	0.005	
25.5	10	0.100	0.059	0.025	**0.013**	0.006		
32.9	20	0.050	0.030	0.013	0.006			
43.9	50	0.020	0.012	0.005				
53.1	100	0.010	0.006					
		Max. frost depth during rainfall [cm]						
		1.7	13.5	21.0	25.2	28.5	32.7	35.5
Max. rainfall during frost [mm]	T [years]	1	2	5	10	20	50	100
5.0	1	**0.981**	0.504	0.195	0.096	0.051	0.020	0.010
15.2	2	0.503	**0.305**	0.125	0.062	0.033	0.013	0.007
23.1	5	0.198	0.127	**0.053**	0.027	0.014	0.006	
28.3	10	0.103	0.067	0.028	**0.014**	0.008		
34.0	20	0.050	0.033	0.014	0.007			
41.6	50	0.020	0.013	0.006				
47.5	100	0.010	0.007					

References

Andradóttir, H. Ó., Arnardóttir, A. R., & Zaqout, T. (2021). Rain on snow induced urban floods in cold maritime climate: Risk, indicators and trends. *Hydrological Processes*, *35*(9), e14298. https://doi.org/10.1002/hyp.14298

Arnalds, O. (2015). *The Soils of Iceland*. Springer Netherlands. https://doi.org/10.1007/978-94-017-9621-7

Bengtsson, L., & Westerström, G. (1992). Urban snowmelt and runoff in northern Sweden. *Hydrological Sciences Journal*, *37*(3), 263–275. https://doi.org/10.1080/02626669209492586

Benninghoff, W. S. (1952). Interaction of Vegetation and Soil Frost Phenomena. *Arctic*, *5*(1), 34–44.

Bras, R. L. (1990). *Hydrology: An Introduction to Hydrologic Science*. Addison-Wesley.

Butler, D., Digman, C., Makropoulos, C., & Davies, J. W. (2018). *Urban Drainage* (4th ed.). CRC Press. https://doi.org/10.1201/9781351174305

Campbell, G. (1974). A Simple Method for Determining Unsaturated Conductivity From Moisture Retention Data. *Soil Science*, *117*. https://doi.org/10.1097/00010694-197406000-00001

Caraco, D., & Claytor, R. (1997). *Stormwater BMP Design: Supplement for Cold Climates*. U.S. Environmental Protection Agency.

Chen, L. (2019). *Copulas and Its Application in Hydrology and Water Resources / by Lu Chen, Shenglian Guo.* (1st ed. 2019.). Springer Singapore. https://doi.org/10.1007/978-981-13-0574-0

Chow, V. T., Maidment, D. R., & Mays, L. W. (1988). *Applied Hydrology*. McGraw-Hill.

Clayton, D. G. (1978). A model for association in bivariate life tables and its application in epidemiological studies of familial tendency in chronic disease incidence. *Biometrika*, *65*(1), 141–151. https://doi.org/10.1093/biomet/65.1.141

Clilverd, H. M., White, D. M., Tidwell, A. C., & Rawlins, M. A. (2011). The Sensitivity of Northern Groundwater Recharge to Climate Change: A Case Study in Northwest Alaska1. *JAWRA Journal of the American Water Resources Association*, *47*(6), 1228–1240. https://doi.org/10.1111/j.1752-1688.2011.00569.x

Crochet, P., Jóhannesson, T., Jónsson, T., Sigurðsson, O., Björnsson, H., Pálsson, F., & Barstad, I. (2007). Estimating the Spatial Distribution of Precipitation in Iceland Using a Linear Model of Orographic Precipitation. *Journal of Hydrometeorology*, *8*(6), 1285–1306. https://doi.org/10.1175/2007JHM795.1

de Vries, D. A. (1963). Thermal properties of soils. In W. R. van Wijk (Ed.), *Physics of plant environment* (2nd ed., pp. 210–235). North Holland Publishing Company.

Dong, C., & Menzel, L. (2020). Recent snow cover changes over central European low mountain ranges. *Hydrological Processes*, *34*(2), 321–338. https://doi.org/10.1002/hyp.13586

Einarsson, M. (1984). *Climate of Iceland*. Elsevier.

Feiccabrino, J., Graff, W., Lundberg, A., Sandström, N., & Gustafsson, D. (2015). Meteorological Knowledge Useful for the Improvement of Snow Rain Separation in Surface Based Models. *Hydrology*, *2*(4), 266–288. https://doi.org/10.3390/hydrology2040266

Flerchinger, G. N., & Pierson, F. B. (1991). Modeling plant canopy effects on variability of soil temperature and water. *Agricultural and Forest Meteorology*, *56*(3), 227–246. https://doi.org/10.1016/0168-1923(91)90093-6

Flerchinger, G., & Saxton, K. (1989a). Simultaneous Heat and Water Model of a Freezing Snow-Residue-Soil System I. Theory and Development. *Transactions of the ASAE*, *32*, 0565–0571. https://doi.org/10.13031/2013.31040

Flerchinger, G., & Saxton, K. (1989b). Simultaneous Heat and Water Model of a Freezing Snow-Residue-Soil System II. Field verification. *Transactions of the ASAE*, *32*, 0573–0576. https://doi.org/10.13031/2013.31041

Fletcher, T. D., Shuster, W., Hunt, W. F., Ashley, R., Butler, D., Arthur, S., Trowsdale, S., Barraud, S., Semadeni-Davies, A., Bertrand-Krajewski, J.-L., Mikkelsen, P. S., Rivard, G., Uhl, M., Dagenais, D., & Viklander, M. (2015). SUDS, LID, BMPs, WSUD and more – The evolution and application of terminology surrounding urban drainage. *Urban Water Journal*, *12*(7), 525–542. https://doi.org/10.1080/1573062X.2014.916314

Ford, C. M., Kendall, A. D., & Hyndman, D. W. (2020). Effects of shifting snowmelt regimes on the hydrology of non-alpine temperate landscapes. *Journal of Hydrology*, *590*, 125517. https://doi.org/10.1016/j.jhydrol.2020.125517

Fouli, Y., Cade-Menun, B. J., & Cutforth, H. W. (2013). Freeze–thaw cycles and soil water content effects on infiltration rate of three Saskatchewan soils. *Canadian Journal of Soil Science*, *93*(4), 485–496. https://doi.org/10.4141/cjss2012-060

Frank, M. J. (1979). On the simultaneous associativity ofF(x, y) andx+y−F(x, y). *Aequationes Mathematicae*, *19*(1), 194–226. https://doi.org/10.1007/BF02189866

Fuchs, M., Campbell, G. S., & Papendick, R. I. (1978). An Analysis of Sensible and Latent Heat Flow in a Partially Frozen Unsaturated Soil. *Soil Science Society of America Journal*, *42*(3), 379–385. https://doi.org/10.2136/sssaj1978.03615995004200030001x

Garvelmann, J., Pohl, S., & Weiler, M. (2015). Spatio-temporal controls of snowmelt and runoff generation during rain-on-snow events in a mid-latitude mountain catchment. *Hydrological Processes*, *29*(17), 3649–3664. https://doi.org/10.1002/hyp.10460

Gellens, D., & Roulin, E. (1998). Streamflow response of Belgian catchments to IPCC climate change scenarios. *Journal of Hydrology*, *210*(1), 242–258. https://doi.org/10.1016/S0022-1694(98)00192-9

Gilbert, R. O. (1987). *Statistical Methods for Environmental Pollution Monitoring* (1st edition). Wiley.

Granger, R., Gray, D., & Dyck, G. (2011). Snowmelt Infiltration to Frozen Prairie Soils. *Canadian Journal of Earth Sciences*, *21*, 669–677. https://doi.org/10.1139/e84-073

Gumbel, E. J. (1960). Bivariate Exponential Distributions. *Journal of the American Statistical Association*, *55*(292), 698–707. Scopus. https://doi.org/10.1080/01621459.1960.10483368

Guymon, G. L., & Luthin, J. N. (1974). A coupled heat and moisture transport model for Arctic soils. *Water Resources Research*, *10*(5), 995–1001. https://doi.org/10.1029/WR010i005p00995

Hammond, M. J., Chen, A. S., Djordjević, S., Butler, D., & Mark, O. (2015). Urban flood impact assessment: A state-of-the-art review. *Urban Water Journal*, *12*(1), 14–29. https://doi.org/10.1080/1573062X.2013.857421

Hansson, K., Šimůnek, J., Mizoguchi, M., Lundin, L.-C., & van Genuchten, M. Th. (2004). Water Flow and Heat Transport in Frozen Soil: Numerical Solution and Freeze-Thaw Applications. *Vadose Zone Journal*, *3*(2), 693–704. https://doi.org/10.2136/vzj2004.0693

He, H., Dyck, M. F., Si, B. C., Zhang, T., Lv, J., & Wang, J. (2015). Soil freezing–thawing characteristics and snowmelt infiltration in Cryalfs of Alberta, Canada. *Geoderma Regional*, *5*, 198–208. https://doi.org/10.1016/j.geodrs.2015.08.001

Iceland Meteorological Office [IMO] (2022a). Incoming and outgoing radiation from Reykjavik station No. 7476. Data delivery May 11, 2022.

Iceland Meteorological Office [IMO] (2020b). Daily weather observations at the Reykjavík Manned Synoptic Station No. 1.

Jansson, P.-E., & Karlberg, L. (2004). Coupled heat and mass transfer model for soil-plant-atmosphere systems. Royal Institute of Technology, Department of Civil and Environmental Engineering. *Stockholm*.

Joe, H. (1997). *Multivariate Models and Multivariate Dependence Concepts*. CRC Press.

Jyrkama, M. I., & Sykes, J. F. (2007). The impact of climate change on spatially varying groundwater recharge in the grand river watershed (Ontario). *Journal of Hydrology*, *338*(3), 237–250. https://doi.org/10.1016/j.jhydrol.2007.02.036

Kane, D. L. (1980). Snowmelt infiltration into seasonally frozen soils. *Cold Regions Science and Technology*, *3*(2–3), 153–161. https://doi.org/10.1016/0165-232X(80)90020-8

Kendall, M. G. (1948). *Rank correlation methods*. Griffin.

Khan, U. T., Valeo, C., Chu, A., & van Duin, B. (2012). Bioretention cell efficacy in cold climates: Part 1 — hydrologic performance. *Canadian Journal of Civil Engineering*, *39*(11), 1210–1221. https://doi.org/10.1139/l2012-110

LeFevre, N. J., Davidson, J. D., & Oberts, G. L. (2009). Bioretention of Simulated Snowmelt: Cold Climate Performance and Design Criteria. *Cold Regions Engineering 2009*, 145–154. https://doi.org/10.1061/41072(359)17

Lian, J., Xu, K., & Ma, C. (2013). Joint impact of rainfall and tidal level on flood risk in a coastal city with a complex river network: A case study of Fuzhou City, China. *Hydrology and Earth System Sciences*, *17*, 679–689. https://doi.org/10.5194/hess-17-679-2013

Lundin, L.-C. (1990). Hydraulic properties in an operational model of frozen soil. *Journal of Hydrology*, *118*(1), 289–310. https://doi.org/10.1016/0022-1694(90)90264-X

Maksimovic, C., Saegrov, S., Milina, J., & Thorolfsson, S. (2000). *Urban drainage in specific climates, v. II: Urban drainage in cold climates—UNESCO Digital Library*. https://unesdoc.unesco.org/ark:/48223/pf0000122599

Mann, H. B. (1945). Non-parametric Tests Against Trend. *Econometrica*, *13*(3), 245–259. JSTOR. https://doi.org/10.2307/1907187

Middelkoop, H., Daamen, K., Gellens, D., Grabs, W., Kwadijk, J. C. J., Lang, H., Parmet, B. W. A. H., Schädler, B., Schulla, J., & Wilke, K. (2001). Impact of climate change on hydrological regimes and water resources management in the Rhine basin. *Climatic Change*, *49*(1–2), 105–128. Scopus. https://doi.org/10.1023/A:1010784727448

Moghadas, S., Leonhardt, G., Marsalek, J., & Viklander, M. (2018). Modeling Urban Runoff from Rain-on-Snow Events with the U.S. EPA SWMM Model for Current and Future Climate Scenarios. *Journal of Cold Regions Engineering*, *32*(1), 04017021. https://doi.org/10.1061/(ASCE)CR.1943-5495.0000147

Muthanna, T. M., Viklander, M., & Thorolfsson, S. T. (2008). Seasonal climatic effects on the hydrology of a rain garden. *Hydrological Processes*, *22*(11), 1640–1649. https://doi.org/10.1002/hyp.6732

Neitsch, S. L., Arnold, J. G., Kiniry, J. R., & Williams, J. R. (2011). *Soil and water assessment tool theoretical documentation version 2009*. Texas Water Resources Institute.

Nelsen, R. B. (2007). *An Introduction to Copulas*. Springer Science & Business Media.

Nygren, M., Giese, M., & Barthel, R. (2021). Recent trends in hydroclimate and groundwater levels in a region with seasonal frost cover. *Journal of Hydrology*, *602*, 126732. https://doi.org/10.1016/j.jhydrol.2021.126732

Ólafsson, H., Furger, M., & Brümmer, B. (2007). The weather and climate of Iceland. *Meteorologische Zeitschrift - METEOROL Z*, *16*, 5–8. https://doi.org/10.1127/0941-2948/2007/0185

Paus, K. H., Muthanna, T. M., & Braskerud, B. C. (2016). The hydrological performance of bioretention cells in regions with cold climates: Seasonal variation and implications for design. *Hydrology Research*, *47*(2), 291–304. https://doi.org/10.2166/nh.2015.084

Penner, E. (1970). Thermal conductivity of frozen soils. *Canadian Journal of Earth Sciences*. https://doi.org/10.1139/e70-091

Petersen, G. N. (2018). Veður í Reykjavík og á Hólmsheiði Desember 2017 – Janúar 2018. *Technical Report GNP/2018-1, Orkuveita Reykjavíkur.*

Qi, J., Zhang, X., & Wang, Q. (2019). Improving hydrological simulation in the Upper Mississippi River Basin through enhanced freeze-thaw cycle representation. *Journal of Hydrology*, *571*, 605–618. https://doi.org/10.1016/j.jhydrol.2019.02.020

Roseen, R. M., Ballestero, T. P., Houle, J. J., Avellaneda, P., Briggs, J., Fowler, G., & Wildey, R. (2009). Seasonal Performance Variations for Storm-Water Management Systems in Cold Climate Conditions. *Journal of Environmental Engineering*, *135*(3), 128–137. https://doi.org/10.1061/(ASCE)0733-9372(2009)135:3(128)

Salvadori, G., & De Michele, C. (2007). On the Use of Copulas in Hydrology: Theory and Practice. *Journal of Hydrologic Engineering*, *12*(4), 369–380. https://doi.org/10.1061/(ASCE)1084-0699(2007)12:4(369)

Sen, P. K. (1968). Estimates of the Regression Coefficient Based on Kendall's Tau. *Journal of the American Statistical Association*, *63*(324), 1379–1389. JSTOR. https://doi.org/10.2307/2285891

Sezen, C., Sraj, M., Medved, A., & Bezak, N. (2020). Investigation of Rain-On-Snow Floods under Climate Change. *Applied Sciences-Basel*, *10*(4), 1242. https://doi.org/10.3390/app10041242

Shanley, J. B., & Chalmers, A. (1999). The effect of frozen soil on snowmelt runoff at Sleepers River, Vermont. *Hydrological Processes*, *13*(12–13), 1843–1857. https://doi.org/10.1002/(SICI)1099-1085(199909)13:12/13<1843::AID-HYP879>3.0.CO;2-G

Šimůnek, J., van Genuchten, M. Th., & Šejna, M. (2016). Recent Developments and Applications of the HYDRUS Computer Software Packages. *Vadose Zone Journal*, *15*(7), vzj2016.04.0033. https://doi.org/10.2136/vzj2016.04.0033

Sklar, M. (1959). Fonctions de repartition a n dimensions et leurs marges. *Undefined*. https://www.semanticscholar.org/paper/Fonctions-de-repartition-a-n-dimensions-et-leurs-Sklar/d017e0a6a9b93dcab7cdcd44b17544c04f7678d2

Slater, A. G., Pitman, A. J., & Desborough, C. E. (1998). Simulation of freeze-thaw cycles in a general circulation model land surface scheme. *Journal of Geophysical Research Atmospheres*, *103*(D10), 11303–11312. Scopus. https://doi.org/10.1029/97JD03630

Sörensen, J., & Bengtsson, L. (2014). *Combined effects of high water level and precipitation on flooding of Gothenburg, Sweden* (p. 12).

Stadler, D., Stahli, M., Aeby, P., & Fluhler, H. (2000). Dye Tracing and Image Analysis for Quantifying Water Infiltration into Frozen Soils. *Soil Science Society of America Journal*, *64*(2), 505–516. https://doi.org/10.2136/sssaj2000.642505x

Stähli, M., Jansson, P.-E., & Lundin, L.-C. (1999). Soil moisture redistribution and infiltration in frozen sandy soils. *Water Resources Research*, *35*(1), 95–103. https://doi.org/10.1029/1998WR900045

Surfleet, C. G., & Tullos, D. (2013). Variability in effect of climate change on rain-on-snow peak flow events in a temperate climate. *Journal of Hydrology*, *479*, 24–34. https://doi.org/10.1016/j.jhydrol.2012.11.021

Theil, H. (1950). A rank-invariant method of linear and polynomial regression analysis, 1-2; confidence regions for the parameters of linear regression equations in two, three and more variables. *Indagationes Mathematicae*, *1*(2). https://ir.cwi.nl/pub/18446

Thorolfsson, S. T. (2012). *Specific Problems in Urban Drainage in Cold Climate (SP-UDCC)*. 888–899. https://doi.org/10.1061/40583(275)86

USDA. (1987). Soil Mechanics Level 1: Module 3—USDA Textural Soil Classification. *Study Guide*.

Wang, G., Hu, H., & Li, T. (2009). The influence of freeze–thaw cycles of active soil layer on surface runoff in a permafrost watershed. *Journal of Hydrology*, *375*(3), 438–449. https://doi.org/10.1016/j.jhydrol.2009.06.046

Watanabe, K., Kito, T., Dun, S., Wu, J. Q., Greer, R. C., & Flury, M. (2013). Water Infiltration into a Frozen Soil with Simultaneous Melting of the Frozen Layer. *Vadose Zone Journal*, *12*(1), vzj2011.0188. https://doi.org/10.2136/vzj2011.0188

Watanabe, K., & Kugisaki, Y. (2017). Effect of macropores on soil freezing and thawing with infiltration: Effect of Macropores on Soil Freezing and Thawing with Infiltration. *Hydrological Processes*, *31*(2), 270–278. https://doi.org/10.1002/hyp.10939

Westerström, G. (1984). *Snowmelt runoff from Porsön residential area, Luleå*. *4*, 315–323. http://urn.kb.se/resolve?urn=urn:nbn:se:ltu:diva-38161

Wever, N., Jonas, T., Fierz, C., & Lehning, M. (2014). Model simulations of the modulating effect of the snow cover in a rain-on-snow event. *Hydrology and Earth System Sciences*, *18*(11), 4657–4669. https://doi.org/10.5194/hess-18-4657-2014

Williams, P. J., & Smith, M. W. (1989). *The frozen earth: Fundamentals of geocryology* (Vol. 306). Cambridge University Press Cambridge.

Wong, T. H. F., & Brown, R. R. (2009). The water sensitive city: Principles for practice. *Water Science and Technology*, *60*(3), 673–682. https://doi.org/10.2166/wst.2009.436

Woods Ballard, B., Wilson, S., Udale-Clarke, H., Illman, S., Scott, T., Ashley, R., & Kellagher, R. (2015). *The SUDS manual (C753). CIRIA: London, UK*. ISBN 978-0-86017-759-3

Würzer, S., & Jonas, T. (2018). Spatio-temporal aspects of snowpack runoff formation during rain on snow. *Hydrological Processes*, *32*(23), 3434–3445. https://doi.org/10.1002/hyp.13240

Würzer, S., Jonas, T., Wever, N., & Lehning, M. (2016). Influence of Initial Snowpack Properties on Runoff Formation during Rain-on-Snow Events. *Journal of Hydrometeorology*, *17*(6), 1801–1815. https://doi.org/10.1175/JHM-D-15-0181.1

Yang, K., Koike, T., Ye, B., & Bastidas, L. (2005). Inverse analysis of the role of soil vertical heterogeneity in controlling surface soil state and energy partition. *Journal of Geophysical Research: Atmospheres*, *110*(D8). https://doi.org/10.1029/2004JD005500

Zaqout, T., & Andradóttir, H. Ó. (2021). Hydrologic performance of grass swales in cold maritime climates: Impacts of frost, rain-on-snow and snow cover on flow and volume reduction. *Journal of Hydrology*, *597*, 126159. https://doi.org/10.1016/j.jhydrol.2021.126159

Zaqout, T., Andradóttir, H. Ó., & Arnalds, Ó. (2022). Infiltration capacity in urban areas undergoing frequent snow and freeze–thaw cycles: Implications on sustainable urban drainage systems. *Journal of Hydrology*, *607*, 127495. https://doi.org/10.1016/j.jhydrol.2022.127495

Zellou, B., & Rahali, H. (2019). Assessment of the joint impact of extreme rainfall and storm surge on the risk of flooding in a coastal area. *Journal of Hydrology*, *569*, 647–665. https://doi.org/10.1016/j.jhydrol.2018.12.028

Zheng, C., Šimůnek, J., Zhao, Y., Lu, Y., Liu, X., Shi, C., Li, H., Yu, L., Zeng, Y., & Su, Z. (2021). Development of the Hydrus-1D freezing module and its application in simulating the coupled movement of water, vapor, and heat. *Journal of Hydrology*, *598*, 126250. https://doi.org/10.1016/j.jhydrol.2021.126250